Steps towards the universal direct current distribution system

Mackay, Laurens

DOI
10.4233/uuid:42a19101-c829-4127-959b-c8ab7d17e37d

Publication date
2018

Document Version
Final published version

Citation (APA)
Mackay, L. (2018). *Steps towards the universal direct current distribution system*. [Dissertation (TU Delft), Delft University of Technology]. https://doi.org/10.4233/uuid:42a19101-c829-4127-959b-c8ab7d17e37d

STEPS TOWARDS THE UNIVERSAL DIRECT CURRENT DISTRIBUTION SYSTEM

STEPS TOWARDS THE UNIVERSAL DIRECT CURRENT DISTRIBUTION SYSTEM

Dissertation

for the purpose of obtaining the degree of doctor
at Delft University of Technology
by the authority of the Rector Magnificus, Prof.dr.ir. T.H.J.J. van der Hagen,
chair of the Board for Doctorates
to be defended publicly on
Wednesday 14 March 2018 at 15:00 o'clock

by

Laurens MACKAY

Master of Science in Electrical Engineering and Information Technology,
Swiss Federal Institute of Technology (ETH), Zürich, Switzerland,
born in Zeist, The Netherlands.

This dissertation has been approved by the promotors.

Composition of the doctoral committee:

Rector Magnificus,	voorzitter
Prof. dr. P. Bauer,	Delft University of Technology, promotor
Dr. L. M. Ramirez Elizondo,	Delft University of Technology, copromotor
Independent members:	
Prof. dr. A. Smets	Delft University of Technology
Prof. dr. P. Palensky	Delft University of Technology
Prof. dr. J. Guerrero	Aalborg University, Denmark
Dr. M. Gibescu	Eindhoven University of Technology
Dr. D. van Hertem	KU Leuven, Belgium

This work was supported by Stichting Innovatie Alliantie under RAAK MKB Grant 2012-20-50M, by STW Perspectief Programma "Smart Energy Systems in the Built Environment", by DC Opportunities and by the Janggen-Pöhn-Stiftung.

Keywords: dc distribution, bipolar dc grids, optimal power flow, protection, lvdc

Front & Back: Printed circuit board layout of solid state circuit breaker of Chapter 5.

ISBN 978-94-6186-905-0

An electronic version of this dissertation is available at
http://repository.tudelft.nl/.

CONTENTS

SUMMARY

The traditional ac power system is challenged by emerging distributed renewable energy sources and an increase in installed load capacity, e.g., electric vehicles. Most of these new resources use inherently dc as do more and more appliances. This poses the question, if they should still be connected on ac in the low voltage grid, which was chosen a century ago, because at that time dc could not be easily transformed to higher voltage levels.

In this dissertation, steps are set towards a universal dc distribution system that has the capability of replacing current low voltage ac grids. Standardization is very important at this voltage level due to the high number of connected devices. Therefore, an analysis of the future power system requirements is made and a modular architecture is proposed that consists of connected nano- and microgrids. The dc distribution grid could be meshed and these nano- and microgrids could be connected without a converter separating them, which has significant implications on the overall design of the system. Modular bipolar voltage levels can increase the efficiency of the system, but complicate its operation as well.

The exact optimal power flow is formulated for bipolar dc distribution grids with asymmetric loading. It can be used to manage congestions that could affect only one pole. Congestions in distribution grids are likely to increase, due to the increase in installed capacity. They are also more severe in dc grids due to the use of power electronic converters that have very hard limits in comparison with ac transformers. A general method to calculate locational marginal prices between any two nodes in the dc grid is formulated. The optimal power flow formulation is extended to multiple periods in order to include storage operation.

Protection is one of the main challenges in creating large dc grids, as short-circuit currents can be very high and there is no current zero crossing as in ac. A low short-circuit current protection philosophy is formulated to deal with this. It also addresses the challenge of very low fault current contribution in case of islanded operation. Solid-state circuit breakers are proposed as the main protection devices for dc distribution grids in combination with fast fault detection and clearance. The challenges regarding fault discrimination and selectivity are addressed. Additionally a classification of protection zones in dc distribution grids based on risk is proposed. Experimental measurements of a developed prototype using current derivative tripping are shown.

Finally, dc ready devices, that can operate on dc as well as ac, are introduced as a means of simplifying the transition towards dc distribution grids. The losses in the rectification components, when operated on dc instead of ac, are analyzed and it is found that the rectification components of wide input range devices do not need to be enhanced.

SAMENVATTING

Het traditionele wisselstroomsysteem wordt uitgedaagd door opkomende gedistribueerde hernieuwbare energiebronnen en een toename in geïnstalleerd vermogen, bijvoorbeeld van elektrische voertuigen. De meeste van deze nieuwe bronnen gebruiken inherent gelijkstroom, evenals steeds meer apparaten. Dit stelt de vraag, of ze nog steeds verbonden moeten zijn op wisselstroom in het laagspanningsnet, dat een eeuw geleden werd gekozen, omdat gelijkstroom op dat moment niet gemakkelijk naar hogere spanningsniveaus kon worden getransformeerd.

In dit proefschrift worden stappen gezet op weg naar een universeel gelijkstroomverdeelsysteem dat de capaciteit heeft om het huidige laagspannings-wisselstroomnet te vervangen. Standaardisatie is erg belangrijk op dit spanningsniveau vanwege het grote aantal aangesloten apparaten. Daarom wordt een analyse van de toekomstige systeemvereisten voor het elektriciteitsnet gemaakt en wordt een modulaire architectuur voorgesteld die bestaat uit verbonden nano- en microgrids. Het DC-distributienet kan vermaasd worden en de nano- en microgrids kunnen worden verbonden zonder een omzetter die hen scheidt, hetgeen significante implicaties heeft op het algehele ontwerp van het systeem. Modulaire bipolaire spanningsniveaus kunnen de efficiëntie van het systeem verhogen, maar maken de werking ervan ook compliceerder.

De exacte Optimal Power Flow is geformuleerd voor bipolaire DC netten met asymmetrische belasting. Het kan worden gebruikt om congesties te beheersen die slechts één pool beïnvloeden. Congesties in distributienetten zullen waarschijnlijk toenemen vanwege de toename van het geïnstalleerde vermogen. Ze zijn ook ernstiger in DC vanwege het gebruik van vermogenselectronica die hardere heeft hebben in vergelijking met wisselstroomtransformators. Een algemene methode wordt geformuleerd om de locale marginale prijzen tussen twee willekeurige knooppunten in het gelijkstroomnet te berekenen. De optimal power flow formulering wordt uitgebreid naar meerdere perioden om de invloed van opslag mee te nemen.

Beveiliging is een van de grootste uitdagingen voor grote gelijkstroomnetten, omdat kortsluitstromen zeer hoog kunnen zijn en er geen stroomnulldoorgang is zoals bij wisselstroom. Een lage kortsluitstroom beveiligingsfilosofie is geformuleerd om hiermee om te gaan. De uitdaging van een zeer lage foutstroombijdrage in het geval van een eilandbedrijf is ook behandeld. Scheiders op basis van halfgeleiders worden voorgesteld als de belangrijkste beveiligingsinrichtingen voor DC-distributienetten in combinatie met snelle foutdetectie. De uitdagingen met betrekking tot foutendiscriminatie en selectiviteit worden beschreven. Daarnaast wordt een classificatie van beschermingszones in DC-distributienetten op basis van risico voorgesteld. Experimentele metingen van een ontwikkeld prototype met behulp van stroomafgeleiding worden getoond.

Ten slotte worden DC-ready-apparaten, die zowel op DC als AC kunnen werken, geïntroduceerd als een middel om de overgang naar DC-distributienetten te vereenvoudigen. De verliezen in de gelijkrichters, wanneer ze worden aangesloten op gelijkstroom

in plaats van wisselstroom, worden geanalyseerd en er is vastgesteld dat de gelijkrichters van apparaten met breed invoerbereik niet behoeven te worden vergroot.

1

INTRODUCTION

The traditional ac power system is challenged by increasing numbers of decentralized energy resources. In the extreme and most challenging case, power would be provided 100 % by intermittent renewable energies. Most of the distributed sources have a fluctuating behavior and as a consequence, demand response, i.e. the adaption of consumption, and/or energy storage will have to be used to keep the system operational. If the generation capacity is too high it may have to be curtailed.

Moreover, the installed power capacity is increasing, e.g. due to an increase in use of electric vehicles. This would lead to more congestion in the distribution grid and corresponding solutions need to be developed. One bottleneck in the distribution grids will be the substations as they are often rated for only 10 or 20 % of the connected peak power, considering that not everyone will use electricity at the same time. However electric vehicles and photo-voltaics might result in more synchronized grid usage, and actions will have to be taken. There are two fundamental possibilities to deal with congestion. One is by control and the other is market based. Market based control of congestion in its purest form leads to nodal prices in the distribution grid.

From these considerations it can be seen that significant changes are needed in the traditional power system in order to satisfy the new requirements. This is a good opportunity to reconsider the whole system and look for other possible improvements such as a dc distribution system.

1.1. COMEBACK OF DIRECT CURRENT

The war of currents between Edison with dc vs. Westinghouse and Tesla with ac was won by ac for good reasons a century ago. However as time passed and new developments were made, the foundations of this victory have become obsolete. Power electronics enable dc/dc conversion and in that way, allow the achievement of what hundred years ago only ac transformers could do properly: the change of voltage levels. From the high voltage side, HVdc lines are now used for long distance power transmission, as dc line losses are much smaller than ac ones. Other benefits achieved are the prevention of

skin effects and a reduction of problems related to cable capacitance and the resulting reactive power flow, especially for submarine cables.

However, also from the low voltage side, dc is having a comeback. Until now, this has taken place mostly inside the devices. First, ac transformers were used to bring down the voltage to usual application levels, e.g. 20 V, and rectification was done thereafter. Nowadays, ac transformers in devices are more and more being replaced by dc/dc converters. Due to their higher switching frequencies, typically 100 kHz instead of 50/60 Hz with ac, much smaller passive components can be used, which reduces size, weight, and material costs. The ac from the grid needs therefore to be rectified and – to prevent distortion of the ac grid – artificial sinusoidal currents are drawn using power factor correction (PFC). Today even ac motors are more and more driven by motor controllers using ac/dc followed by dc/ac conversion, which allows variable speed control.

It is important to note that distributed renewable energy sources are mostly either dc inherently, e.g. photovoltaics, or use a dc link to decouple rotations speeds from the ac grid such as wind power. Furthermore, batteries are dc in general and their application is evolving in electric vehicles and other devices. For these reasons it is now plausible to consider bringing dc one level higher and to transform the distribution grid from ac to dc, eliminating dc/ac and ac/dc conversions. This is one of the main motivations for having dc distribution networks.

Microgrids have the potential to improve reliability in the case of an outage occurring at a higher voltage level in the network by using available distributed sources and storage. DC microgrids can have some advantages over ac microgrids. For example, balancing local supply and demand and establishing financial compensation for grid losses could be done using the dc voltage. Due to the lack of synchronization requirements in dc, the re-connection to a higher level grid is straightforward. The centralized ac/dc conversion from low voltage or medium voltage ac grid can be made more efficient and can even help stabilize the ac grid, for example by supplying reactive power. The reduction of conversion steps and the lack of synchronization requirements motivate further research in dc distribution networks.

1.2. DC DISTRIBUTION SYSTEM

The hypothesis for this dissertation is that with a dc distribution system, the previously mentioned smart grid challenges could be solved more easily and more reliably than with ac distribution networks. The transition from ac to dc is very challenging. However, for countries with little ac infrastructure the option of going directly for dc and skipping the traditional ac power system, has the potential to be more suitable. DC ready devices that work on both ac and dc would not need to be more expensive than ac-only devices and would simplify the transition with economics of scale.

When just looking inside buildings or small houses, many options for dc are already available on the market. For example, the USB Type-C connector with USB Power Delivery up to 100 W will make the transition to a dc system considerably smoother, as small devices will not come with an ac connection anymore.

The NEN and IEC standardization process started in 2014 and is currently ongoing. Designing a complete system from scratch gives a unique chance to include features for the future smart grid. For this reason it is essential to explore at this moment what are

the potential opportunities that dc systems could provide. In this way, the requirements related to new applications can be directly included into standardization.

Of the whole power system, the low voltage grid connecting households and buildings is the most important section to be developed. Due to the many entities involved (grid operators, owners, device manufacturers), standardization in this level is most essential. In medium voltage for example, grid operators can autonomously decide on its system, and therefore system standardization is not mandatory.

Until now, in the literature of dc microgrids, it is generally assumed that the electrical installations inside and outside the buildings are separated by a converter to be located at the entrance of each building.This is a convenient assumption as it decouples the internal grid from the one in the street. However when thinking of a future dc distribution system, this will probably not be the optimal solution as these converters would have to be rated for the peak load of every house. In present ac systems – at least in Europe – there is no transformer at every house entrance; instead there is one for several of them. This allows to use a smaller power rating, as not all houses have their peak power at the same time. The important conclusion is that for the dc distribution system one should start considering a system that comprises both the electrical installation inside and outside the building as a whole, as it is done in ac distribution grids. This is what will be considered in this dissertation.

In ac grids, distribution is done often in two or three phase systems. This allows to connect small devices to a single phase and larger devices to multiple phases with a higher voltage in between. Similarly in dc distribution grids bipolar grids could be used to provide a lower voltage to small devices and double the voltage to large ones. As the two poles of the dc distribution grid in this case are unlikely to be loaded evenly, special care has to be taken if the system is to be operated close to its limits.

Protection in dc distribution systems is a crucial topic but it has had little attention in previous research. The use of traditional protection strategies with high short-circuit currents is a possibility, but converters need to be designed for higher peak currents. The same would also be necessary in ac systems when there is no rotating inertia. Therefore a new protection philosophy with low short-circuit currents should be used for dc distribution systems.

Several aspects of protection will be considered in this work and will serve as a contribution to this challenge. This has to be done in coordination with all other parts of the system.

One of the major challenges is that the field is young and a lot of inter-dependencies exist among the components of the system; especially linked to the possible protection strategies and control methods.

1.3. RESEARCH OBJECTIVE

The main objective of this dissertation is the following:

> To enable an *universal dc distribution system* that can accommodate a significant share of distributed renewable energy sources, by considering *optimal power flow*, *storage operation* and *protection* in such systems.

1.4. RESEARCH QUESTIONS

The main objective is approached by the formulation of several research questions. The following research questions are considered in this dissertation:

1. How can the dc distribution system be designed to allow for resilience with significant share of distributed renewable energy sources?

2. How should optimal power flow be implemented in meshed bipolar dc distribution grids in order to achieve minimum operation cost respectively maximization of social welfare, while respecting operation limits of lines and converters?

3. How can nodal prices for prosumers be derived in dc distribution grids such that they allow for independent economics agents to optimize for their own profit and encourage congestion management?

4. How is storage operated optimally in bipolar dc distribution grids and what effect does the operation of storage have on the nodal prices.

5. What protection philosophy should be applied to large dc distribution grids such that both connected and islanded operation of individual dc microgrids is possible?

6. Do the rectification components of ac devices need to be enhanced if they are operated on dc instead of ac?

1.5. OUTLINE

This dissertation is based on publications. The publications are referred to on the first page of each chapter. In Figure 1.1 a visual overview of this dissertation and the relation of the chapters is shown. The dissertation is structured by the following chapters:

Chapter 2: Towards the Universal DC Distribution System addresses the first research question by making a system level synthesis of the envisioned universal dc distribution system. First a general analysis of future use-cases is done. A modular dc distribution system is described that can include modular connection of different nano- and microgrids without converters. This design can make the system more resilient in the presence of distributed renewable energy sources as the nano- and microgrids could continue operation in case of higher level outages. Further, meshed grids are discussed to better interconnect the system and provide alternative power paths in case of congestion and outages. Modular voltage levels are introduced to accommodate the needs of both low and high power sources and loads in the same standardized dc distribution system. Furthermore, operational aspects such as *electricity market design* and *protection* are addressed. The challenges in the *transition* to a dc distribution system are covered towards the end. These three emphasized topics are covered in more detail by the following chapters as illustrated in Figure 1.1.

Chapter 3: Optimal Power Flow for Unbalanced Bipolar DC Distribution Grids derives the exact optimal power flow for bipolar dc distribution grids that could be used for electricity market design. It addresses the second research question. The exact optimal

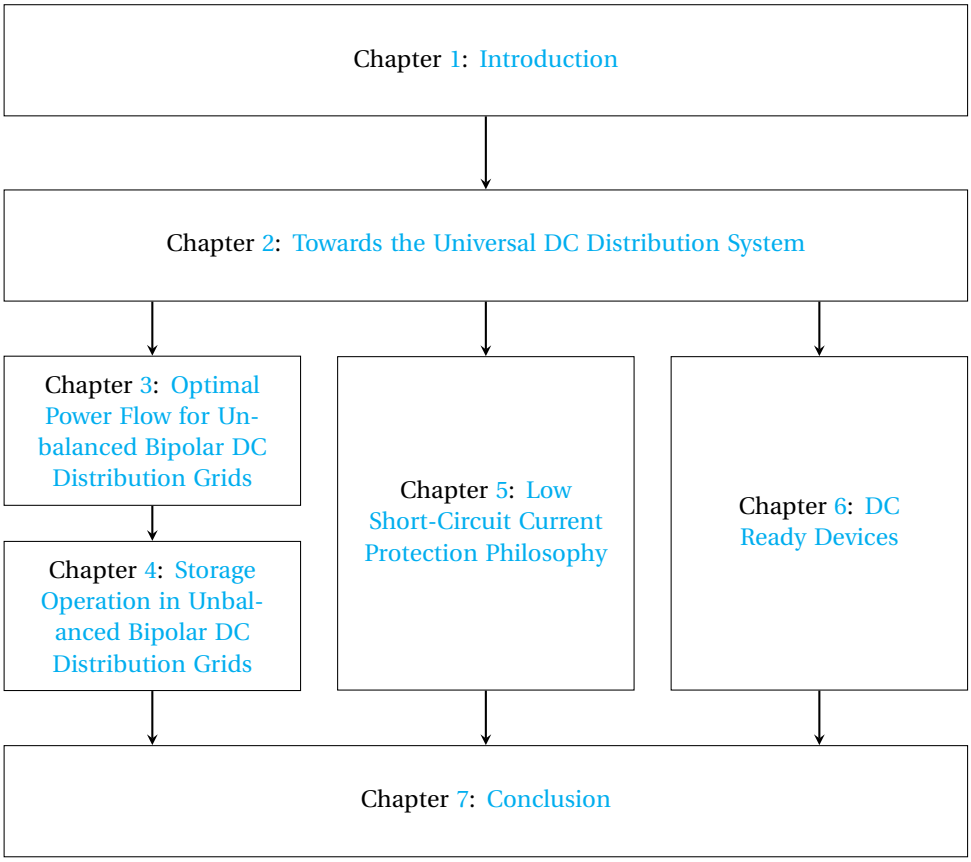

Figure 1.1: Visualization of the outline of this dissertation and its chapters. Chapters 2 covers the overall system, from which three selected topics are covered in more detail. Chapters 3 and 4 build up on each other.

power flow will be formulated in terms of current and voltage and includes current limits for lines and converters instead of only power limits.

Additionally, the third research question is addressed by deriving a general way of obtaining locational marginal prices between any two connection points in a bipolar dc distribution grid. This can include pole-to-pole and pole-to-neutral connections.

Chapter 4: Storage Operation in Unbalanced Bipolar DC Distribution Grids extends Chapter 3 to multiple time periods. In this way the fourth research question can be addressed by modeling the energy storage system equations behind a grid interface. The effect on the locational marginal prices is shown in several examples. Further, variable time periods are used to reduce the computational effort.

Chapter 5: Low Short-Circuit Current Protection Philosophy for DC Distribution Grids addresses the fifth research question. Based on the architecture and modularity derived in Chapter 2, the challenges of using traditional protection strategies are elaborated. Solid-state protection is identified as the suitable method for dc distribution grids. In or-

der to not destroy solid-state circuit breakers by high currents, a low short-circuit current protection philosophy is formulated. The challenges of the necessary fast fault clearance regarding fault detection, discrimination, and selectivity are addressed. Moreover, a classification of protection zones by risk is proposed. The chapter is concluded with measurement results from an operational street lighting system and an experimental solid-state circuit breaker using current derivative for fault detection.

Chapter 6: DC Ready Devices – Is Redimensioning of the Rectification Components Necessary? introduces dc ready devices and analyses the losses in the rectifying components. DC ready devices could simplify a transition towards dc distribution grids as described in Chapter 2. In this chapter, the sixth research question is addressed.

Chapter 7: Conclusions draws the conclusions of the overall dissertation. Every research question is readdressed and it is shown how they were answered in the individual chapters / publications.

2

TOWARDS THE UNIVERSAL DC DISTRIBUTION SYSTEM

Due to an increasing number of power generation units and load devices operating with direct current (dc) at distribution level, there is a potential benefit of leading efforts towards building a dc distribution system. However, the implementation of dc distribution systems faces important challenges, including the market inertia of ac systems and standardization. Many of the benefits that are attributed to dc can only be realized if a complete dc system is developed, and not if only a few components are replaced. This chapter presents the concept of a universal dc distribution system.The universal dc distribution system could be implemented in various use cases, but could also completely replace ac distribution grids. The chapter covers the possibilities of having dc nanogrids inside buildings, dc microgrids in neighbourhoods, and the connection to ac and dc medium voltage grids. Furthermore, considerations regarding flexibility, electricity market design, control and protection are presented.

This chapter is based on L. Mackay, N. H. van der Blij, L. Ramirez-Elizondo, and P. Bauer, "Toward the Universal DC Distribution System," Taylor and Francis, Electric Power Components and Systems, 2017.

2.1. INTRODUCTION

The electrical power system is significantly changing in order to cope with the increasing participation of various distributed energy resources. These changes are required to ensure the reliability, efficiency, power quality, protection, and cost effectiveness of the system. This presents a good opportunity to reflect about the overall system and reconsider certain design choices.

AC is nowadays the standard for transmission and distribution grids. The dominance of ac was facilitated by the ease of transforming ac electrical energy to different voltage levels through the ac transformer, needed for efficient transportation over long distances [1, 2]. However, the advances in power electronics nowadays allow for an equally simple transformation of dc voltages.

Currently, the employment of dc is growing at various voltage levels in the power system. The adoption of HVDC lines for the transport of electrical energy over long distances is one example. The advantages of HVDC over HVAC are reported to be low cost, decreased losses, and absence of restrictions on long distance cables [3].

At device level dc is also having a comeback. The high switching frequencies of dc/dc converters result in smaller passive components and consequently a reduction in size, weight, and cost. In systems where previously an ac transformer was used to step down the voltage before it was rectified, rectification is now be immediately applied. Moreover, dc is being adopted for an ever increasing amount of applications including data centers, telecommunication, buildings and ships. The benefits of adopting dc in, for example, data centers includes improved efficiency, lower capital cost, increased reliability, and improved power quality [4].

Due to the increasing number of dc applications, it becomes potentially beneficial to build the distribution system on dc instead of ac. In literature, dc is seen to have several advantages over ac in terms of transmission, efficiency, converters, and control [5]. However, the broad application of dc distribution systems still faces challenges including the market inertia of ac systems and the lack of standardization. A comparison of ac and dc will not be covered in this chapter, since the full benefits of dc over ac can only be quantified once a complete dc system is developed.

The lack of a general standard has lead to diverse architectures and operations of dc distribution systems. Most literature focuses on local dc grids in buildings [6], e.g. for lighting applications and data centers [7]. Many of the design choices have been made for specific applications, without taking the potential advantages of having a complete low voltage dc distribution system into account. Furthermore, local generation and storage is often assumed [8], while sharing of resources and the location of renewable sources is neglected.

Most of the work on dc distribution grids assumes that converters are installed at each household, which connect the local dc or ac nanogrids [9–11]. These converters provide a convenient separation and could also be used for protection purposes [10]. However, since these converters need to be rated for peak power they are generally expensive. By taking an integral view on the overall distribution system, these disadvantages could be avoided by removing the converters at each household. However, more complex interactions and interdependencies, e.g. in control and protection, have to be dealt with.

This chapter contributes to the discussion towards a universal dc distribution system that could be generally applied to various use cases. An integral view is taken on the larger distribution system, and the challenges and opportunities that can be found in system interdependencies are highlighted. For example, standardization, meshed distribution grids, modular voltage levels, flexibility, market design, control and protection are discussed. It does not only consider near future applications of local dc nanogrids, but aims at a universal system with the capability of completely replacing low voltage ac distribution grids in a longer term. This includes tackling the challenges introduced by intermittent renewable energy sources. It is a continuation of two previous papers in which the opportunities and challenges of dc distribution systems were presented [12, 13].

The remainder of this chapter is organized as follows: in Section 2.2, important elements of the future power system are discussed. The envisioned architecture of the universal dc distribution system is described in Section 2.3. Section 2.4 introduces the operational aspects of this system. Subsequently, possible steps toward the introduction of the universal dc distribution system are discussed in Section 2.5. Ultimately, conclusions are drawn in Section 2.6.

2.2. FUTURE POWER SYSTEM

To enable the broad adoption of dc distribution grids, economics of scale should be achieved. A universal dc distribution system that meets future requirements should be envisioned, so that economics of scale can be realized earlier. In this section possible future use cases are discussed, to be later covered in the envisioned system. This is important in order to prevent over-optimization for specific near-future applications, which could lead to drawbacks for a more widespread adoption.

2.2.1. CENTRALIZED GENERATION

The share of renewable energy generation in the electrical energy production is rising in many countries. Therefore, the future power system should be able to cope with 100% renewable energy supply. It is often assumed that renewable energy is inherently decentralized, however this is not necessarily true.

Traditionally distribution systems are built in a centralized fashion. Future distribution systems may still contain centralized power generation, for example in cases where conventional power plants are replaced by large-scale renewable generation plants. An important difference is that the location of the centralized generation sites will not likely be determined by the consumption centers anymore, but by the location of renewable resources.

For example, wind farms can be built at sea to exploit the higher average wind speeds. Large scale solar thermal power plants can be located in deserts to exploit the higher solar radiation. Hydro power plants are likely placed in mountain regions where also large-scale hydro-storage can be realized. Just like in the case of conventional power plants, large-scale renewable generation plants also need appropriate transmission systems since consumption and generation are often far apart. HVDC will play an important role in making this possible. Furthermore, a MV grid and a LV distribution grid are

required in order to bring the power to the customers.

2.2.2. DISTRIBUTED ENERGY RESOURCES

In this chapter the term distributed energy resources is used to refer to distributed forms of generation, storage, and controllable loads. Distributed renewable sources introduce intermittency to the distribution grid due to varying availability of sun and wind. Distributed storage and controllable loads could provide flexibility to cope with this intermittency.

Currently many new small-scale (renewable) energy sources are distributed in the low voltage grid. Examples of these small-scale sources include rooftop photovoltaic systems, and small-scale wind and hydro plants, but could also include diesel generators. Moreover, many new applications such as electric vehicles have built-in storage capacity that could be utilized to benefit the grid. Likewise, the flexibility in loads such as heat-pumps can do indirect energy storage by shifting the load to a more convenient time.

It is important to note that most of these resources are owned by consumers. A prosumer market model would allow to model the role of consumers and producers of energy in a more abstract way. Consequently, this could enable a more economical utilization of these resources for both the prosumers and the overall distribution system. [14]

2.2.3. NANO- AND MICROGRIDS

The reliability of a (centralized) power system is unlikely to increase when the system becomes more complex by the addition of distributed resources. However, distributed energy resources enable the isolated operation of parts of the grid in case of outages at a higher level. Therefore, it would be beneficial for the future distribution grid to consist of interconnected microgrids. In this case the grid could sustain operation if parts of the grid fail.

In these isolated systems, demand response is likely to play an important role, as supply could be limited due to weather conditions. Storage and (conventional) backup supply could be installed in important locations, however in many countries this is financially not viable.

2.2.4. OFF-GRID SYSTEMS

With the increasing participation of distributed energy resources we can ask ourselves if the grid is actually needed. Independent distribution grids are often envisioned as an inevitable destination. Off-grid systems can be more economical for remote locations, where the cost of interconnection exceeds the cost of additional storage and/or energy generation.

However, in more densely populated areas, the advantages of sharing resources outweigh the additional cost due to the low cost of interconnection and the high utilization factor. Moreover, it is unlikely that everyone will use high power loads at the same time. Additionally, weather conditions can make it expensive to cover 100% of the demand by local renewable energy and storage, as it is unlikely that load peaks will coincide with the peaks in supply.

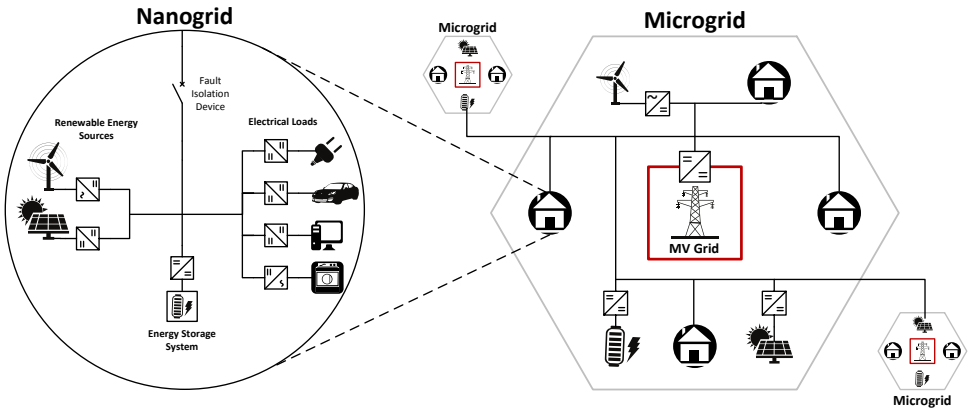

Figure 2.1: On the right: a dc microgrid connecting a neighbourhood with multiple dc nanogrids inside buildings and some larger distributed energy resources. It can be connected to other dc microgrids on the same voltage levels and/or to the medium voltage grid at the substation depicted in the center. On the left: a dc nanogrid inside a building with various energy resources is shown in detail. A fault isolation device can separate it from the microgrid.

2.2.5. STANDARDIZATION

Economics of scale are very important in order to realize reduced cost and consequently to encourage a broad adoption of dc distribution grids. It is therefore important to arrive at a standardized system that can be used for various applications.

2.3. THE UNIVERSAL DC DISTRIBUTION SYSTEM

The envisioned standardized dc distribution system should be universal in a sense of being appropriate for various applications, conditions and sizes as described in the previous section. In order to show the full potential and the affiliated considerations, a complete dc distribution grid architecture, that could be built in cities, is described in this section. However, for specific or initial applications it is possible to implement only certain parts.

2.3.1. MODULAR DC DISTRIBUTION GRID ARCHITECTURE

The dc distribution grid architecture should consist of several subsystems that can be connected together. Moreover, it is not necessary that the complete grid is built on dc, any part on any level in the grid could be ac and connected to the dc grid via an ac/dc converter. Especially during a transition to a full dc distribution grid.

DC NANOGRID

The grid inside buildings (or on private property) could be operated independently from the main grid in islanding mode if distributed energy resources exist. In order to enable the utilization of this energy supply potential in case of faults in the distribution grid, it could be beneficial if this part of the grid would be able to operate independently as a nanogrid. Nanogrids can be owned and controlled by independent entities. They can be connected to the dc distribution grid by a smart meter and a protection device, or

to an ac distribution grid by an ac/dc converter. An example of such a nanogrid and its connection is shown in Fig. 2.1 on the left. A typical power rating of a nanogrid could be 10 kW.

Inside the nanogrid, extra low voltage subsystems could be implemented. Typical voltages for these systems are 48 V, 24 V or 12 V [15]. They could, for example, be used for low power LED lighting, or for connecting loads by USB Type-C connector and USB Power Delivery [16]. These are not in the scope of this chapter as their design does not directly affect the distribution grid, because they always need to be galvanically isolated by a full power converter.

DC MICROGRID

In order to allow the sharing of distributed energy resources between nanogrids (neighbours) in a resilient way, even if higher level grids fail, dc microgrids should connect a neighbourhood. The size of these microgrids could be, for example, one street block, one low-voltage feeder or the low voltage distribution grid under one substation (e.g., 500 kVA) of today's 400 V ac grids.

Such a dc microgrid could have a connection to higher level grids but could also directly connect to neighbouring dc microgrids as shown in Fig. 2.1 on the right. As such, the low voltage grid is built out of interconnected microgrids [17] and could be extended to a large grid, connecting a whole city. These dc microgrids should be able to operate independently and therefore protection devices should separate them. In order to allow economic dispatch, even in islanded operation, local electricity markets could be implemented on this level. Also the power flow and congestion should be controlled.

MEDIUM VOLTAGE GRID

Fig. 2.2 shows an example of a medium voltage and a high voltage grid overlaying the connected dc microgrids. The medium voltage grid can be implemented in dc and could connect large scale energy resources such as onshore windfarms. These grids could also be implemented in ac with a modular ac/dc converter at the substation connecting it to the low voltage dc grid, allowing for high partial load efficiency [18]. A connection to a medium voltage grid is optional and may not be implemented for remote locations. Microgrids could only connect to neighbouring microgrids, which may or may not be connected to the medium voltage grid, or operate fully independently.

2.3.2. MESHED DC DISTRIBUTION GRIDS

Nowadays ac distribution grids are often operated in a radial structure as this has advantages in protection and power flow control. Grids in densely populated areas are often constructed in a meshed architecture, but the meshes are not closed in order to keep the operation radial. This allows for more flexibility in, for example, maintenance and repair.

With the increased utilization of the grid infrastructure due to electrical vehicles, heat pumps and solar panels, it would be preferable to take advantage of available meshed connections [19]. In dc distribution grids, dc/dc or ac/dc converters take the role of traditional ac transformers. These power electronic converters cannot be overloaded for extended periods of time, like ac transformers can be. Meshing the low voltage grid

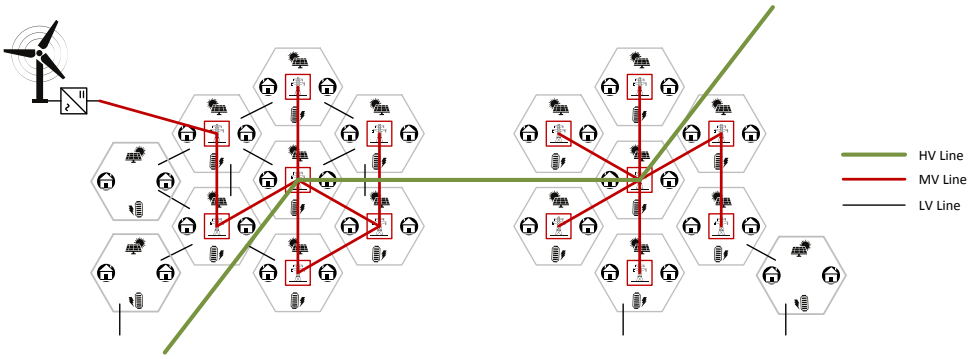

Figure 2.2: An overview of a distribution area with multiple dc microgrids that are directly connected (black) to each other forming some meshes. On top of that, a medium voltage dc grid (red) connecting most of these microgrids at substations. Furthermore, a high voltage transmission system is depicted in green.

can allow for the utilization of a neighbouring substation in case of congestion at one converter.

It has to be ensured that the power flow does not exceed the line limits for extended time periods. Power flow control converters, that impose voltages in series with lines, can be added to influence the power flow. In this way the infrastructure can be better utilized if this is necessary, however, they increase control complexity and cost and can decrease reliability. Power flow control converters are built using partial power converters to enhance efficiency and reduce cost. However, therefore they do not provide galvanic isolation because a major part of the power is directly transferred from one side to the other. Large galvanically connected low voltage grids could emerge which have to be taken into account for power flow control and protection. Ensuring line limits can be done in a decentralized way without communication [19].

2.3.3. NO CONVERTERS AT THE NANOGRID'S INTERFACE

Low voltage dc grids have emerged from applications such as lighting and data centers. From this perspective it is normally assumed that dc nanogrids are interfaced with ac grids by a central ac/dc converter [20]. In literature, dc distribution grids are considered to have dc/ac inverters for each costumer, allowing the usage of legacy ac devices [9, 21].

When combining these two approaches one would naturally end up with a dc/dc converter at the entrance of every house [11]. The advantage of this system architecture is that the nano- and microgrid systems are electrically separated. Consequently, the control and protection of this system is easier as only well defined parts of the subsystem have to be taken into consideration.

However, when considering a universal dc distribution grid, that can be used for all use cases, this solution is, in general, suboptimal. This is best illustrated with an example of two neighbouring buildings. The first buildings has solar panels while the other has storage facilities. During the day when little of the power is used, the solar power from the first building is stored in the second building's storage. Later, when demand is highest, the stored electrical energy is (partially) transferred back to the first building.

Consequently, the two extra converters at the interfaces of the two nanogrids with the microgrid introduce 4 additional conversion steps, significantly decreasing efficiency.

Another problem with a converter at the nanogrids interface is that these converters would need to be designed for the peak demand of the nanogrid, which is expensive. Consequently, this converter will have a low utilization factor as the average demand is significantly lower. Most of the time these converters would operate at partial load condition with poor efficiency, as modular converters might not be economically feasible at these power levels due to the overhead of modularity. If the converters at the interface are replaced with a combined converter at a substation, it could be designed with a much lower rating than the sum of each nanogrid's peak demand. In ac grids, substation transformers are commonly designed for 10-20% of the total connected peak demand. Furthermore, since the power from distributed sources can take a direct path to the demand inside the microgrid, converter power capacity can further be reduced.

To summarize, removing the converters at the interface between nanogrids and the microgrid can reduce investment cost significantly. Nevertheless, in remote locations with long distances between nanogrids or for dc nanogrids connected to ac distribution grids a converter at the interfaces could still be favorable.

2.3.4. MODULAR BIPOLAR VOLTAGE LEVELS

One of the challenges in low voltage dc is to standardize the voltage levels. Extra low voltage levels are often seen in dc nanogrids, such as 24 V proposed by EMerge Alliance [7], 48 V in the telecommunication industry [22], or the 20 V of the USB Power Delivery Standard [16]. They are, however, not suitable for a distribution grid with higher power and longer distances as they would result in high losses or thick and expensive cables.

It is expected that the standardization of input voltage levels for generic devices will converge to a value between 350 V and 400 V. These voltage levels are also widely used in the dc links of ac power supplies today. Therefore, these voltage levels would allow easy implementation of dc ready devices [23].

Most of the low voltage dc literature focuses on these local dc grids and does not consider the expansion to a complete dc distribution grid. EMerge Alliance proposes to use midpoint grounding, effectively making ±190 V out of the 380 V [7]. This can be applied to isolated local dc grids, such as today's data centers.

When it comes to transporting power over longer distances, higher system voltages are necessary. Using true bipolar systems where devices with their defined input voltage are connected pole-to-neutral instead of pole-to-pole could half the line losses for balanced systems while copper could be reduced. Device interfaces should then be made such that they can be connected to a midpoint grounded system ground but also between a pole and the neutral. Bigger devices, that today are connected to three phase ac, could then be connected directly between a positive and a negative pole.

Fig. 2.3 shows an example of a modular bipolar system of ±350 V, as proposed by Direct Current B.V. [24]. A ±700 V grid could then be made for applications where a lot of large loads are to be connected. With a margin for overvoltage droop regulation considered, this voltage stays under 1500 V low voltage limit imposed by the IEC. However, also ±375 V and ±750 V have recently been discussed and might be a good compromise [15]. Regardless of the chosen nominal voltage levels, there is always an operation

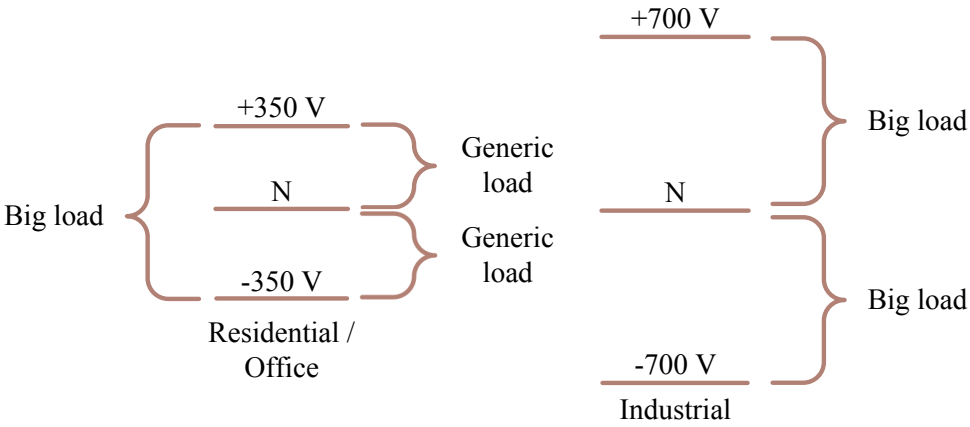

Figure 2.3: Modular bipolar voltage levels can be implemented for industrial applications with ±700 V and for residential applications with ±350 V. Small appliances connect to 350 V while large appliances connect to 700 V by connecting to both poles. Isolation consideration have to be made for 700 V devices.

range around the chosen values that has to be specified. Modular voltage levels, if used from the beginning, would allow for the scaling of the system and increase compatibility with systems of different sizes.

In these bipolar systems it can be, in some cases, beneficial to remove the neutral conductor. This might be relevant when refurbishing 4-cable 3-phase ac cables where then two conductors could be used for each pole. However, if the neutral is removed the currents flowing in both (independent) poles must be balanced. This can be done by means of a balancing converter shifting power between the two poles or by balancing local supply and demand on both poles (by using distributed energy resources or demand response).

2.4. OPERATIONAL ASPECTS

The standardization of a new systems gives the unique opportunity to incorporate features that may be desirable in the future. Trade-offs will have to be made as optimal solutions for some applications may cause problems for other applications. This section highlights some of these aspects.

A key challenge in the operation of the universal dc distribution system is that the size and composition of different systems can vary. Moreover, the size and composition of a distribution grid could also vary over time due to grid extension, faults, or maintenance reasons. For example, microgrids and nanogrids should be able to island themselves and continue operation when other parts of the grid experience difficulties. After the problems have been resolved, the microgrids should reconnect (de-island) to reestablish the sharing of resources. Furthermore, the nanogrids should independently be able to black start to facilitate the usage of available energy sources as soon as they are available after a grid collapses.

2.4.1. ENABLE FLEXIBILITY

To facilitate operation when supply is scarce, enabling flexibility in demand and supply is crucial [25]. This will be more common as intermittent renewable sources are introduced.

Load shedding can be used as a last resort to prevent the collapse of the system. In dc grids load shedding can be done based on the local voltage, which is a direct indicator of the system's power balance [26]. The voltage thresholds, at which load shedding occurs, should be standardized and incorporated into all devices. Priority of loads can be realized by employing different voltage thresholds for different types of loads. In order to increase system stability loads should ramp down proportionally to the voltage if possible (e.g. lighting) [27]. It is important to note that this will prevent a grid outage in cases where nowadays ac grids would already be blacked out, increasing user satisfaction.

The increasing flexibility in appliances such as electric vehicles can, if enabled, reduce infrastructure investments significantly. While the overall system benefits can be high, individual benefits are often so small that this certainly has to be automated and no user interaction should be required. In case of demand response the users should be able to actively increase the importance in order to override automatic action at any given time.

The smaller the devices get the worse the trade-off is in implementing these features. Therefore, a good balance has to be found. Local economical demand response could be achieved by combining a smart meter with a power flow controller. In this case the smart meter, which is connected to the market, could accomplish economical load shedding by reducing the voltage inside the nanogrid (triggering load shedding). Such a system could be interesting in, for example, developing countries when a cost limit should be achieved.

2.4.2. ELECTRICITY MARKET DESIGN

Electricity market design is important to stimulate the utilization of distributed resources [14]. Until now this has often been regarded as an independent topic on top of the technical aspects and independent of ac or dc. However, better utilization of the infrastructure could be realized if the market is seen as part of the (optimal) control system.

Prosumer market models in which each participant is equally able to consume and produce power seem to be the proper answer for emerging distributed resources as they do not penalize the storage of energy [14, 27]. Furthermore, grid fee and electricity fee should be explicitly separated to allow for economic dispatch based on marginal cost in an energy only based market. The grid fee, which is used to cover infrastructure investment and maintenance, can still depend on the rating of the connection to the grid.

Dynamic prices in an energy market could enable the utilization of distributed demand and storage flexibility. The faster the dynamic prices are updated the less reserve power is needed. However, as a consequence the cost and complexity of communication and clearing may rise, and thus a balance has to be found. The market model should incorporate price forecasts to allow adequate utilization of resources (such as load shifting and/or storage).

Increases in installed power by, for example, PV or electric vehicles are expected to lead to congestion in the low voltage grids and this should be taken into account when

building dc grids. Also in dc distribution grids the stricter limit of ac/dc and dc/dc converters may lead more easily to congestion than ac transformers (which can be overloaded for some time). Therefore, the market model should manage congestion by, for example, dynamic nodal pricing [25] using exact optimal power flow calculations [28]. Cost functions of demand need to be assumed in order to incorporate demand response. Exact optimal power flow in bipolar grid can lead to nodal or local marginal prices that depend on the pole of connection when only individual poles are congested due to unbalance. Losses of converters, lines, and power flow control converters (that modify the power flow) should also be included [28].

Market clearing should be implemented in a (partially) distributed way in order to allow independent operation of microgrids, but also to reduce complexity and communication needs [29, 30]. Microgrids could act as an aggregator of the information that is shared with connected microgrids and higher level grids in order to converge towards a more globally optimal operation. While centralized optimization can (in theory) always outperform or be equivalent to distributed control (because it could implement the same actions as distributed agents), in practice the problem complexity, communication effort and resilience speak in favor of suboptimal distributed solutions.

Preliminary work indicates that for dc new solutions for distributed market clearing might be possible. This could include “physical market clearing”, where price information is broad-casted and market participants act directly (only giving physical feedback). Moreover, local measurements might be taken into account for distributed real-time optimization iterations.

2.4.3. CONTROL

A large amount of research has been done on the control of dc microgrids [31]. Often, full knowledge of the system components and parameters is assumed, which should not be a requirement for the universal dc distribution system. Rules for the control should be developed and standardized that allow reconfiguration of the system and enable economics of scale.

In normal operation, optimization could be done by the real-time market. The control should be implemented in a hierarchical way such that lower parts can continue operation even if communication is lost, increasing resilience of the system. Therefore, not only set points should be defined, but the current-voltage (IV) characteristics should be defined for the full operation range of the converters. In Fig. 2.4 an example of such an operation range is shown for a storage system. It can include current limits, power limits, droop control for the operation of parallel sources, and optionally a deadband where the converter is off. Ideally these parameters can be modified based on the market clearing or environment.

Moreover, the rules should consider the behavior and development of power electronics towards higher switching frequencies and smaller passive components. The low inertia of dc distribution grids results in strict requirements on the control system [32]. It should be noted that low inertia grids are also a problem for future ac grids. Constant power loads complicate this challenge due to their negative impedance. Possible solutions could be standardized control bandwidths and converter ramp rates to ensure system stability. Slower behavior of loads on the grid side results in better stability, but

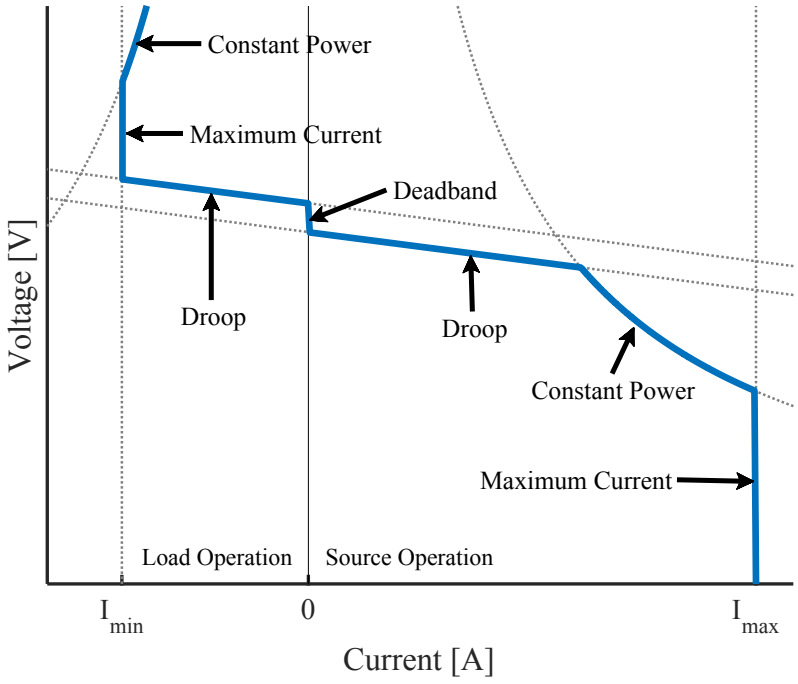

Figure 2.4: Possible current-voltage characteristic for the local control of a storage converter. In general current limits, power limits and droop rates should be defined if it is desired to increase the resilience of the system.

as a trade-off intermediate storage is needed for devices that need fast power changes.

For long line lengths active damping could be necessary and limits may have to be defined. Disconnection and connection events of microgrids, especially in case of faults, should be given considerable attention in the design of the control guidelines.

2.4.4. PROTECTION

The protection of dc grids is considered as one of the biggest challenges in the field and it is getting more and more attention [33]. Unlike in ac systems, the current has no zero crossing that extinguishes arcs, resulting in high fault currents in dc systems. Moreover, series arcing can be an issue when high power loads are unplugged. Special plugs with leading pins is one of the possible solutions, but also selective load side arc detection could be implemented [34]. Furthermore, coordination with frequency based backup protection would need to be standardized.

Traditional protection schemes in the low voltage grid rely on high short circuit currents, a radial system, and unidirectional power flow for selectivity. However, since these three elements are not necessarily present in dc distribution systems new short circuit protection strategies need to be developed.

Advances in power electronics have lead to a reduction of capacitor size and conse-

quently their contribution to short-circuit currents. It should be noted that freewheeling diodes of converters (e.g. ac/dc) can lead to additional short circuit current in case of protection failure. Oversizing the converters is sometimes employed for ac systems [35] and could be considered for dc but is an expensive solution. Also, a small nanogrid in islanded operation might not be able to produce high enough short-circuit currents, even with oversized converters. Since high fault currents are not inherently desirable, a new low short-circuit current protection philosophy is favorable [36].

Low short-circuit currents allow for solid state breakers to be used, which enables fast fault clearing and avoids arcing. Fast selectivity in meshed grids with bidirectional power flow is therefore essential and an important research challenge. Current limiting inductors that limit the rate of change of the current need to be used. The significant impact of these limiting inductors on the control system which needs to be taken into account. Inrush currents and ramp rates must be specified in order to allow fast fault discrimination. [36]

Grounding is another important topic to be taken into consideration since dc can cause corrosion if it flows trough metallic structures in the environment for an extended period [33]. High impedance grounding schemes have often been used in dc microgrids (e.g. data centers), since it allows to sustain operation during a single ground fault. However, selectivity is not possible because only the voltage change is detected but no fault current is flowing to the fault. As selectivity is important in larger systems, this is not feasible for dc distribution grids. Solid grounding in one point allows for selective protection for residual ground currents, however if there are multiple grounding points, ground currents would flow. Multiple grounding points would be needed in order to be able to island individual nanogrids. The development of advanced grounding schemes is therefore fundamental. Preliminary research indicates that capacitive grounding could be an interesting alternative since it provides low impedance for fault transients and blocks dc currents.

2.5. HOW TO GET THERE?

This chapter discusses many technological challenges of the universal dc distribution grid. However, the biggest challenge for the adoption of universal dc distribution grids is the market inertia of ac systems. Even if there are technological and economical benefits it is challenging to select dc systems over the well-established proved ac systems. Therefore, this section discusses possible paths for the adoption of the universal dc distribution grid.

There are several technologies that are in development or already available that could benefit the adoption of dc distribution grids. Firstly, a important development is the introduction of USB Type-C and USB Power Delivery, which allows up to 100 W (5 A at 20 V) to be transferred [16]. Therefore, USB Type-C could be used to provide power to most consumer electronic devices, even those that traditionally are connected to the ac grid. It is expected that in the near future many types of low power devices will be available with USB Power Delivery. As a result, fewer devices would be directly connected to the ac power system. This means that all these devices could be connected to a dc distribution grid by means of a USB wall socket, thus simplifying a transition.

Secondly, dc ready devices that can work on both ac and dc, could allow for eco-

nomics of scale for higher power appliances. DC ready devices are not significantly more expensive than ac only devices and enable the flexibility of choosing between ac and dc [23].

Currently, dc systems are mostly used for specific (industrial) applications such as telecommunication and data centers. In the near future it is expected that the number of these industrial applications of dc systems further increases due to the scale of the applications. Some examples are LED street lighting, greenhouse lighting, motors with speed control, and shipboard power systems.

Upcoming is the application of dc distribution systems for commercial buildings. Commercial buildings adopt early as the benefits of dc outweigh the engineering effort at this larger scale. For example, LED lighting combined with USB Power Delivery and PV interconnected on dc can be an early business case for office buildings.

Once a market is established from industrial applications and commercial buildings, economics of scale are applied. As a result more dc devices will become available and the cost of these devices will decrease. At this point residential dc houses could become feasible. Most of the higher power appliances (such as heat pumps, washing machines, cooking facilities and lighting) are fixed inside the building. Consequently, residential dc appliances could be installed during construction by the housing corporations (even if the supply is still limited).

A subsequent opportunity would present itself when in neighbourhoods the majority of buildings operate on dc. In this case, using a dc distribution grid to connect these buildings would be beneficial. Moreover, in some cases parallel street lighting systems could be switched to dc and offer an alternative connection.

It is likely that ac and dc grids will co-exist at some locations for a transition period because of market development. However in long term, these hybrid systems will not produce a benefit, as virtually all appliances connected to the voltage grid use a dc bus inside or could be designed with lower or comparable cost for dc.

When thinking about future dc distribution grids one must realize that the transition is challenging. DC will only become a real alternative to ac once a market for dc devices is established. When working infrastructure exists, the benefits of dc are unlikely to outweigh the cost of replacing a working system. However, opportunities in these systems present themselves when line capacity has to be expanded or if changes have to be made anyway to the existing system. When new infrastructure is built, a true choice exists. This would be for example the case in not-electrified areas in developing countries, which could be built completely on dc, once a standard and market is established.

2.6. CONCLUSION

In this chapter considerations for a universal dc distribution system that is capable of completely replacing nowadays ac distribution grids have been presented. Starting from the need for economics of scale, the various use cases of the power system in the future and desired system properties were discussed. The universal dc distribution system was described as a system that can come in many different forms. Starting from dc nanogrids inside buildings and dc microgrids in neighbourhoods to the connection to ac and dc medium voltage grids, and with that to higher voltage systems. The advantages and challenges of meshed dc distribution grids were discussed.

One important aspect is that full power converters should not separate nano- and microgrids at building entrances. In this way the voltage levels inside buildings and in the street will be equal. Furthermore, bipolar grids with modular voltage levels can satisfy the different power needs.

Operational aspects of the envisioned system were briefly discussed including flexibility, market design, control and protection. Moreover, the challenging transition to the universal dc distribution system was discussed with USB Type-C connector and USB Power Delivery as important enablers for the millions of small devices.

In conclusion, this chapter encourages to look at the big picture and longer term future applications of low voltage dc. Only considering near future applications and business cases lead to (de-facto) standards that are suboptimal for a widespread adoption of dc. These standards would complicate the large scale utilization and rollout of dc distribution systems. The ongoing standardization efforts pose a unique opportunity to do it right in the first place and create a system that can cope with most future challenges to come and the various use cases in the different regions of this planet.

REFERENCES

[1] J. W. Coltman, "The transformer [historical overview]," *IEEE Industry Applications Magazine*, vol. 8, no. 1, pp. 8–15, Jan 2002.

[2] T. McNichol, *AC/DC: The Savage Tale of the First Standards War*. Wiley, 2006.

[3] M. P. Bahrman, "Hvdc transmission overview," in *2008 IEEE/PES Transmission and Distribution Conference and Exposition*, April 2008, pp. 1–7.

[4] G. AlLee and W. Tschudi, "Edison redux: 380 vdc brings reliability and efficiency to sustainable data centers," *IEEE Power and Energy Magazine*, vol. 10, no. 6, pp. 50–59, Nov 2012.

[5] D. M. Larruskain, I. Zamora, O. Abarrategui, and Z. Aginako, "Conversion of AC distribution lines into DC lines to upgrade transmission capacity," *Electric Power Systems Research*, vol. 81, no. 7, pp. 1341 – 1348, 2011.

[6] R. Weiss, L. Ott, and U. Boeke, "Energy efficient low-voltage DC-grids for commercial buildings," in *2015 IEEE First International Conference on DC Microgrids (ICDCM)*. IEEE, jun 2015, pp. 154–158. [Online]. Available: http://ieeexplore.ieee.org/document/7152030/

[7] EMerge Alliance, "Occupied Space Standard, Data/Telecom Center Standard."

[8] R. Singh and K. Shenai, "DC microgrids and the virtues of local electricity," *IEEE Spectrum*, vol. 6, 2014.

[9] P. Salonen, T. Kaipia, P. Nuutinen, P. Peltoniemi, and J. Partanen, "An LVDC distribution system concept," in *NORPIE/2008, Nordic Workshop on Power and Industrial Electronics*, 2008.

[10] D. Boroyevich, I. Cvetkovic, D. Dong, R. Burgos, F. Wang, and F. Lee, "Future electronic power distribution systems - A contemplative view," in *Proceedings of the International Conference on Optimisation of Electrical and Electronic Equipment, OPTIM*, 2010, pp. 1369–1380.

[11] A. Werth, N. Kitamura, and K. Tanaka, "Conceptual Study for Open Energy Systems: Distributed Energy Network Using Interconnected DC Nanogrids," *IEEE Transactions on Smart Grid*, vol. 6, no. 4, pp. 1–1, 2015. [Online]. Available: http://ieeexplore.ieee.org/lpdocs/epic03/wrapper.htm?arnumber=7070698

[12] L. Mackay, T. G. Hailu, G. R. Chandra Mouli, L. Ramirez-Elizondo, J. A. Ferreira, and P. Bauer, "From DC Nano- and Microgrids Towards the Universal DC Distribution System – A Plea to Think Further Into the Future," in *PES General Meeting*. IEEE, 2015.

[13] L. Mackay, T. Hailu, L. Ramirez-Elizondo, and P. Bauer, "Towards a DC Distribution System – Opportunities and Challenges," in *DC Microgrids, IEEE First International Conference on*, 2015.

[14] Y. Parag and B. K. Sovacool, "Electricity market design for the prosumer era," *Nature Energy*, vol. 1, no. 4, p. 16032, 2016. [Online]. Available: http://www.nature.com/articles/nenergy201632

[15] E. Rodriguez-Diaz, F. Chen, J. C. Vasquez, J. M. Guerrero, R. Burgos, and D. Boroyevich, "Voltage-Level Selection of Future Two-Level LVdc Distribution Grids: A Compromise Between Grid Compatibiliy, Safety, and Efficiency," *IEEE Electrification Magazine*, vol. 4, no. 2, pp. 20–28, jun 2016.

[16] USB Promoter Group, "Universal Serial Bus Revision 3.1 Specification," 2014. [Online]. Available: http://www.usb.org/developers/docs/

[17] J. M. Guerrero, M. Chandorkar, T.-L. Lee, and P. C. Loh, "Advanced Control Architectures for Intelligent Microgrids—Part I: Decentralized and Hierarchical Control," *IEEE Transactions on Industrial Electronics*, vol. 60, no. 4, pp. 1254–1262, apr 2013.

[18] X. She, A. Q. Huang, S. Lukic, and M. E. Baran, "On Integration of Solid-State Transformer With Zonal DC Microgrid," *IEEE Transactions on Smart Grid*, vol. 3, no. 2, pp. 975–985, jun 2012.

[19] L. Mackay, T. Hailu, L. Ramirez-Elizondo, and P. Bauer, "Decentralized Current Limiting in Meshed DC Distribution Grids," in *DC Microgrids, IEEE First International Conference on*, 2015.

[20] E. Rodriguez-Diaz, M. Savaghebi, J. C. Vasquez, and J. M. Guerrero, "An overview of low voltage DC distribution systems for residential applications," in *2015 IEEE 5th International Conference on Consumer Electronics - Berlin (ICCE-Berlin)*. IEEE, sep 2015, pp. 318–322.

[21] P. Nuutinen, T. Kaipia, P. Peltoniemi, a. Lana, a. Pinomaa, a. Mattsson, P. Silventoinen, J. Partanen, J. Lohjala, and M. Matikainen, "Research Site for Low-Voltage Direct Current Distribution in a Utility Network - Structure, Functions, and Operation," *Smart Grid, IEEE Transactions on*, vol. PP, no. 5, p. 1, 2014.

[22] T. Dragicevic, J. C. Vasquez, J. M. Guerrero, and D. Skrlec, "Advanced LVDC Electrical Power Architectures and Microgrids: A step toward a new generation of power distribution networks." *IEEE Electrification Magazine*, vol. 2, no. 1, pp. 54–65, mar 2014.

[23] L. Mackay, L. Ramirez-Elizondo, and P. Bauer, "DC Ready Devices – Is Redimensioning of the Rectification Components Necessary?" in *Mechatronika 2014 - 16th International Conference on Mechatronics*. IEEE, 2014.

[24] H. Stokman, "Direct Current B.V." [Online]. Available: http://www.directcurrent.eu

[25] P. D. Lund, J. Lindgren, J. Mikkola, and J. Salpakari, "Review of energy system flexibility measures to enable high levels of variable renewable electricity," *Renewable and Sustainable Energy Reviews*, vol. 45, pp. 785–807, 2015.

[26] L. Mackay, P. Kolios, L. Ramirez-Elizondo, and P. Bauer, "Voltage Dependent Demand Response with Dynamic Hysteresis Thresholds in DC Microgrids," in *IEEE PowerTech 2015 Conference Eindhoven*, 2015.

[27] L. Mackay, M. Imhof, R. Wiget, and G. Andersson, "Voltage dependent pricing in DC distribution grids," in *IEEE PowerTech 2013 Conference Grenoble*. IEEE, jun 2013.

[28] L. Mackay, A. Dimou, R. Guarnotta, G. Morales-Espania, L. Ramirez-Elizondo, and P. Bauer, "Optimal Power Flow in Bipolar DC Distribution Grids with Asymmetric Loading," in *IEEE Energycon Leuven*, 2016.

[29] A. Kargarian, J. Mohammadi, J. Guo, S. Chakrabarti, M. Barati, G. Hug, S. Kar, and R. Baldick, "Toward Distributed/Decentralized DC Optimal Power Flow Implementation in Future Electric Power Systems," *IEEE Transactions on Smart Grid*, pp. 1–1, 2016. [Online]. Available: http://ieeexplore.ieee.org/document/7581042/

[30] J. Mohammadi, J. Zhang, S. Kar, G. Hug, and J. M. F. Moura, "Multilevel distributed approach for DC Optimal Power Flow," in *2015 IEEE Global Conference on Signal and Information Processing (GlobalSIP)*. IEEE, dec 2015, pp. 1121–1125.

[31] T. Dragicevic, X. Lu, J. Vasquez, and J. Guerrero, "DC Microgrids - Part I: A Review of Control Strategies and Stabilization Techniques," *IEEE Transactions on Power Electronics*, pp. 1–1, 2016.

[32] T. Hailu, L. Mackay, L. Ramirez-Elizondo, J. Gu, and J. A. Ferreira, "Voltage Weak DC Microgrids," in *DC Microgrids, IEEE First International Conference on*, 2015.

[33] T. Dragicevic, X. Lu, J. C. Vasquez, and J. M. Guerrero, "DC Microgrids - Part II: A Review of Power Architectures, Applications, and Standardization Issues," *IEEE Transactions on Power Electronics*, vol. 31, no. 5, pp. 3528–3549, may 2016.

[34] L. Mackay, A. Shekhar, B. Roodenburg, L. Ramirez-Elizondo, and P. Bauer, "Series Arc Extinction in DC Microgrids using Load Side Voltage Drop Detection," in *DC Microgrids, IEEE First International Conference on*. IEEE, 2015.

[35] T. L. Vandoorn, J. C. Vasquez, J. De Kooning, J. M. Guerrero, and L. Vandevelde, "Microgrids: Hierarchical Control and an Overview of the Control and Reserve Management Strategies," *IEEE Industrial Electronics Magazine*, vol. 7, no. 4, pp. 42–55, dec 2013.

[36] L. Mackay, N. Gouvalas, T. Hailu, H. Stokman, L. Ramirez-Elizondo, and P. Bauer, "Low Short Circuit Current Protection Philosophy for DC Distribution Grids".

3

Optimal Power Flow for Unbalanced Bipolar DC Distribution Grids

The emergence of distributed energy resources can lead to congestion in distribution grids. DC distribution grids are becoming more relevant as more sources and loads connected to the low voltage grid use dc. Bipolar dc distribution grids with asymmetric loading can experience partial congestion resulting in a nodal price difference between the two polarities if a respective market model is applied. In order to take into account this price difference, this chapter presents an optimal power flow (OPF) model formulated in terms of voltage and current. In the case of bipolar dc distribution grids, the single line approximation is no longer valid because current can flow in the neutral conductors as well. Moreover, loads and sources can be connected between any two nodes in the network. The proposed exact OPF formulation includes bilinear equations. The locational marginal prices (LMP) are derived by linearizing the problem at the optimal solution. Example cases show the various phenomena that can appear under asymmetric loading, such as pole-to-pole connections combined with pole-to-neutral connections, parallel sources, meshed grids and their effect on the LMP.

This chapter is based on L. Mackay, R. Guarnotta, A. Dimou, G. Morales-Espania, L. Ramirez-Elizondo, and P. Bauer, "Optimal Power Flow for Unbalanced Bipolar DC Distribution Grids," in IEEE Access, 2018

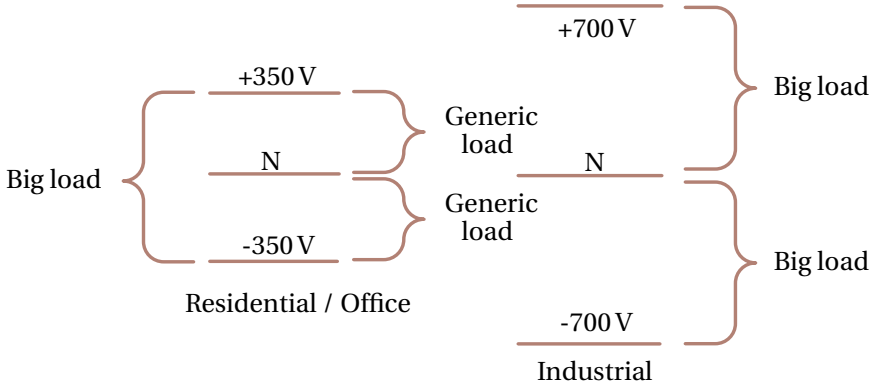

Figure 3.1: Modular bipolar LVdc voltage levels and how devices could be connected [2].

3.1. Introduction

Distribution grids are expected to experience more congestion problems due to the emergence of electrical vehicles, renewable energy sources, and other distributed energy resources. Locational marginal prices (LMP) can enable optimal utilization of distributed energy resources owned by different entities. DC distribution grids have advantages over ac distribution grids due to their inherently higher power transfer capacity, and due to the fact that most loads and sources connected to the low voltage grid nowadays are already dc. In the future, more and more, will be either inherently dc or use a dc link to couple variable rotation speeds [1].

Bipolar dc grids have a neutral conductor in addition to the positive and negative conductor of unipolar dc grids. Their configuration can be compared to that of a 3-phase or 2-phase ac grid. As shown on the left side of Fig. 3.1, small devices (comparable to single phase devices in 400 V ac systems) can be connected between the positive pole and the neutral or between the neutral and the negative pole. Without loss of generality, in this chapter a nominal voltage of ±350 V is assumed [1]. Bigger devices can be connected directly between the positive pole and the negative pole. Therefore, a voltage of 700 V is available to these devices. This voltage is close to the double the peak of 230 V ac which would be the minimum dc voltage after activ rectification of three phase 400 V ac when neutral is connected ($400\,\text{V}/\sqrt{3}\cdot\sqrt{2}\cdot 2 \approx 650\,\text{V}$). The power available on a 700 V dc connection corresponds to the one of a 400 V 3-phase ac connection with same rms current rating I, while using one wire less ($\sqrt{3}\cdot 400\,\text{V}\cdot I = 693\,\text{V}\cdot I \approx 700\,\text{V}\cdot I$). For bigger industrial applications, e.g., photovoltaic power plants, a bipolar 700 V grid can be made as shown on the right side of Fig. 3.1 [2].

Bipolar dc distribution grids offer twice the power transfer capacity (+100 %) of unipolar dc grids, while only one conductor is added (+50 %). The total losses in a balanced system remain the same as does the voltage rating of the small devices. Small devices in

general have galvanic isolation inside or do not refer their potential to ground. Therefore, no increase in component cost is expected. Longer distances could be bridged without a neutral conductor saving additional 33 % of conductor material, if both poles are balanced at each end or a balancing converter that shifting power between polarities is added to do so. This balancing converter is not in the scope of this chapter.

Optimal power flow (OPF) is a method to optimize the dispatch of generation and load in order to minimize the total cost or maximize the social welfare while respecting operation limits. In literature for bipolar dc grids, OPF has been done for HVdc and a combined approximated OPF for hybrid ac and dc networks [3–5]. Bipolar HVdc lines are normally operated symmetrically, hence a single line approximation can be used in these dc networks [6]. DC microgrid literature contains a vast amount of research on local energy managment systems. Mostly local dc nano- or microgrids are considered where network constraints are not included [7] and, if they are, only unipolar dc grids are considered [8].

In bipolar dc distribution grids [1] the lines can be loaded asymmetrically (unbalanced), i.e., devices connected between pole and neutral, to allow smaller devices to connect to lower voltage. Due to this likely asymmetric loading of both polarities in distribution grids, partial line congestion can appear. Congestion of distribution grids occur when power flows are subject to physical or operational limitations. These are likely to occur in distribution networks in the future due to the increase of installed power capacity (e.g. electric vehicles and photovoltaics). Partial line congestion means that for example only the positive pole is overloaded while more power could be transferred on the negative pole. This can be related to congestions in unbalanced 3-phase ac distribution feeders. Moreover, asymmetric congestion should result in differing LMP on the two polarities at the same location. Furthermore, parts of the grid may be built with only one of the two polarities, or the neutral conductor can be left out for longer distances. The voltages in the low voltage grid can have significant variations due to losses and have to be kept within bounds.

This chapter proposes a method to model the OPF problem for unbalanced bipolar dc grids. It can also be used for bipolar dc grids under symmetric loading. The problem is formulated in terms of voltage and current, instead of the usual formulation in power. The formulation does not use the usual single line approximation, as the current in the neutral conductor influences the potentials of the neutral nodes. The present chapter builds up on previous work [9], however, the LMP results are different. Instead of only fixing the voltage at the optimal solution, this chapter uses a first order linearization. This ensures the same optimal solution in the linear program. Thereby the applicability is extended and allows for the optimization of meshed grids, which was not possible before. The new formulation leads to the incorporation of marginal losses into the LMP, which means that the current prices within non-congested areas are no longer equal. Furthermore the proposed mathematical formulation is more precise and allows multiple sources at the same location. More complex examples and special cases can therefore be demonstrated.

The remainder of this chapter is organized as follows. Section 3.2 introduces the modeling method without single line model. Based thereon, the exact OPF problem is formulated and the LMP are derived in Section 3.3. In Section 3.4 some numerical ex-

ample cases are presented in order to demonstrate the methodology developed. Finally, in Section 3.5 conclusions are drawn and future work is identified.

Nomenclature

Indices and Sets

$\mathcal{N} = \mathcal{N}_+ \cup \mathcal{N}_- \cup \mathcal{N}_N$	Positive, negative and neutral nodes.
$\mathcal{N}^\emptyset$	Nodes $\mathcal{N}$ without reference node.
$m, n \in \mathcal{N}$	Nodes of the bipolar grid.
$(m, n) \in \mathcal{G}$	Pair of nodes with connecting line.
$(m, n, s) \in \mathcal{S}$	Individual sources s at nodes (m, n).

Variables

u_m	Voltage at node m [V].
i_m	Total current at node m, going from the source layer into the resitive network [A] (see Fig. 3.2b).
$i_{m,n}$	Line current from node m to n [A].
$i^S_{m,n,s}$	Current of one source, defined as negative (−), or a load defined as positive (+) [A].
$p^S_{m,n,s}$	Power of source s connected at (m, n) [W].
λ^I_m	LMP for node m in terms of current [m.u./Ah].
$\lambda^P_{m,n}$	LMP for nodes (m, n) in terms of power [m.u./Wh].
$(\cdot)^*$	Superscript for variable value at optimal solution.

Parameters

$G_{m,n}$	Branch conductance [S].
$\underline{U}, \overline{U}$	Voltage limits for both poles [V].
$\underline{U}_N, \overline{U}_N$	Voltage limits for neutral conductor [V].
$\underline{I}_{m,n}, \overline{I}_{m,n}$	Line current limits [A].
$\underline{I}^S_{m,n,s}, \overline{I}^S_{m,n,s}$	Current limits for source [A].
$\underline{P}^S_{m,n,s}, \overline{P}^S_{m,n,s}$	Power limits for source [W].
$\Pi^S_{m,n,s}$	Marginal cost/value of sources [m.u./Wh].

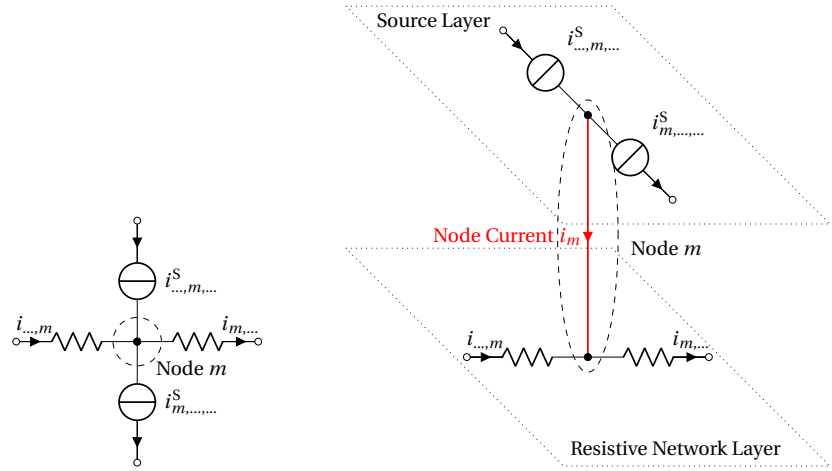

Figure 3.2: (a) Traditional representation of a node with connected lines and sources that can be either generators or loads. (b) The node with connected lines and sources split up into source layer (top) and resistive network layer (bottom). The node current i_m connects both layers in every node. It represents the total current flowing into the resistive network from all generators and loads connected in the source layer.

3.2. MATHEMATICAL MODEL OF THE EXACT POWER FLOW IN BIPOLAR DC DISTRIBUTION GRIDS

Instead of the usual OPF representation in terms of power [6], in this chapter the problem is formulated in terms of currents and voltages. In this way, constraints can be formulated as upper and lower bounds in terms of currents and voltages. The network of sources and lines, as shown in Fig. 3.2a, is split into a resistive network and a source layer, as illustrated in Fig. 3.2b. This is done by putting all lines into the resistive layer and all loads and generators into the source layer. The resistive grid is modeled similar to the traditional dc OPF. The source layer structures the positive and negative connections of all sources and loads and assigns them to the right nodal current. This nodal current i_m links both layers and is used later for the derivation of the LMP.

3.2.1. MODELING OF THE GRID

The exact linear power flow in the network is represented by explicitly modeling voltage and current variables. The voltage magnitude differences between two nodes and the respective resistances of the connecting branches impose the current flow pattern [4].

The bipolar dc grid consists of the nodes in set $\mathcal{N}$, for which the following equations are true:

$$i_{m,n} = G_{m,n} \cdot (u_m - u_n) \qquad \forall (m,n) \in \mathcal{G} \tag{3.1}$$

$$i_m = \sum_{n|(m,n)\in\mathcal{G}} i_{m,n} - \sum_{n|(n,m)\in\mathcal{G}} i_{n,m} \qquad \forall m \in \mathcal{N} \tag{3.2}$$

where node current i_m is equal to the algebraic sum of the currents flowing into the connected branches. This is the Kirchhof's current law of the resistive network at the bottom of Fig. 3.2b.

3.2.2. Modeling Generators and Loads

In order to allow a more generic modeling of prosumers, that can both consume and produce power, loads are also modeled as sources. For a more elegant mathematical formulation later on, sources that feed power into the grid (generators) have negative current and power, while sources that consume power (loads) have positive current and power. All sources are modeled as current sources because they can be connected in parallel which would not be possible with voltage sources. The positive current of a current source (load) is defined as flowing from the more positive pole to the more negative pole. That means that current is extracted out of the resistive network at the positive pole and fed into the resistive network at the negative pole (Fig. 3.2b).

In a bipolar grid, sources and loads can be connected between various points in the network: between positive polarity and neutral conductor, between neutral conductor and negative polarity conductor, or directly between positive and negative conductors, advisable for bigger sources and loads. It is evident that in actual applications this could lead to asymmetric loading of the grid, causing increased voltage magnitudes for the nodes of the neutral conductor. Therefore, also the neutral conductor is modeled and all sources and loads are connected between two nodes (m, n).

Multiple sources connected to the same nodes could be useful, e.g., to model a building with PV together with the loads of the building. In order to allow multiple sources with different characteristics at the same location an additional sum is made over all individual sources between the same nodes. The node currents are then the algebraic sum of all sources connected on a specific node m:

$$\begin{aligned} -i_m = &\sum_{n|(m,n,s)\in\mathcal{S}} \sum_{s|(m,n,s)\in\mathcal{S}} i^{\mathrm{S}}_{m,n,s} \\ &- \sum_{n|(m,n,s)\in\mathcal{S}} \sum_{s|(n,m,s)\in\mathcal{S}} i^{\mathrm{S}}_{n,m,s} \end{aligned} \qquad \forall m \in \mathcal{N}^{\emptyset} \tag{3.3}$$

Equations (3.2) together with (3.3) are essentially constituting Kirchhoff current law. The node current i_m is the variable used to describe the interface between the resistive network and the sources together with the loads connected on various nodes as shown in Fig. 3.2b. For a node m of the system, where no current injection or extraction occurs due to the lack of a source or a load, the node current i_m will be zero. Otherwise the node current i_m, according to (3.3), is equal to the total balance of current injected and extracted from this specific node.

While the power flow in the network can be described fully by previous equations, the power of the sources will be necessary for modeling power limits and marginal cost in terms of energy. The power of the sources is

$$p^{\mathrm{S}}_{m,n,s} = (u_m - u_n) \cdot i^{\mathrm{S}}_{m,n,s} \qquad \forall (m,n,s) \in \mathcal{S} \tag{3.4}$$

which is a bilinear equation, thus making the problem quadratic.

3.2.3. LIMITS

The reference node is assumed to be grounded and its voltage is fixed to zero:

$$u_0 = 0\,\mathrm{V} \tag{3.5}$$

Under normal operating conditions the acceptable voltage variation is limited to certain percentage of the nominal operating voltage. Moreover, operational constraints due to line current limits are taken into account. The nodes of the network $\mathcal{N}$ are divided into three groups: $\mathcal{N}_+$ for the positive pole, $\mathcal{N}_-$ for the negative pole, and $\mathcal{N}_\mathrm{N}$ for the neutral conductor. The voltage and line current limits are

$$\underline{U} \le u_m \le \overline{U} \qquad \forall m \in \mathcal{N}_+ \tag{3.6}$$

$$\underline{U} \le -u_m \le \overline{U} \qquad \forall m \in \mathcal{N}_- \tag{3.7}$$

$$\underline{U}_\mathrm{N} \le u_m \le \overline{U}_\mathrm{N} \qquad \forall m \in \mathcal{N}_\mathrm{N} \tag{3.8}$$

$$\underline{I}_{m,n} \le i_{m,n} \le \overline{I}_{m,n} \qquad \forall (m,n) \in \mathcal{G} \tag{3.9}$$

The sources can be constrained by current and power limits:

$$\underline{I}^\mathrm{S}_{m,n,s} \le i^\mathrm{S}_{m,n,s} \le \overline{I}^\mathrm{S}_{m,n,s} \qquad \forall (m,n,s) \in \mathcal{S} \tag{3.10}$$

$$\underline{P}^\mathrm{S}_{m,n,s} \le p^\mathrm{S}_{m,n,s} \le \overline{P}^\mathrm{S}_{m,n,s} \qquad \forall (m,n,s) \in \mathcal{S} \tag{3.11}$$

Current can be used to model the limits of power electronics while power is more appropriate for process limits. The separation of these two limits may be preferable when significant voltage deviations appear in the distribution grids. The power constraint (3.11) is a indirectly a quadratic inequality constraint due to (3.4) being quadratic.

3.3. OPTIMAL POWER FLOW

After modeling the grid, sources and constraints, the OPF is solved in order to minimize total cost. A two-step method following a similar approach as that in [10] is used to solve the economic dispatch and derive the LMP. Firstly the exact model is used to find the optimal solution. Secondly the problem is linearized at the found optimal solution to derive the LMP.

3.3.1. COST/VALUE FUNCTION OF SOURCES

The operation cost of each generator and load is defined by a given marginal cost $\Pi^\mathrm{S}_{m,n,s}$ (cost of increasing the output by one unit). Demand response of loads could be implemented by giving them a marginal value (defined as opposite of marginal cost) and allowing its power consumption to be variable. Load shedding with different priorities could also be implemented by giving different values to loads. If the resulting price is higher, they would automatically turn off [1].

3.3.2. SOLVING FOR THE ECONOMIC DISPATCH

The optimal economic dispatch is found by minimizing the total cost and this is equivalent to maximizing the social welfare [11]. The problem formulation is presented as

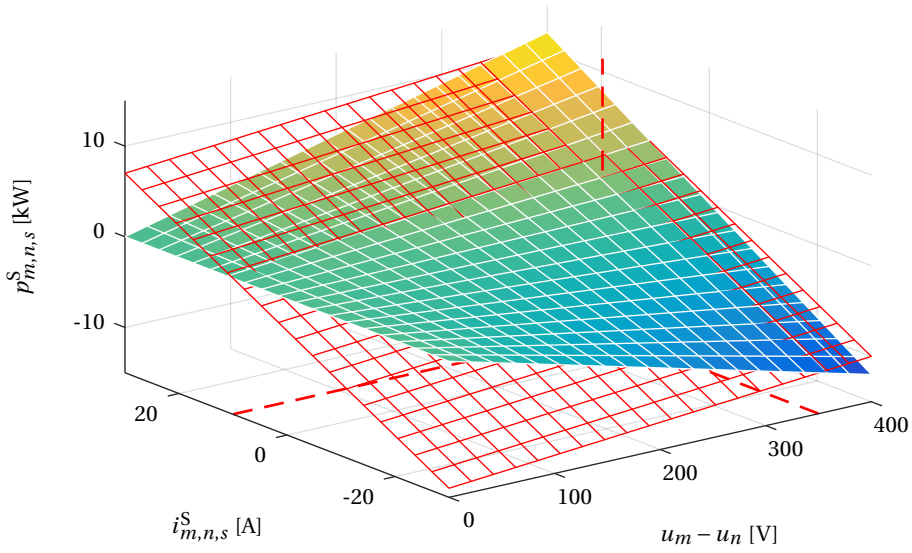

Figure 3.3: Visualization of the linearization around the solution of the bilinear power equation (surface). The linearized power equation (at 350 V, 10 A) is shown as red mesh.

follows:

$$\begin{aligned} \min \quad & \sum_{(m,n,s)\in\mathscr{S}} -p^{S}_{m,n,s} \cdot \Pi^{S}_{m,n,s} \\ \text{s.t.} \quad & (3.1) - (3.11) \end{aligned} \tag{3.12}$$

The choice of sign is important for the marginal values used in the next section. The multiplication of the two variables in (3.4) makes the problem bilinear, a special case of quadratic programming for which the problem is not convex.

It is important to note that due to the non-convexity of the problem, an optimal solution is not guaranteed to be the global optimum. This aspect has to be dealt with by the optimization algorithm, which is not in the scope of this chapter. It is assumed that the found solution is acceptable because it is feasible, even though it is possibly not globally optimal.

3.3.3. Locational Marginal Prices (LMP)

Non-convex problems suffer from weak duality. In order to derive the LMP for the non-convex problem, the problem is linearized at the optimal solution [10].

Linearization

Firstly, the quadratic problem (3.12) is solved and the optimal voltages u^{*}_{m} and source currents $i^{S*}_{m,n,s}$ are obtained. Then, the problem is linearized around this optimal solution. This means that power equation (3.4), the only non-linear equation in the problem,

has to be linearized. By using the first order Taylor appoximation this finally results in

$$\begin{aligned} p^{\mathrm{S}}_{m,n,s} = {} & (u^*_m - u^*_n) \cdot i^{\mathrm{S}}_{m,n,s} \\ & + (u_m - u_n) \cdot i^{\mathrm{S}*}_{m,n,s} \\ & - (u^*_m - u^*_n) \cdot i^{\mathrm{S}*}_{m,n,s} \end{aligned} \qquad \forall (m,n,s) \in \mathscr{S} \tag{3.13}$$

In Fig. 3.3 a visualization of the bilinear power equation (3.4) and its linearization (3.13) is shown. Herewith a linear optimization problem can be formulated as

$$\begin{aligned} \min \quad & \sum_{(m,n,s)\in\mathscr{S}} -p^{\mathrm{S}}_{m,n,s} \cdot \Pi^{\mathrm{S}}_{m,n,s} \\ \text{s.t.} \quad & (3.1) - (3.3), (3.13), (3.5) - (3.11) \end{aligned} \tag{3.14}$$

The problem formulation (3.14) is now linear, thus convex and with strong duality. The linear problem is initialized at the solution of (3.12). In this way, the same solution is obtained, also for the case of multiple solutions at the same optimum. In other words, the variables computed using linear programming are then the same as for quadratic programming. The linearization is thus exact at the solution. Therefore, the dual variables can be used to derive the LMP for the original problem [12]. Depending on the solver, the dual variables might also be obtained from the original problem.

LMP is the marginal cost of supplying the next increment of energy at a given location. LMP are commonly expressed in terms of power and reflect also losses and congestion [13–15]. In this case, dual variables obtained from the equality constraint (3.2) for each node are given in terms of current (instead of power) and denoted by λ^{I}_m. Using linear programming enables to interpret these dual variables as the LMP for all m. However they are in terms of current [m.u./Ah], which is not the usual unit (m.u. stands for Monetary Unit).

LMP IN TERMS OF POWER

LMP in power terms are calculated for all generators and loads connected between different polarities $m, n \in \mathscr{N}$. Their value can be derived as follows: Let $\alpha_{m,n,s}$ be the amount payable by a prosumer per time interval, which is by definition the power times the LMP:

$$\alpha_{m,n,s} = p^{\mathrm{S}}_{m,n,s} \cdot \lambda^{\mathrm{P}}_{m,n} \tag{3.15}$$

On the other hand this amount has to be equal to the amount payable for extracting the source current $i^{\mathrm{S}}_{m,n,s}$ in one node and injecting it in the other, because that is what is physically happening:

$$\begin{aligned} \alpha_{m,n,s} &= \lambda^{\mathrm{I}}_m \cdot i^{\mathrm{S}}_{m,n,s} + \lambda^{\mathrm{I}}_n \cdot (-i^{\mathrm{S}}_{m,n,s}) \\ &= (\lambda^{\mathrm{I}}_m - \lambda^{\mathrm{I}}_n) \cdot i^{\mathrm{S}}_{m,n,s} \end{aligned} \tag{3.16}$$

Table 3.1: Line Currents

	$\mathcal{N}_+$		$\mathcal{N}_N$		$\mathcal{N}_-$	
Case 1	$i_{4,5}$	68.03	$i_{0,1}$	29.66	$i_{8,9}$	-97.69
	$i_{5,6}$	40.67	$i_{1,2}$	29.33	$i_{9,10}$	-70.00
	$i_{6,7}$	-0.48	$i_{2,3}$	-0.70	$i_{10,11}$	1.18
Case 2	$i_{2,3}$	13.62	$i_{0,1}$	-13.62	$i_{5,6}$	0.00
	$i_{3,4}$	-22.51	–	–	$i_{6,7}$	22.51
Case 3	$i_{3,4}$	70.00	$i_{0,1}$	0.00	$i_{6,7}$	-70.00
	$i_{4,5}$	-40.96	$i_{1,2}$	5.96	$i_{7,8}$	35.00
	$i_{3,5}$	29.04	$i_{0,2}$	5.96	$i_{6,8}$	-35.00

By solving (3.15) for $\lambda^{\mathrm{P}}_{m,n}$ and substituting (3.16) and (3.4), the LMP in terms of power between nodes (m,n) can be derived as

$$\lambda^{\mathrm{P}}_{m,n} = \frac{\alpha_{m,n,s}}{p^{\mathrm{S}}_{m,n,s}} = \frac{(\lambda^{\mathrm{I}}_m - \lambda^{\mathrm{I}}_n)\cdot i^{\mathrm{S}}_{m,n,s}}{(u_m - u_n)\cdot i^{\mathrm{S}}_{m,n,s}} = \frac{\lambda^{\mathrm{I}}_m - \lambda^{\mathrm{I}}_n}{u_m - u_n} \qquad \forall m,n \in \mathcal{N} \tag{3.17}$$

So the LMP between two nodes in terms of power is equal to the difference of current LMP λ^{I}_m divided by the voltage difference of the nodes u_m.

MARGINAL LOSSES

Using the marginal values of the OPF as LMP, includes marginal losses into the price. Thereby the losses have a greater impact on the price than the physical power loss. The marginal losses are approximately twice as high as the cost of the physical losses. This phenomenon is known from literature for ac grids [16] and is therefore not further discussed in this chapter.

3.4. NUMERICAL EXAMPLES

This section presents three cases that were selected to show the special phenomenon that can occur in bipolar dc grids with asymmetric loading, which cannot be modeled using OPF with single line approximation. Case 1 illustrates the method and shows partial congestion on only one line of a bipolar cable. Case 2 shows the effect of sources connected directly between two poles, and multiple sources between the same nodes, as well as interdependence between the two poles. Case 3 shows a meshed grid with partial line congestion. In this last case the LMP on the non-congested lines are of special interest.

The problems are modeled using GAMS and solved using the CONOPT solver [17]. The networks consist of 25 mm^2 cables with $\overline{I}_{m,n} = -\underline{I}_{m,n} = 70$ A current limit and 50 mm^2

Table 3.2: Node Voltages

	$\mathcal{N}_+$		$\mathcal{N}_N$		$\mathcal{N}_-$	
Case 1	u_4	367.50	u_0	0.00	u_8	-367.50
	u_5	364.10	u_1	-1.48	u_9	-362.62
	u_6	360.03	u_2	-4.42	u_{10}	-355.62
	u_7	360.06	u_3	-4.38	u_{11}	-355.67
Case 2	u_2	367.06	u_0	0.00	u_5	-332.50
	u_3	366.37	u_1	0.68	u_6	-332.50
	u_4	367.50	–	–	u_7	-333.63
Case 3	u_3	367.50	u_0	0.00	u_6	-367.50
	u_4	360.50	u_1	0.00	u_7	-360.50
	u_5	364.60	u_2	-0.60	u_8	-364.00

cables with $\overline{I}_{m,n} = -\underline{I}_{m,n} = 100\,\text{A}$ current limit. The voltage limits are set to $350\,\text{V} \pm 5\%$ and the neutral conductor has the same operating range:

$$\overline{U} = 367.5\,\text{V}$$
$$\underline{U} = 332.5\,\text{V}$$
$$\overline{U}_\text{N} = 17.5\,\text{V}$$
$$\underline{U}_\text{N} = -17.5\,\text{V}$$

The upper nodes of Fig. 3.5, 3.6 and 3.7 are in $\mathcal{N}_+$, the lower nodes in $\mathcal{N}_-$, and the nodes in the middle are in $\mathcal{N}_\text{N}$.

Each case has its own tables to show specific configuration of loads and generators, and LMP. Table 3.1 presents the line currents for all cases. Table 3.2 shows the nodal voltages.

3.4.1. CASE 1: BIPOLAR GRID WITH PARTIAL LINE CONGESTION

The goal of this case is to show the congestion of only one of three conductors in a line. Fig. 3.5 shows the example grid. The central 4 sources operate as loads. On the left and the right each two generators are connected between neutral and the poles. Table 3.3 shows the marginal costs $\Pi^\text{S}_{m,n,s}$ of the generators. The left ones are cheap (5 m.u./kWh) while the right ones are expensive (10 m.u./kWh). The power limits of the generators on the right are -20 kW and on the left -25 kW on top and -50 kW on the bottom. The loads in the middle on the left side are fixed to 10 kW and on the right side on the top 15 kW and on the bottom 25 kW. The lines on the left and right are 100 m long and have 50 mm^2 cross section with a current limit $\overline{I}_{m,n}$ of 100 A. The lines in the middle between the two loads have the same length but are thinner and have a current limit of 70 A which is reached on the negative conductor $i_{9,10}$ as can be seen in Table 3.1.

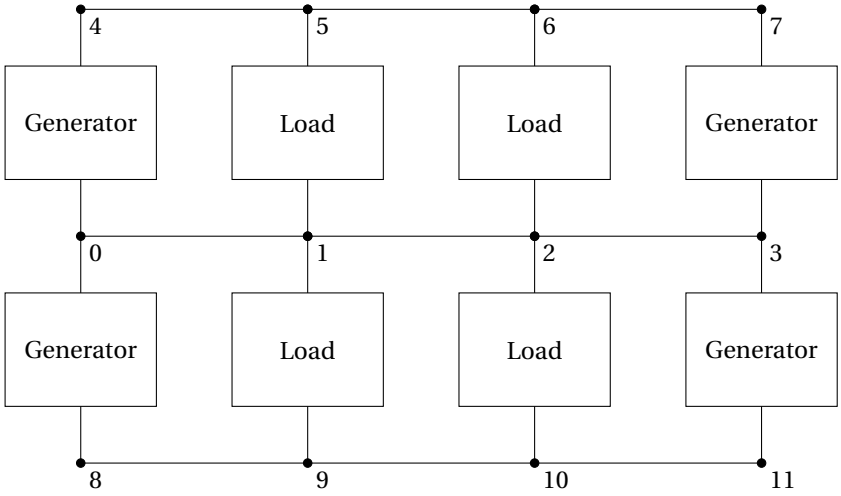

Figure 3.4: Bipolar dc grid with positive (top), neutral (middle) and negative conductors (bottom). Generators and loads are shown as two port and are connected between the respective pole and neutral.

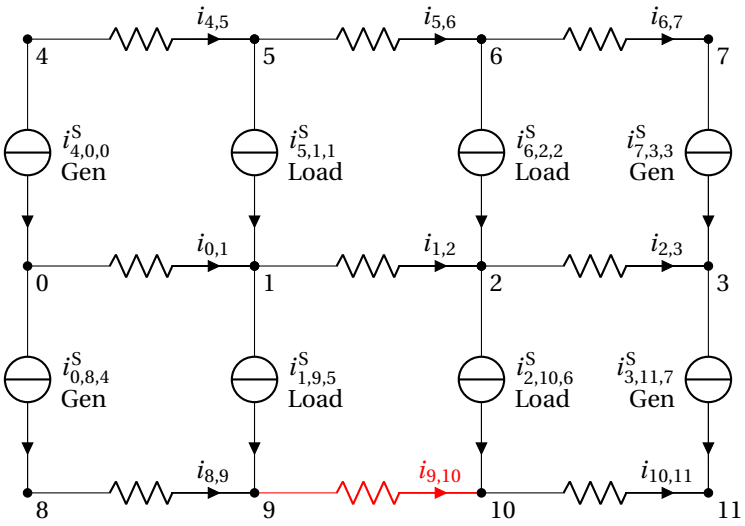

Figure 3.5: Bipolar dc grid with positive (top), neutral (middle) and negative conductors (bottom). The 4 central sources are loads while the 4 outer sources are generators. A line congestion occurs on the negative conductor in the middle.

Table 3.3: Case 1: Source Variables

Parameter / Variables	Sources' Inputs and Outputs			
$(\mathcal{N}_+, \mathcal{N}_N)$	(4,0,0)	(5,1,1)	(6,2,2)	(7,3,3)
$\Pi^{\mathrm{S}}_{m,n,s}$ [m.u./kWh]	5	0	0	10
$\underline{P}^{\mathrm{S}}_{m,n,s}$ [kW]	-25	10	15	-20
$\overline{P}^{\mathrm{S}}_{m,n,s}$ [kW]	0	10	15	0
$p^{\mathrm{S}}_{m,n,s}$ [kW]	-25.00	10.00	15.00	-0.18
$i^{\mathrm{S}}_{m,n,s}$ [A]	-68.03	27.35	41.16	-0.48
$(\mathcal{N}_N, \mathcal{N}_-)$	(0,8,4)	(1,9,5)	(2,10,6)	(3,11,7)
$\Pi^{\mathrm{S}}_{m,n,s}$ [m.u./kWh]	5	0	0	10
$\underline{P}^{\mathrm{S}}_{m,n,s}$ [kW]	-50	10	25	-20
$\overline{P}^{\mathrm{S}}_{m,n,s}$ [kW]	0	10	25	0
$p^{\mathrm{S}}_{m,n,s}$ [kW]	-35.90	10.00	25.00	-0.42
$i^{\mathrm{S}}_{m,n,s}$ [A]	-97.60	27.69	71.18	-1.18

Table 3.4: Case 1: Locational Marginal Prices

$(m,n) \in \mathcal{N}$	(4, 0)	(5, 1)	(6, 2)	(7, 3)
$u_m - u_n$ [V]	367.50	365.58	364.45	364.44
$\lambda^{\mathrm{P}}_{m,n}$ [m.u./kWh]	9.82	9.94	10.00	10.00
λ^{I}_{m} [m.u./Ah]	3607.36	3641.28	3681.95	3681.71
λ^{I}_{n} [m.u./Ah]	0.00	8.33	37.70	37.35
$(m,n) \in \mathcal{N}$	(0, 8)	(1, 9)	(2, 10)	(3, 11)
$u_m - u_n$ [V]	367.50	361.13	351.20	351.29
$\lambda^{\mathrm{P}}_{m,n}$ [m.u./kWh]	5.00	5.23	10.01	10.00
λ^{I}_{m} [m.u./Ah]	0.00	8.33	37.70	37.35
λ^{I}_{n} [m.u./Ah]	-1837.50	-1879.76	-3476.18	-3475.59

Voltage differences $u_m - u_n$ and the LMP of each connection point are displayed in Table 3.4. The LMP are shown in terms of power ($\lambda^{\mathrm{P}}_{m,n}$) but also in terms of current for both connecting nodes (λ^{I}_{m} and λ^{I}_{n}).

On top for the positive conductor the locational marginal price is related to the expensive generator at the right, which is needed only to cover the losses. The line current $i_{6,7}$ is so low, that almost no losses occur and due to rounding the price at (6,2) is the same. The current in the neutral conductor $i_{2,3}$ even slightly overcompensates for those losses in the positive conductor such that the prices is slightly lower (9.999 rounded to 10.00). Further to the left the power is flowing from the left hand side and therefore prices decrease due to less losses on the way.

On the negative conductor at the bottom, a line congestion occurs and $i_{9,10}$ is limited to -70 A. This is not the case for the neutral conductor, as positive and negative currents are superimposed. The prices on the both sides on the congestion diverge. The left side is fed by generator (0,8,4) and the LMP increases due to the losses at (1,9). Additional supply is needed from the right generator and, with some additional losses, the LMP at (2,10) is slightly above the marginal cost of the generator.

This case presented the partial congestion (in line $i_{9,10}$) which only appears in unbalanced bipolar dc grids. This congestion cannot be modeled and observed with traditional OPF formulations.

3.4.2. Case 2: Parallel Sources, Pole to Pole Source and Demand Response

Fig. 3.6 shows the example grid for Case 2. All lines are 100 m long and 50 mm^2 thick. The two sources on the left are generators with a marginal cost as shown in Table 3.5. In the

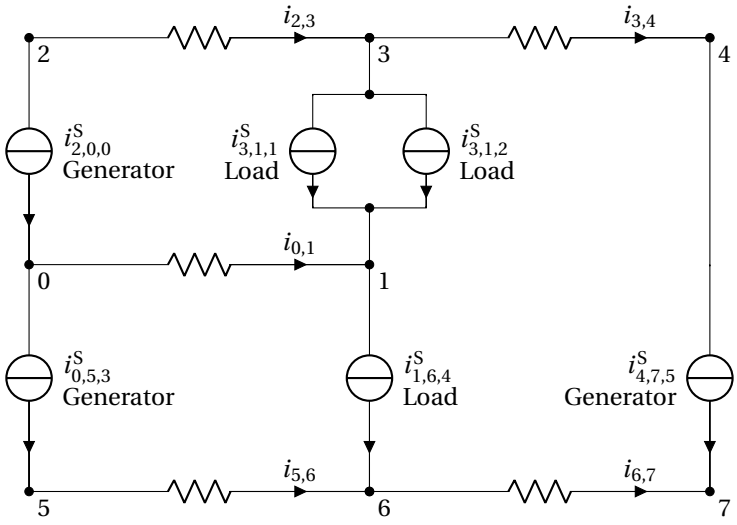

Figure 3.6: Bipolar grid with parallel sources and a source from pole to pole. The two sources on the left and the one on the right are generators, the 3 sources in the middle are loads with varying value (demand response).

Table 3.5: Case 2: Source Variables

Parameter / Variables	Sources' Inputs and Outputs		
$(\mathcal{N}_+, \mathcal{N}_N)$	(2,0,0)	(3,1,1)	(3,1,2)
$\Pi^{\mathrm{S}}_{m,n,s}$ [m.u./kWh]	5	3	10
$\underline{P}^{\mathrm{S}}_{m,n,s}$ [kW]	-5	0	0
$\overline{P}^{\mathrm{S}}_{m,n,s}$ [kW]	0	10	15
$p^{\mathrm{S}}_{m,n,s}$ [kW]	-5.00	0.00	13.21
$i^{\mathrm{S}}_{m,n,s}$ [A]	-13.62	0.00	36.132
$(\mathcal{N}_N, \mathcal{N}_-)$ & $(\mathcal{N}_+, \mathcal{N}_-)$	(0,5,3)	(1,6,4)	(4,7,5)
$\Pi^{\mathrm{S}}_{m,n,s}$ [m.u./kWh]	5	3	0
$\underline{P}^{\mathrm{S}}_{m,n,s}$ [kW]	-5	0	-20
$\overline{P}^{\mathrm{S}}_{m,n,s}$ [kW]	0	7.5	0
$p^{\mathrm{S}}_{m,n,s}$ [kW]	0.00	7.50	-15.78
$i^{\mathrm{S}}_{m,n,s}$ [A]	0.00	22.51	-22.51

Table 3.6: Case 2: Locational Marginal Prices

$(m,n) \in \mathcal{N}$	(2, 0)	(3, 1)	–
$u_m - u_n$ [V]	367.06	365.69	–
$\lambda^{\mathrm{P}}_{m,n}$ [m.u./kWh]	9.86	10.00	–
λ^{I}_{m} [m.u./Ah]	3619.84	3626.55	–
λ^{I}_{n} [m.u./Ah]	0.00	-30.38	–
$(m,n) \in \mathcal{N}$	(0, 5)	(1, 6)	(4, 7)
$u_m - u_n$ [V]	332.50	332.50	710.13
$\lambda^{\mathrm{P}}_{m,n}$ [m.u./kWh]	-10.84	-10.94	0.00
λ^{I}_{m} [m.u./Ah]	0.00	-30.38	3615.20
λ^{I}_{n} [m.u./Ah]	3602.88	3615.203	3615.203

middle there are two loads in parallel on the positive conductor. They implement demand response with variable power between 0 and $\overline{P}^{S}_{m,n,s}$ by setting a constant marginal value to $\Pi^{S}_{m,n,s}$ which is below the generator cost for the left load and above the for the right one. The bottom load also can apply demand response with a maximum power of only 7.5 kW. On the right a renewable energy source with zero marginal cost and plenty of supply capacity is connected directly from positive pole to negative pole.

The voltage differences $u_m - u_n$ and the LMP of each connection point are shown in Table 3.6. This case is constructed in order to show the challenges in asymmetric bipolar grids. While energy could be provided at zero cost in the system, still not all load can be supplied at the given willingness to pay. The load on the bottom and a part of the right top load is supplied by the zero marginal cost generator between two poles. The load on the bottom is at maximum power, therefore there is no path for additional current to the negative pole. The voltages difference on the negative pole is reduced to the limit in order to increase the current for the same power to the maximum.

On the positive pole the generator on the left supplies maximum power at a relatively high price to meet the demands of the right load (3,1,2). The LMP are defined by the willingness to pay of the right load. The price at the left generator is a bit lower due to the losses in between. The LMP on the negative pole are negative because an increase in load there would allow a higher current trough load (3,1,2) and thus to generate more value. This means that loads/consumers receive money for their consumption. The prices are even more negative than the marginal value because, for an increase in load on the positive pole, less power is needed on the negative pole due to the lower voltage difference there. The price between positive and negative conductor is zero due to the available renewable energy from source (4,7,5).

3.4.3. Case 3: Meshed Bipolar Grid with Congestion

Fig. 3.7 shows the meshed bipolar dc grid for Case 3. The two sources on the left are generators with a marginal cost of zero as shown in Table 3.7. In the middle there are two loads with demand response. The top one has a high marginal value, while the bottom one has a low marginal value. On the right there are two more generators with, on top, relatively low marginal cost and, on bottom, high marginal cost. The lines are 100 m long, 25 mm^2 think and have a current limit of ± 70 A. This current limit is reached for $i_{3,4}$ and $i_{6,7}$. Even though the other path is not congested, the power flow cannot be increased as the current distribution is defined by the difference in resistance. Current limiting devices [18] or power flow control converters [19] would allow an impedance adaption and better utilization of grid infrastructure. In this case however, the congestion leads to a price divergence as shown in Table 3.8. The top right generator is producing additional power while the bottom one is too expensive for the bottom load, which does demand response instead.

The LMP on the negative pole are derived from the value of the curtailed load (1,7,4) as shown in Table 3.8. At nodes (2,8) the LMP is a bit less than half of that value. If an additional unit of load would be connected here, the load (1,7,4) would only need to be reduced by half a unit as additional power can come directly from the source. This decrease will reduce the voltage drop in line (7,8), therefore the voltage drop in line (6,8) could be increased to supply the rest of the unit.

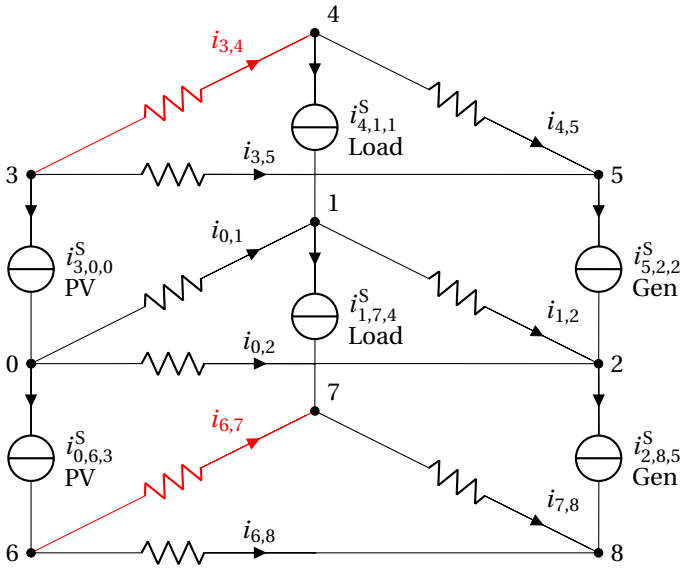

Figure 3.7: Meshed bipolar dc grid with renewable sources on the left, variable loads in the middle and generators on the right.

Table 3.7: Case 3: Source Variables

Parameter / Variables	Sources' Inputs and Outputs		
$(\mathcal{N}_+, \mathcal{N}_N)$	(3,0,0)	(4,1,1)	(5,2,2)
$\Pi^{S}_{m,n,s}$ [m.u./kWh]	0	15	5
$\underline{P}^{S}_{m,n,s}$ [kW]	-50	0	-50
$\overline{P}^{S}_{m,n,s}$ [kW]	0	40	0
$p^{S}_{m,n,s}$ [kW]	-36.40	40.00	-4.35
$i^{S}_{m,n,s}$ [A]	-99.04	110.96	-11.91
$(\mathcal{N}_N, \mathcal{N}_-)$ & $(\mathcal{N}_+, \mathcal{N}_-)$	(0,6,3)	(1,7,4)	(2,8,5)
$\Pi^{S}_{m,n,s}$ [m.u./kWh]	0	6	10
$\underline{P}^{S}_{m,n,s}$ [kW]	-50	0	-50
$\overline{P}^{S}_{m,n,s}$ [kW]	0	40	0
$p^{S}_{m,n,s}$ [kW]	-38.59	37.85	0.00
$i^{S}_{m,n,s}$ [A]	-105.00	105.00	0.00

Table 3.8: Case 3: Locational Marginal Prices

$(m,n) \in \mathcal{N}$	(3, 0)	(4, 1)	(5, 2)
$u_m - u_n$ [V]	367.50	360.50	365.19
$\lambda^{\mathrm{P}}_{m,n}$ [m.u./kWh]	0.00	10.16	5.00
λ^{I}_{m} [m.u./Ah]	0.00	3632.63	1813.34
λ^{I}_{n} [m.u./Ah]	0.00	-31.19	-12.62
$(m,n) \in \mathcal{N}$	(0, 6)	(1, 7)	(2, 8)
$u_m - u_n$ [V]	367.50	360.60	363.40
$\lambda^{\mathrm{P}}_{m,n}$ [m.u./kWh]	0.00	6.00	2.98
λ^{I}_{m} [m.u./Ah]	0.00	-31.19	-12.62
λ^{I}_{n} [m.u./Ah]	0.00	-2194.19	-1097.10

On the positive pole, the LMP are derived from the generator at the right. The LMP at the load is approximately double, because an increase in load by one unit would need an increase of generation at (5,2,2), which results in higher voltage drops in line (4,5). To keep the $i_{3,4}$ below its limit, the voltage difference from node 3 to 4 needs to stay the same. Hence, $i_{3,5}$ would have to be reduced and the loss in power needs to be additionally generated at (5,2,2). Therefore, approximately 2 units of power have to be provided at price 5.00 m.u./kWh for one additional unit of load. Due to marginal losses the price at the load is slightly more than double.

3.5. CONCLUSION

In this chapter a method to exactly model bipolar dc distribution grids with asymmetric loading has been presented. This method can also be used for bipolar dc distribution grids with symmetric loading. The problem is formulated in terms of current and voltage instead of power in order to model the grid exactly and allows limits in voltages and currents. The objective function for the OPF problem is therefore bilinear. By linearizing the problem at the optimal solution, the LMP can be calculated. Different case studies showed how the LMP differ between the different polarities depending on the asymmetric loading and congestion. Moreover, connection to only positive and negative poles can lead to negative prices on one pole. The presented formulation can be used as a foundation for future application of LMP in bipolar dc distribution grids. Because this is the first time unbalanced bipolar dc grids are modeled the method could not be gen-

erally compared with a reference case. However, during the development the validity has been tested on samples. Also manual calculations have been performed to confirm results.

Future work includes the modeling of multiple voltage levels and the converters connecting them. Decentralized current limiters [18] or power flow control converters [19] could be included into meshed grids in order to better utilize the grid. Further, the operation of storage in the presented OPF formulation and the resulting operation of bipolar dc grids has to be further investigated. Finally, it is relevant to investigate distributed solutions in order to allow connected dc microgrids to robustly run their own economic dispatch and increase system resilience.

REFERENCES

[1] L. Mackay, N. H. van der Blij, L. Ramirez-Elizondo, and P. Bauer, "Toward the Universal DC Distribution System," *Electric Power Components and Systems*, vol. 45, no. 10, pp. 1032–1042, 2017.

[2] L. Mackay, T. G. Hailu, G. R. Chandra Mouli, L. Ramirez-Elizondo, J. A. Ferreira, and P. Bauer, "From DC Nano- and Microgrids Towards the Universal DC Distribution System – A Plea to Think Further Into the Future," in *PES General Meeting*. IEEE, 2015.

[3] R. Wiget and G. Andersson, "Optimal Power Flow for Combined AC and Multi-Terminal HVDC Grids based on VSC Converters," in *IEEE Power and Energy Society General Meeting*, 2015.

[4] J. Beerten, S. Cole, and R. Belmans, "A sequential AC/DC power flow algorithm for networks containing Multi-terminal VSC HVDC systems," in *IEEE PES General Meeting*. IEEE, jul 2010, pp. 1–7.

[5] J. Rimez and R. Belmans, "A combined AC/DC optimal power flow algorithm for meshed AC and DC networks linked by VSC converters," *International Transactions on Electrical Energy Systems*, vol. 25, no. 10, pp. 2024–2035, oct 2015.

[6] L. Gan and S. H. Low, "Optimal Power Flow in Direct Current Networks," *IEEE Transactions on Power Systems*, vol. 29, no. 6, pp. 1–13, 2014.

[7] Y.-K. Chen, Y.-C. Wu, C.-C. Song, and Y.-S. Chen, "Design and Implementation of Energy Management System With Fuzzy Control for DC Microgrid Systems," *IEEE Transactions on Power Electronics*, vol. 28, no. 4, pp. 1563–1570, apr 2013.

[8] J. Ma, L. Yuan, Z. Zhao, and F. He, "Transmission Loss Optimization-Based Optimal Power Flow Strategy by Hierarchical Control for DC Microgrids," *IEEE Transactions on Power Electronics*, vol. 32, no. 3, pp. 1952–1963, mar 2017.

[9] L. Mackay, A. Dimou, R. Guarnotta, G. Morales-Espania, L. Ramirez-Elizondo, and P. Bauer, "Optimal Power Flow in Bipolar DC Distribution Grids with Asymmetric Loading," in *IEEE Energycon Leuven*, 2016.

[10] R. P. O'Neill, P. M. Sotkiewicz, B. F. Hobbs, M. H. Rothkopf, and W. R. S. Jr., "Efficient market-clearing prices in markets with nonconvexities," *European Journal of Operational Research*, vol. 164, no. 1, pp. 269 – 285, 2005.

[11] G. Stamtsis, "Power transmission cost calculation in deregulated electricity market," Ph.D. dissertation, Universität Duisburg-Essen, 2003. [Online]. Available: http://purl.oclc.org/NET/duett-12102003-112744

[12] T. Wu, M. Rothleder, Z. Alaywan, and A. D. Papalexopoulos, "Pricing Energy and Ancillary Services in Integrated Market Systems by an Optimal Power Flow," *IEEE Transactions on Power Systems*, vol. 19, no. 1, pp. 339–347, 2004.

[13] Y. F. Y. Fu and Z. L. Z. Li, "Different models and properties on LMP calculations," *2006 IEEE Power Engineering Society General Meeting*, 2006.

[14] D. Gautam and M. Nadarajah, "Influence of distributed generation on congestion and LMP in competitive electricity market," *World Academy of Science, Engineering and Technology*, vol. 39, no. 3, pp. 822–829, 2009.

[15] M. S. H. Nabavi, S. Hajforoosh, and M. A. Masoum, "Placement and Sizing of Distributed Generation Units for Congestion Management and Improvement of Voltage Profile using Particle Swarm Optimization," *IEEE PES Innovative Smart Grid Technologies, ISGT Asia 2011 Conference: Smarter Grid for Sustainable and Affordable Energy Future*, 2011.

[16] E. Litvinov, "Design and operation of the locational marginal prices-based electricity markets," *IET Generation, Transmission & Distribution*, vol. 4, no. 2, p. 315, 2010.

[17] *GAMS: The Solvers Manuals*. GAMS, 2015, vol. CPLEX 12. [Online]. Available: http://gams.com/help/topic/gams.doc/solvers/allsolvers.pdf

[18] L. Mackay, T. Hailu, L. Ramirez-Elizondo, and P. Bauer, "Decentralized Current Limiting in Meshed DC Distribution Grids," in *DC Microgrids, IEEE First International Conference on*, 2015.

[19] P. Purgat, L. Mackay, R. Adilardi Prakoso, L. Ramirez-Elizondo, and P. Bauer, "Power flow control converter for meshed LVDC distribution grids," in *2017 IEEE Second International Conference on DC Microgrids (ICDCM)*. IEEE, jun 2017, pp. 476–483.

4

Storage Operation in Unbalanced Bipolar DC Distribution Grids

The emergence of distributed energy resources can lead to congestions in distribution grids. DC distribution grids are becoming more relevant as more sources and loads connected to the low voltage grid use dc. Bipolar dc distribution grids with asymmetric loading can experience partial congestion resulting in a nodal price difference between the two polarities, as has been shown in the previous chapter. The addition of storage to a bipolar dc distribution grid requires the optimization over a prediction horizon in order to achieve optimal power flow. Variable time steps are used to increase precision in short term future while reducing computation time for longer term future. The impact of storage operation on the LMP in bipolar dc grids is shown. Examples illustrate the effect and special cases that can occur when operating energy storage systems in bipolar dc distribution grids.

This chapter is based on a future publication.

4.1. INTRODUCTION

Distribution grids are expected to experience more congestion problems due to the emergence of electrical vehicles, renewable energy sources, and other distributed energy resources. Using locational marginal prices (LMP) can enable optimal utilization of distributed energy resources owned by different entities. DC distribution grids have advantages over ac distribution grids due to their inherently higher power transfer capacity and due to the fact that most loads and sources connected to the low voltage grid nowadays are dc already. In the future more and more, will be either inherently dc or use a dc link to couple variable rotation speeds [1, 2].

Bipolar dc grids have, in addition to the positive and negative conductor of unipolar dc grids, a neutral conductor. Their configuration can be compared to that of a 3-phase or 2-phase (180° phase angel difference with neutral) ac grid. As shown in Fig. 3.1 on the left, small devices can be connected between the positive pole and the neutral or between the neutral and the negative pole. [3]

The operation of storage is an important element in future distribution grids with high share of distributed renewable energy resources. They can be used to deal with the challenges caused by fluctuating renewable energies. Energy storage systems link different time periods together. This principal problem has been well addressed in literature [4–6]. The market model has a important impact on the economical operation of storage. In some market models storage is inherently uneconomical due to concepts such as net-metering, where the time of consumption or production has no effect on the cost. In other market models a part of the fixed grid cost is added to the electricity prices which results in additional penalty and reduces the utilization of existing storage potential. There are many heuristic storage operation approaches, such as maximizing self consumption, which may address specific market designs but do not optimize the total operation cost of the power system.

When using LMP the operation of storage can be used to maximize social welfare. The LMP take into account factors such as line losses and the location in a distribution system. Additionally congestion management can be accomplished.

The main contribution of this chapter is the extension of the single period exact optimal power flow[3] by the operation of storage in bipolar dc distribution grids with asymmetric loading. This comprises the optimization over multiple interlinked time steps. The time steps can be of variable size which allows a more precise modeling of the short term future with small time steps, while the longer term future can be modeled with larger time steps in order to save computation time. Further the impact of storage operation on congestion, it's capability of balancing the poles to some extend and the influence on the LMP is shown.

The remainder of this chapter is organized as follows. Section 4.2 introduces the modeling method without single line model and the storage equations and constraints that interlink the variable time steps. Based thereon, the OPF problem for multiple time steps is formulated and the LMP are derived in Section 4.3. In Section 4.4 some example cases are presented in order to demonstrate the methodology developed. Finally, in Section 4.5 conclusions are drawn and future work is identified.

NOMENCLATURE

INDICES AND SETS

$\mathcal{N} = \mathcal{N}_+ \cup \mathcal{N}_- \cup \mathcal{N}_N$	Positive, negative and neutral nodes.
$\mathcal{N}^{\emptyset}$	Nodes $\mathcal{N}$ without reference node.
$m, n \in \mathcal{N}$	Nodes of the bipolar grid.
$(m, n) \in \mathcal{G}$	Pair of nodes with connecting line.
$(m, n, s) \in \mathcal{S}$	Individual sources s at nodes (m, n).
$\mathcal{S} = \bigcup_v \mathcal{S}_v$	All sources are assigned to a set of voltage limits.
$(m, n, s) \in \mathcal{B}$	Energy storage system s at nodes (m, n).
$\mathcal{B} = \mathcal{B}^{\text{fix}} \cup \mathcal{B}^{\text{var}}$	Storage can be of fixed or variable size.
$k \in \mathcal{K} = \{0, ..., K\}$	Time steps.

VARIABLES

$u_{m,k}$	Voltage of node m at time step k [V].
$i_{m,k}$	Current at node m, going from the source layer into the resitive network [A].
$i_{m,n,k}$	Line current from node m to n [A].
$i^{\text{S}}_{m,n,s,k}$	Current of one source, defined as negative (−), or a load defined as positive (+) [A].
$p^{\text{S}}_{m,n,s,k}$	Power of source s connected at (m, n) [W].
$e_{m,n,s,k}$	Energy content [Wh].
$\lambda^{\text{I}}_{m,k}$	LMP for node m in terms of current [m.u./A].
$\lambda^{\text{P}}_{m,n,k}$	LMP for nodes (m, n) in terms of power [m.u./W].
$\lambda^{\|\text{P}\|}_{m,n,k}$	Normalized LMP for nodes (m, n) in terms of power [m.u./Wh].
$b_{m,n,s,k}$	Binary variable for charge (=1) and discharge of storage.
$q_{m,n,s}$	Integer variable for the quantity of storage systems at (m,n,s).
$(\cdot)^*$	Superscript for variable value at optimal solution.

Parameters

$G_{m,n}$	Branch conductance [S].
$\underline{U}, \overline{U}$	Voltage limits for both poles [V].
$\underline{U}_{\mathrm{N}}, \overline{U}_{\mathrm{N}}$	Voltage limits for neutral conductor [V].
$\underline{U}_v, \overline{U}_v$	Voltage limits for sources $\in \mathscr{S}_v$ [V].
$\underline{I}_{m,n}, \overline{I}_{m,n}$	Line current limits [A].
$\underline{I}^{\mathrm{S}}_{m,n,s}, \overline{I}^{\mathrm{S}}_{m,n,s}$	Current limits for source [A].
$\underline{P}^{\mathrm{S}}_{m,n,s}, \overline{P}^{\mathrm{S}}_{m,n,s}$	Power limits for source [W].
$\underline{E}_{m,n,s,k}, \overline{E}_{m,n,s,k}$	Energy limits for energy storage system [Wh].
$\underline{Q}_{m,n,s}, \overline{Q}_{m,n,s}$	Limits for the quantity of storage systems at (m,n,s).
$\Pi^{\mathrm{S}}_{m,n,s}$	Marginal cost / value of sources [m.u./Wh].
$\Pi^{\mathrm{ESS}}_{m,n,s}$	Investment cost of one storage unit [m.u./unit].
$\eta_{m,n,s}$	Storage converter efficiency.
t_k	Time at time step k [h].

4.2. Power Flow Model Including Storage in Bipolar DC Distribution Grids

Instead of the usual representation in terms of power [7], in this chapter the problem is formulated in terms of currents and voltages. This allows the straightforward exact modeling of the network including losses and allows exact constraints in terms of currents and voltages. The network of sources and lines is split into two layers. This is illustrated on the network in Fig. 3.2a that is split up in Fig. 3.2b by putting all lines into the resistive layer and all loads and generators into the source layer. The resistive grid is modeled similar to the traditional dc OPF. The source layer structures the positive and negative connections of all sources and loads and assigns them to the right nodal current. This nodal current $i_{m,k}$ links both layers and is used later for the derivation of the LMP.

4.2.1. Modeling of the Grid

By explicitly modeling voltage and current variables, the exact linear power flow in the network is represented. Voltage magnitude differences between two nodes and the respective resistances of the connecting branches impose the current flow pattern [8].

The bipolar dc grid consists of the nodes in set $\mathscr{N}$ for which the following equations are true:

$$i_{m,n,k} = G_{m,n} \cdot (u_{m,k} - u_{n,k}) \qquad \forall (m,n) \in \mathscr{G} \tag{4.1}$$

$$i_{m,k} = \sum_{n|(m,n)\in\mathscr{G}} i_{m,n,k} - \sum_{n|(n,m)\in\mathscr{G}} i_{n,m,k} \qquad \forall m \in \mathscr{N} \tag{4.2}$$

where node current $i_{m,k}$ is equal to the algebraic sum of the currents flowing into the

connected branches. The Kirchhofs current law of the resistive network at the bottom of Fig. 3.2b is discribed by (4.2).

4.2.2. MODELING GENERATORS AND LOADS

In order to allow a more abstract modeling of prosumers that can both consume and produce power, loads are also modeled as sources. For a more elegant mathematical formulation later on, sources that feed power into the grid (generators) have negative current and power, while sources that consume power (loads) have positive current and power. The positive current of a current source (load) is defined as flowing from the more positive pole to the more negative pole. That means that current is extracted out of the resistive network at the positive pole and fed into the resistive network at the negative pole.

In a bipolar grid, sources and loads can be connected between various points in the network: between positive polarity and neutral conductor, between neutral conductor and negative polarity conductor, or directly between positive and negative conductors, advisable for bigger sources and loads. It is evident that in actual applications this could lead to asymmetric loading of the grid, causing increased voltage magnitudes for the nodes of the neutral conductor. Therefore, also the neutral conductor is modeled and all sources and loads are connected between two nodes (m, n).

Multiple sources connected to the same nodes could be useful, e.g., to model a building with solar panels together with the loads of the building. In order to allow multiple sources with different characteristics at the same location an additional sum is made over all individual sources between the same nodes. The node currents are then the algebraic sum of all sources connected on a specific node m:

$$-i_{m,k} = \sum_{n|(m,n,s)\in\mathscr{S}} \sum_{s|(m,n,s)\in\mathscr{S}} i^{\mathrm{S}}_{m,n,s,k} - \sum_{n|(n,m,s)\in\mathscr{S}} \sum_{s|(n,m,s)\in\mathscr{S}} i^{\mathrm{S}}_{n,m,s,k} \qquad \forall m \in \mathscr{N}^{\emptyset} \tag{4.3}$$

Equations (4.2) together with (4.3) are essentially constituting Kirchhoff current law. The node current $i_{m,k}$ is the variable used to describe the interface between the resistive network and the sources together with the loads connected on various nodes as shown in Fig. 3.2b. For a node m of the system, where no current injection or extraction occurs due to the lack of a source or a load, the node current $i_{m,k}$ will be zero. Otherwise the node current $i_{m,k}$, according to (4.3), is equal to the total balance of current injected and extracted from this specific node.

While the power flow in the network can be described fully by previous equations, the power of the sources will be necessary for modeling power limits and marginal cost in terms of energy. The power of the sources is

$$p^{\mathrm{S}}_{m,n,s,k} = (u_{m,k} - u_{n,k}) \cdot i^{\mathrm{S}}_{m,n,s,k} \qquad \forall (m,n,s) \in \mathscr{S} \tag{4.4}$$

which is a bilinear equation, thus making the problem quadratic.

4.2.3. Constraints

A reference node is assumed to be grounded and its voltage is fixed to zero:

$$u_{0,k} = 0\,\mathrm{V} \tag{4.5}$$

Under normal operating conditions the acceptable voltage variation is limited to certain percentage of the nominal operating voltage. Moreover, operational constraints due to line current limits are taken into account. The nodes of the network $\mathcal{N}$ are divided in three groups: $\mathcal{N}_+$ for positive pole, $\mathcal{N}_-$ negative pole and $\mathcal{N}_\mathrm{N}$ neutral conductor. The voltage and line current limits are

$$\underline{U} \le u_{m,k} \le \overline{U} \qquad \forall m \in \mathcal{N}_+ \tag{4.6}$$

$$\underline{U} \le -u_{m,k} \le \overline{U} \qquad \forall m \in \mathcal{N}_- \tag{4.7}$$

$$\underline{U}_\mathrm{N} \le u_{m,k} \le \overline{U}_\mathrm{N} \qquad \forall m \in \mathcal{N}_\mathrm{N} \tag{4.8}$$

$$\underline{I}_{m,n} \le i_{m,n,k} \le \overline{I}_{m,n} \qquad \forall (m,n) \in \mathcal{G} \tag{4.9}$$

The absolute voltage limits above can be relaxed if the differential voltage for the sources is limited:

$$\underline{U}_v \le u_{m,k} - u_{n,k} \le \overline{U}_v \qquad \forall (m,n) \in \mathcal{S}_v, \forall v \tag{4.10}$$

The sources can be constrained by current and power limits:

$$\underline{I}^\mathrm{S}_{m,n,s} \le i^\mathrm{S}_{m,n,s,k} \le \overline{I}^\mathrm{S}_{m,n,s} \qquad \forall (m,n,s) \in \mathcal{S} \setminus \mathcal{B}^\mathrm{var} \tag{4.11}$$

$$\underline{P}^\mathrm{S}_{m,n,s,k} \le p^\mathrm{S}_{m,n,s,k} \le \overline{P}^\mathrm{S}_{m,n,s,k} \qquad \forall (m,n,s) \in \mathcal{S} \setminus \mathcal{B} \tag{4.12}$$

Current can be used to model limits of power electronics while power is more appropriate for process limits. The separation of these two limits may be preferable when significant voltage deviations in the distribution grids are considered. The power constraint (4.12) can be seen as a quadratic inequality constraint due to (4.4) being quadratic.

4.2.4. Mixed Integer Storage Model and Constraints

Energy storage systems are assumed to have a converter connecting them to the grid. They are modeled using a source as described in Section 4.2.2 and augmented with additional equations. The converter is modeled with constant efficiency $\eta_{m,n,s}$ for charging and discharging. The storage itself is assumed to be without losses and thus is modeled as an integrator of the secondary converter power. The energy content of the storage system is limited with and upper and lower bound:

$$\underline{E}_{m,n,s,k} \le e_{m,n,s,k} \le \overline{E}_{m,n,s,k} \qquad \forall (m,n,s) \in \mathcal{B}^\mathrm{fix} \tag{4.13}$$

These limits can change over time to model minimum backup requirements or minimum range of electric vehicles.

Renewable energy sources often have zero marginal cost. In case of abundant energy supply or congestions it can happen that the locational marginal prices become zero. In

that case losses in the system would not have an impact on the objective function. Without integer variables the model would be prone to multiple optimal solutions that could include charging and discharging at the same time. This would be invalid solutions as a converter can physically only do either at the same time. The double losses would have impact on all other system variables. Therefore a binary variable $b_{m,n,s,k}$ is introduced to indicate if a storage system is charging ($b_{m,n,s,k} = 1$) or discharging ($b_{m,n,s,k} = 0$). The power is limited to be positive if charging and negative if discharging:

$$(1 - b_{m,n,s,k}) \cdot \underline{P}^{\mathrm{S}}_{m,n,s,k} \leq p^{\mathrm{S}}_{m,n,s,k} \leq b_{m,n,s,k} \cdot \overline{P}^{\mathrm{S}}_{m,n,s,k} \qquad \forall (m,n,s) \in \mathscr{B}^{\mathrm{fix}} \tag{4.14}$$

The initial energy content of all storage systems have to be defined:

$$e_{m,n,s,0} = E_{m,n,s,0} \qquad \forall (m,n,s) \in \mathscr{B}^{\mathrm{fix}} \tag{4.15}$$

The main storage equation is coupling the energy content for adjacent time steps. It is integrating the secondary power of the storage converter over the time difference between the time steps.

$$\begin{aligned} e_{m,n,s,k+1} = & e_{m,n,s,k} + p_{m,n,s,k} \cdot (t_{k+1} - t_k) \cdot \\ & \left(b_{m,n,s,k} \cdot \eta_{m,n,s} + (1 - b_{m,n,s,k}) \cdot \frac{1}{\eta_{m,n,s}} \right) \end{aligned} \qquad \forall (m,n,s) \in \mathscr{B} \tag{4.16}$$

The time difference is modeled explicitly in order to allow for variable time steps. In this way the near future can be modeled with high resolution while memory and computation power is saved when modeling longer future events. The secondary power is reduced by the converter efficiency while charging. However when discharging the secondary power is greater than the primary one in order to compensate for the converter losses.

4.3. MULTI PERIOD OPTIMAL POWER FLOW

After modeling the grid, sources, constraints and energy storage systems, the OPF is solved in order to minimize total operation cost. A two-step method following a similar approach as that in [9] is used to solve the economic dispatch and derive the LMP. After introducing the function in the next section, firstly the exact model is used to find the optimal solution for the economic dispatch of generators and loads. Secondly the problem is linearized at the found optimal solution in order to derive the LMP.

4.3.1. COST / VALUE FUNCTION OF SOURCES

The operation cost of each generator and load is defined by a given marginal cost $\Pi^{\mathrm{S}}_{m,n,s,k}$. Demand response of loads can be implemented by giving them a marginal value and allowing the power to be variable. Load shedding with different priorities is implemented by giving different values to loads and not setting the maximum and minimum power equal but allowing for an operation range. If the price is higher they will turn off. The marginal cost of generators and especially the marginal value of demand can change over time. In this way time dependent preferences can be modeled.

4.3.2. SOLVING FOR THE ECONOMIC DISPATCH

The multiplication of two variables in (4.4) makes the objective function bilinear, a special case of quadratic programming for which the problem is not convex. Further the binary variable $b_{m,n,s,k}$ makes it a mixed integer quadratic program. The energy storage systems link all time steps together in (4.16). The objective function (4.17) is computed using mixed integer quadratic programming while being constrained by the network's model for a given grid topology. The economic dispatch is then defined by $i^{\mathrm{S}}_{m,n,s,k}$ and branch currents are calculated for all $(m,n) \in \mathscr{G}$ and node voltages and currents for all $m \in \mathscr{N}$.

The problem formulation is presented as follows:

$$\begin{aligned} \min \quad & \sum_{k=0}^{K-1} \sum_{(m,n,s)\in\mathscr{S}} -p^{\mathrm{S}}_{m,n,s,k} \cdot \Pi^{\mathrm{S}}_{m,n,s,k} \cdot (t_{k+1} - t_k) \\ \text{s.t.} \quad & (4.1) - (4.16) \end{aligned} \tag{4.17}$$

The power of each source and load is multiplied by the marginal cost and weighted by the duration of the respective time step. This represents the minimization of the total cost over the optimization horizon and is equivalent to the maximization of the social welfare. The lifetime degradation of the energy storage systems due to usage is neglected. The choice of sign and minimization is important for the marginal values that will be used in the next section.

It is important to note that due to the non-convexity of the problem an optimal solution is not guaranteed to be the global optimum. This aspect has to be dealt with by the optimization algorithm, which is not in the scope of this chapter. It is assumed that the found solution is the acceptable, even if possibly not globally optimal.

4.3.3. LOCATIONAL MARGINAL PRICES (LMP)

After having found a optimal solution in the previous section, the LMP are now to be calculated. Non-convex problems suffer from a weak duality between the objective function and constraints. As opposed to linear programming, dual variables cannot generally be used to interpret LMP when non-convex quadratic programming is used. To price the non-convex problem, the problem is linearized at the optimal solution [9].

LINEARIZATION

Firstly, the quadratic problem (4.17) is solved and the optimal voltages $u^*_{m,k}$ and source currents $i^{\mathrm{S}*}_{m,n,s,k}$ are obtained. Then the problem is linearized around this optimal solution. This means that power equation (4.4) has to be linearized. By using the first order Taylor approximation this results in

$$\begin{aligned} p^{\mathrm{S}}_{m,n,s,k} = {} & (u^*_{m,k} - u^*_{n,k}) \cdot i^{\mathrm{S}}_{m,n,s,k} \\ & + (u_{m,k} - u_{n,k}) \cdot i^{\mathrm{S}*}_{m,n,s,k} \\ & - (u^*_{m,k} - u^*_{n,k}) \cdot i^{\mathrm{S}*}_{m,n,s,k} \end{aligned} \qquad \forall (m,n,s) \in \mathscr{S} \tag{4.18}$$

Further the binary variable distinguishing charging and discharging of energy storage systems is fixed to the optimal value thus making a constant parameter out of it:

$$b_{m,n,s,k} = b^*_{m,n,s,k} \tag{4.19}$$

Herewith a linear optimization problem can be re-formulated as

$$\begin{aligned} \min \quad & \sum_{k=0}^{K-1} \sum_{(m,n,s)\in\mathscr{S}} -p^{\mathrm{S}}_{m,n,s,k} \cdot \Pi^{\mathrm{S}}_{m,n,s,k} \cdot (t_{k+1} - t_k) \\ \text{s.t.} \quad & (4.1) - (4.3), (4.18), (4.5) - (4.16), (4.19) \end{aligned} \tag{4.20}$$

The problem formulation (4.20) is now linear without integer variables, thus convex and with strong duality. Under the assumption that (4.20) provide the same optimal solution as (4.17), the dual variables of the latter can be used to obtain the LMP. The global objective will be the same if the variables computed using linear programming are the same as for quadratic programming. Therefore, the dual variables can be used to derive the LMP for the original problem [10].

LMP is the marginal cost of supplying the next increment of energy at a location. LMP are commonly expressed in terms of power and reflect losses and congestions [11–15]. In the model proposed, generation levels of all sources define the economic dispatch. Accordingly, the dual variables obtained from the equality constraint (4.2) for each node are given in terms of current and denoted by $\lambda^{\mathrm{I}}_{m,k}$. Using linear programming enables the interpretation of these dual variables as the LMP for all m. However they are terms of current [m.u./A], which is not the usual unit.

LMP IN TERMS OF POWER

LMP in power terms are calculated for all generators and loads connected between different nodes (m,n). Their value can be derived as follows: Let $\alpha_{m,n,s,k}$ be the amount payable by a prosumer per time interval, which is by definition the power times the LMP:

$$\alpha_{m,n,s,k} = p^{\mathrm{S}}_{m,n,s,k} \cdot \lambda^{\mathrm{P}}_{m,n,k} \tag{4.21}$$

On the other hand this amount has to be equal to the amount payable for extracting the source current $i^{\mathrm{S}}_{m,n,s,k}$ in one node and injecting it in the other:

$$\begin{aligned} \alpha_{m,n,s,k} &= \lambda^{\mathrm{I}}_{m,k} \cdot i^{\mathrm{S}}_{m,n,s,k} + \lambda^{\mathrm{I}}_{n,k} \cdot (-i^{\mathrm{S}}_{m,n,s,k}) \\ &= (\lambda^{\mathrm{I}}_{m,k} - \lambda^{\mathrm{I}}_{n,k}) \cdot i^{\mathrm{S}}_{m,n,s,k} \end{aligned} \tag{4.22}$$

By solving (4.21) for $\lambda^{\mathrm{P}}_{m,n,k}$ and substituting (4.22) and (4.4), the LMP in terms of power between nodes (m,n) can be derived as

$$\begin{aligned} \lambda^{\mathrm{P}}_{m,n,k} &= \frac{\alpha_{m,n,s,k}}{p^{\mathrm{S}}_{m,n,s,k}} = \frac{(\lambda^{\mathrm{I}}_{m,k} - \lambda^{\mathrm{I}}_{n,k}) \cdot i^{\mathrm{S}}_{m,n,s,k}}{(u_{m,k} - u_{n,k}) \cdot i^{\mathrm{S}}_{m,n,s,k}} \\ &= \frac{\lambda^{\mathrm{I}}_{m,k} - \lambda^{\mathrm{I}}_{n,k}}{u_{m,k} - u_{n,k}} \end{aligned} \tag{4.23}$$

So the LMP between two nodes in terms of power is equal to the difference of current LMP $\lambda^{\mathrm{I}}_{m,k}$ divided by the voltage difference of the nodes $u_{m,k}$.

The LMP $\lambda^{\mathrm{I}}_{m,k}$ and $\lambda^{\mathrm{P}}_{m,k}$ depend on the duration of the time period because a change in power for a longer time period have a greater influence on the total system cost than one of a short period. Therefore a normalized LMP $\lambda^{\|\mathrm{P}\|}_{m,k}$ is calculated as follows:

$$\lambda^{\|\mathrm{P}\|}_{m,k} = \frac{\lambda^{\mathrm{P}}_{m,k}}{(t_{k+1} - t_k)} = \frac{\lambda^{\mathrm{I}}_{m,k} - \lambda^{\mathrm{I}}_{n,k}}{(u_{m,k} - u_{n,k})(t_{k+1} - t_k)} \tag{4.24}$$

This normalized LMP can be directly related to the marginal cost $\Pi^{\mathrm{S}}_{m,n,s,k}$ of generators and loads and will be used for the presentation in the following section.

4

MARGINAL LOSSES

Using the marginal values of the exact OPF as LMP, results in the inclusion of marginal losses into the price. The LMP are not only enhanced by the power lost on the line but they reflect the losses that would occur if an incremental unit of load was added. Thereby the line losses have a greater impact on the price than the their physical value. The marginal losses are approximately twice as high as the cost of the physical losses. This is known from literature for ac grids and is therefore not in detail discussed in this chapter [16].

4.4. EXAMPLES

In this section several examples are shown in order to demonstrate the methodology presented in the previous sections. It is not the intention to show realistic average use scenarios but rather to show extreme cases that show case special conditions that could occur in bipolar dc distribution grids. The timelines show the steady state power flow without any dynamics or uncertainties.

4.4.1. CASE 1: BALANCING BY STORAGE TO REDUCE LINE LOSSES

The first case study is to show the how storage can balance the power flow in long lines with asymmetric loading. In Fig. 4.1 the schematic for this case is shown. The cables made of aluminum with 95 mm^2 and have an resistance of 0.2975 Ω/km (3.361 S) with a current limit of 186 A. The middle part has a length of 1000 m the left and right part are of 100 m length. The operating voltage range for all sources are defined from 325 to 375 V.

On the left and right there are each two energy storage systems connected between pole and neutral. For this case each of these storage systems have the approximate specifications of two Tesla Powerwalls. With a maximum charge and discharge power of 6.6 kW and 12.8 kWh of energy capacity. A round trip efficiency of 90% is assumed. The initial state of energy content is assumed to be 0 kWh.

There is a generator with a marginal cost of 5 m.u/kWh at each pole on the left middle. The load on the positive pole uses 3 kW normally but has a higher power need from 01:00 till 04:00 of 18 kW. The load on the negative pole uses 2 kW normally and has a higher power need from 02:00 till 05:00 of 15 kW. This will create a large unbalance from 01:00 till 02:00 and from 04:00 till 05:00.

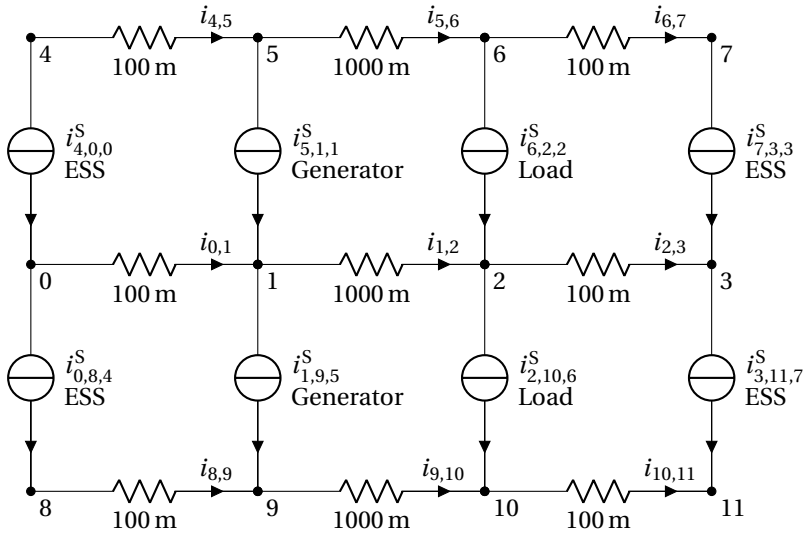

Figure 4.1: Case 1: Bipolar dc grid with two storage systems on the left and two generators, a long cable in the middle and two loads with two energy storage systems on the right.

The multi-period optimal power flow is computed. The energy storage system on the negative pole on the right is being used to balance the current in the long line during this times.

An interesting observation can be made when analyzing the resulting voltages. It can be seen that in the case of heavy unbalance (from 01:00 to 02:00 and from 04:00 to 05:00) the voltage of the less loaded pole is reduced to the minimum. This seems on the first look counter-intuitive. This occurs when the current in the neutral conductor is higher than the that in the less loaded pole conductor. For the same power on the less loaded conductor the current in the pole can be increased and the one in the neutral conductor can be reduced by reducing the voltage on the less loaded pole.

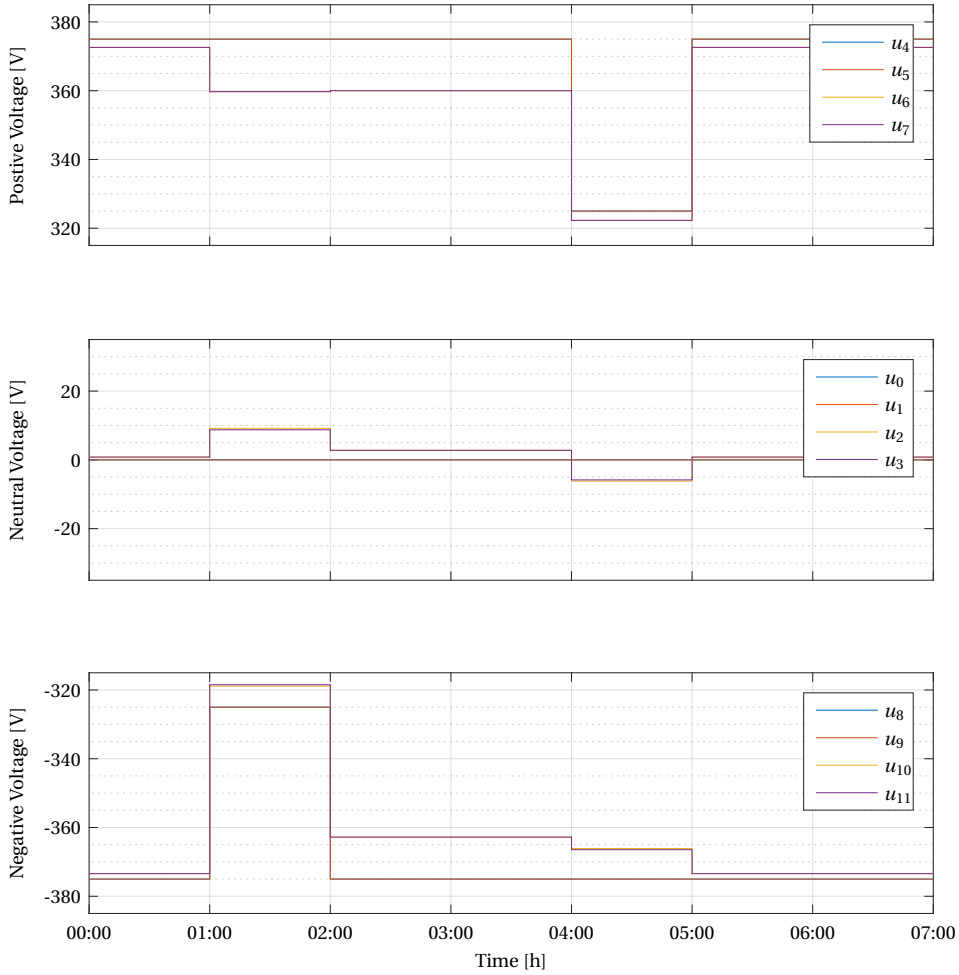

Figure 4.2: The voltages over time. It can be seen that the negative voltage is reduced to the minimum between 01:00 and 02:00 and the positive voltage is reduced to the minimum between 04:00 and 05:00. This reduces the losses in the neutral conductor.

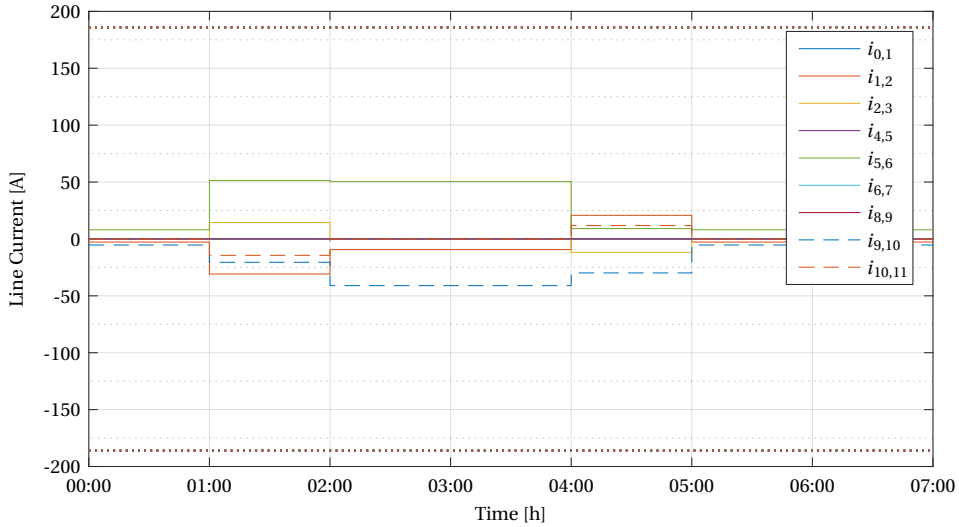

Figure 4.3: The line currents never reach the cable limit. It can be seen that the neutral line current $i_{1,2}$ has a higher magnitude than the negative line current $i_{9,10}$ between 01:00 and 02:00. This is the reason for the voltage to go to the minimum. The equivalent can be seen on the positive conductor between 04:00 and 05:00.

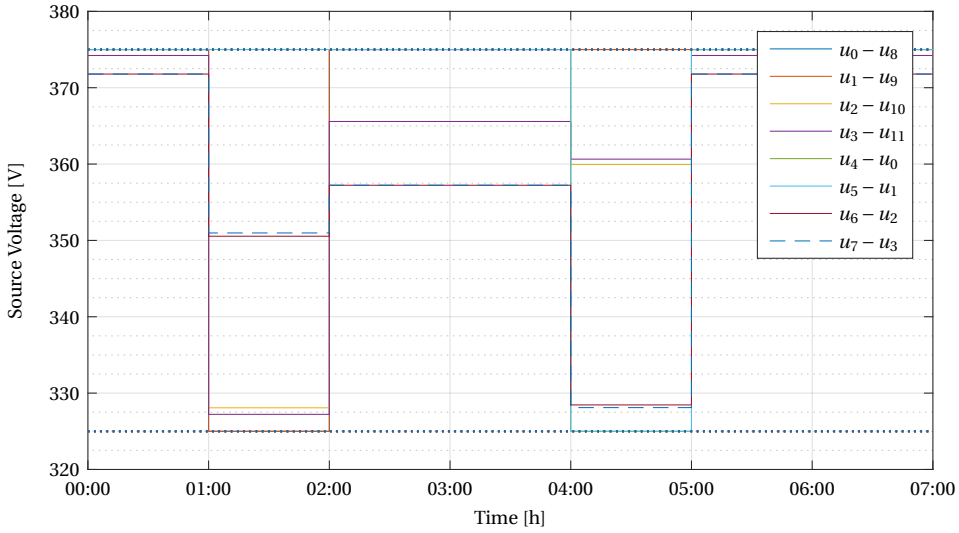

Figure 4.4: Voltages across the source terminals. The upper and lower limits are shown as dotted lines. It can be seen how the voltage is reduced to the minimum between 01:00 and 02:00 and 04:00 and 05:00 on the negative and positive pole respectively.

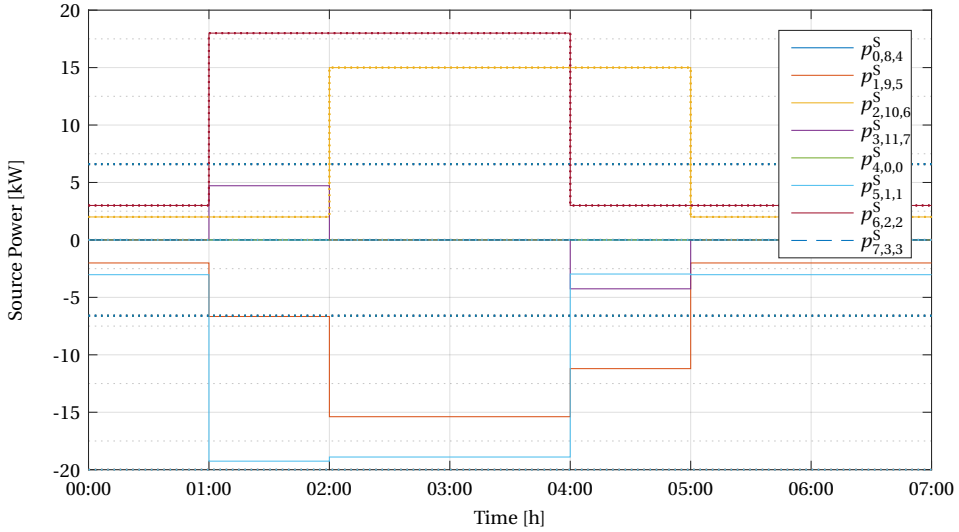

Figure 4.5: Power of the sources. The positive pole load $p^S_{6,2,2}$ goes to 18 kW from 01:00 till 04:00. The negative pole load $p^S_{2,10,6}$ goes to 15 kW one hour later. This creates the large unbalance. The storage unit on the negative pole $p^S_{3,11,7}$ charges at the first unbalance and discharges at the second. The limits are shown as dotted lines.

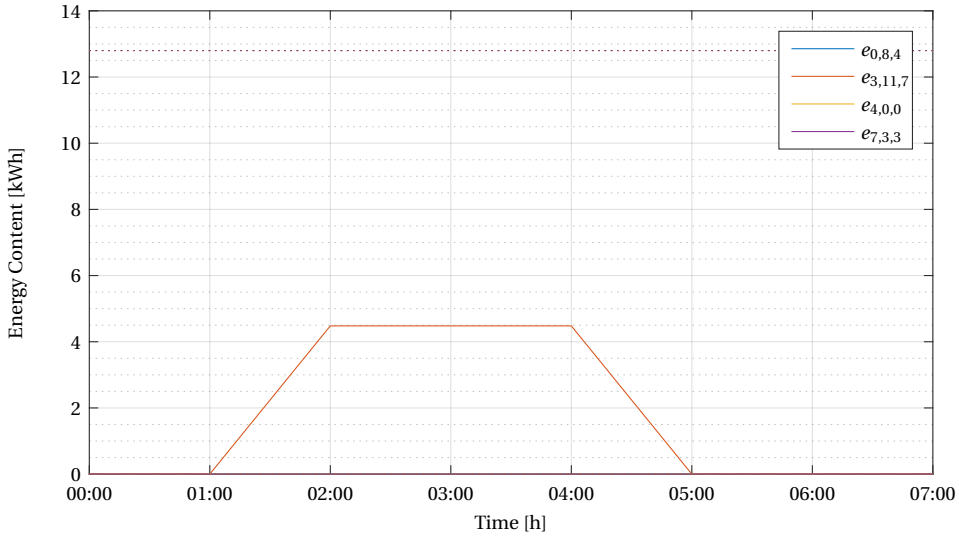

Figure 4.6: The energy content of all energy storage systems. Only one of the storage systems ($e_{3,11,7}$) is charging from 01:00 till 02:00 to balance the grid and discharging from 04:00 till 05:00. The capacity limits are shown as dotted lines.

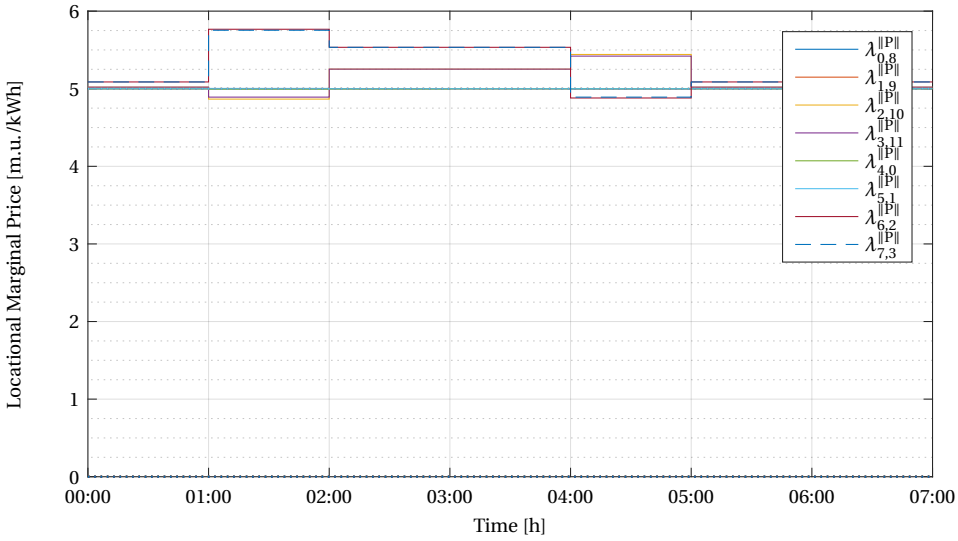

Figure 4.7: The LMP in the grid change over time. Due to the unbalance the prices increase during two time periods. This is when it is economical to use the storage systems. On the pole that is less loaded the prices even fall below the marginal cost of the source. This is caused by the voltage rise in the neutral conductor that provides power from the other pole. The marginal costs are shown as dotted lines.

4.4.2. CASE 2: ±350 V DC GRID WITH 700 V PV AND STORAGE

The second case study shows the effect of pole-to-pole connected sources. In Fig. 4.8 the grid schematic is shown. Two pole-to-neutral loads are connected on the left followed by two generators. In the middle two pole-to-neutral energy storage systems are connected. On the right a photovoltaic system is connected pole-to-pole in parallel with an energy storage system. The neutral conductor is left unconnected.

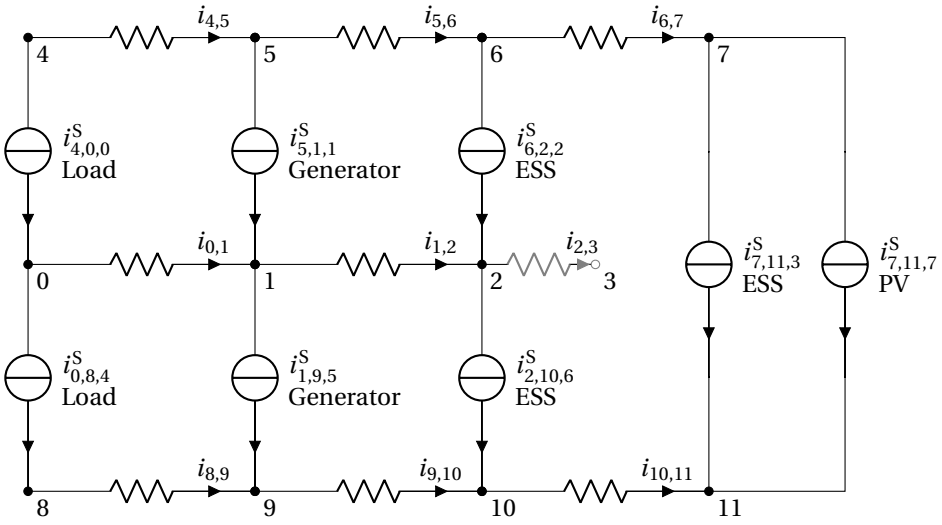

Figure 4.8: Circuit diagram of Case 2. Two loads and two expensive generators are connected on the left. In the middle two pole-to-neutral energy storage systems can be used for balancing. On the right a more efficient energy storage system is connected pole-to-pole in parallel with a large PV system.

In the following figures the individual values of the optimal power flow are shown and described in the figure captions.

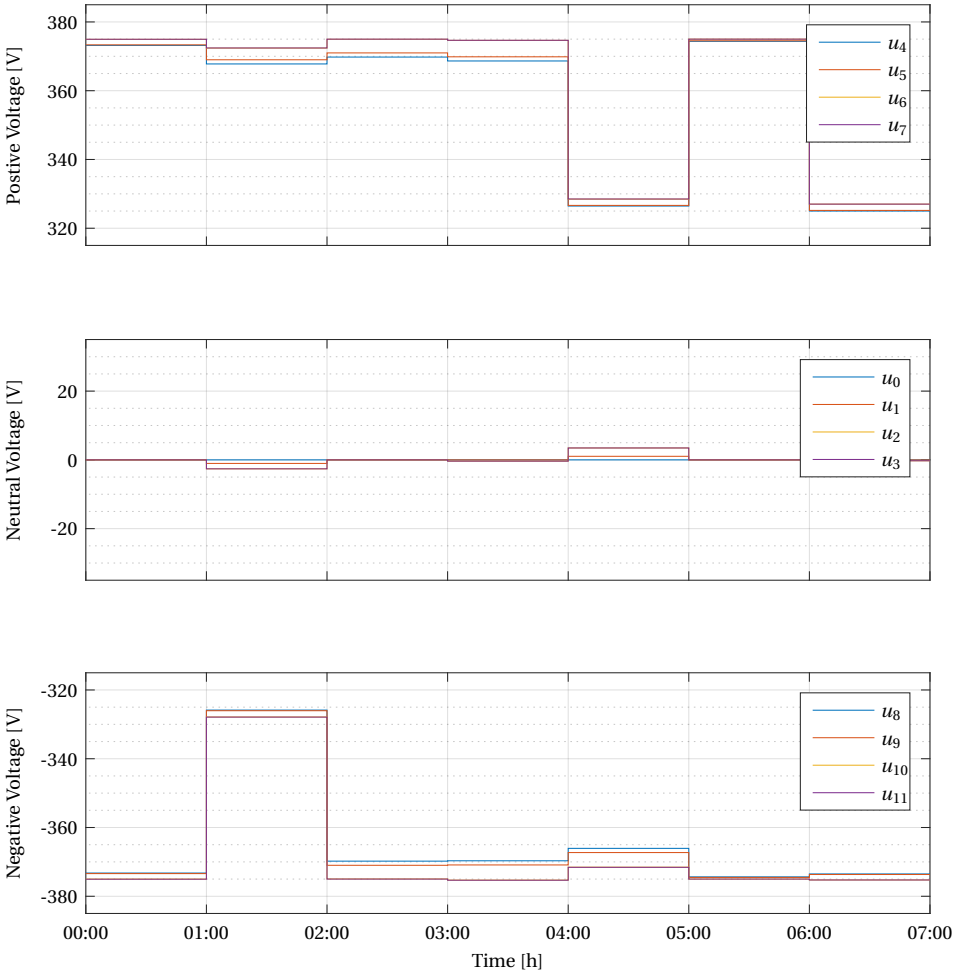

Figure 4.9: The voltages over time. It can be seen that the the negative voltage is minimized between 01:00 and 02:00 and the positive voltage between 04:00 and 05:00. This is to reduce the net current in the neutral conductor and minimize losses.

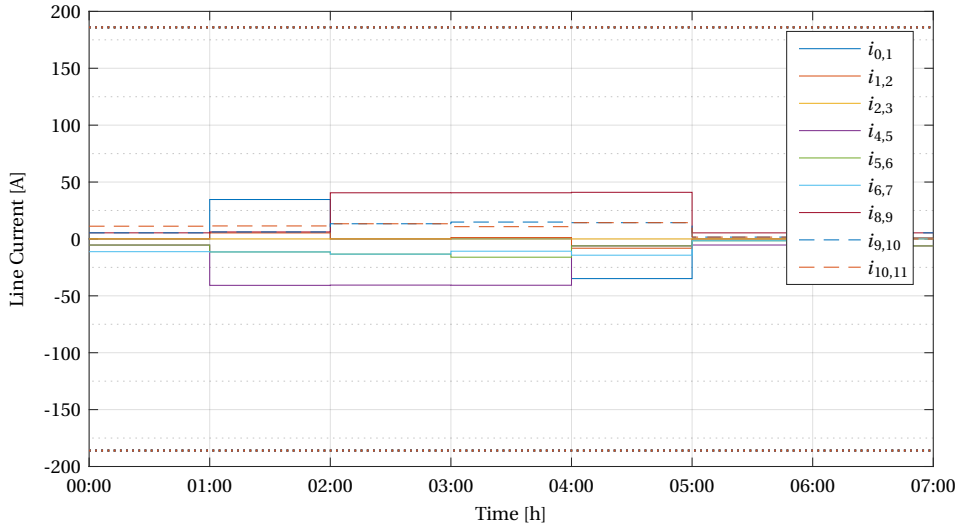

Figure 4.10: The current in all individual lines. The constraints are shown in dotted lines. No constraints are active. It can be seen between 01:00 and 02:00, that the neutral current $i_{0,1}$ is much higher than the negative current $i_{8,9}$ this is the reason it is more efficient to reduce the negative voltage to the minimum and increase the current in the negative conductor.

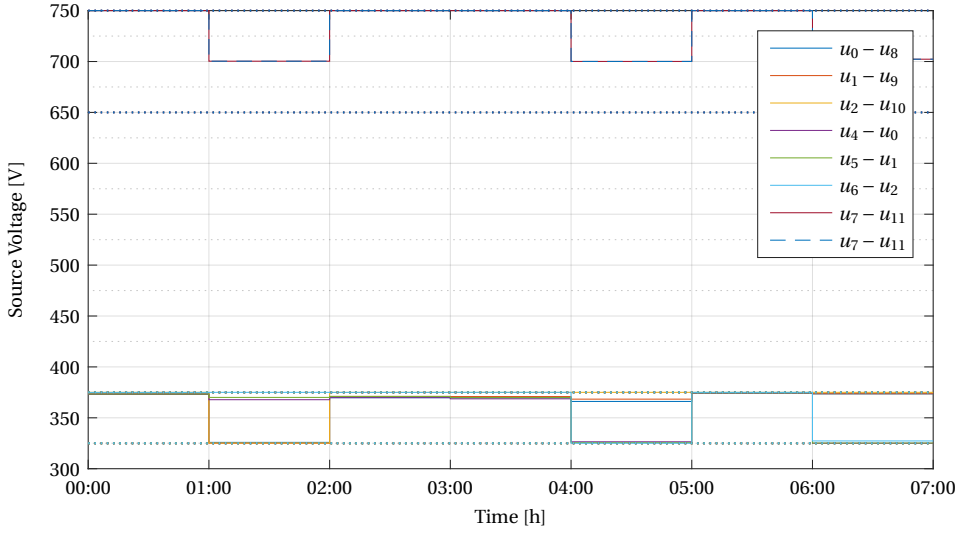

Figure 4.11: Voltages across the source terminals. The pole to pole voltages are seen to be reduced where one of the poles reduces to minimum voltage. The limits are shown with dotted lines.

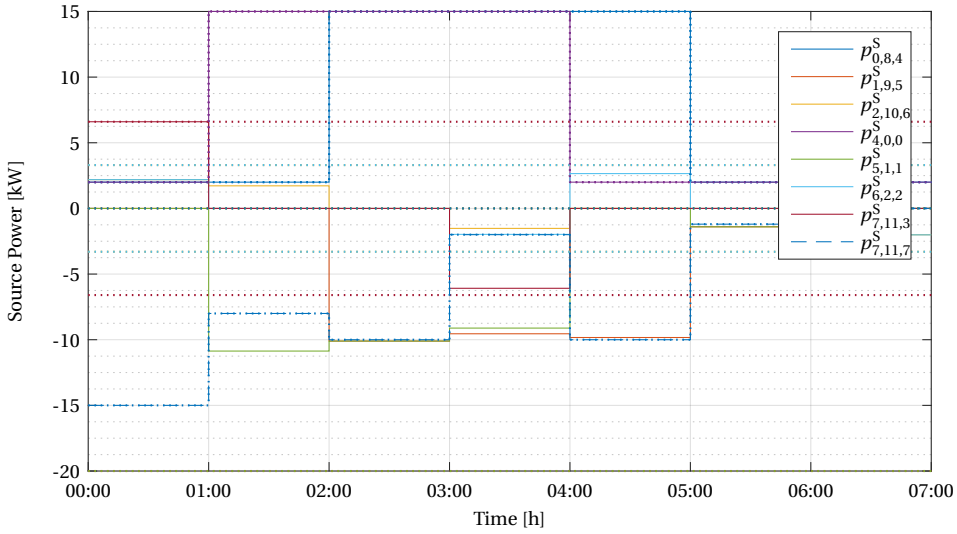

Figure 4.12: Power of the sources. The limits of the sources are shown in dotted lines. The two loads $p^S_{4,0,0}$ and $p^S_{0,8,4}$ are changing in a time shifted and cause a unbalance between the poles. Further the PV source $p^S_{7,11,7}$ is fluctuating. This causes the storage units to balance the power. The pole-to-pole connected ESS $p^S_{7,11,7}$ is reaching the charging power limit.

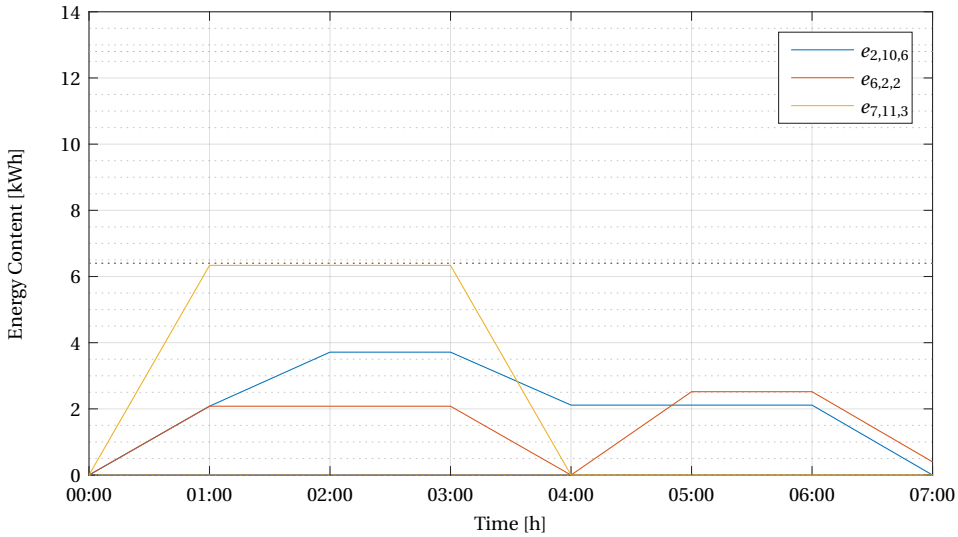

Figure 4.13: The stored energy with the energy limits shown by dotted lines. The pole-to-pole connected storage unit is limited in power not in energy. It is charging at higher power, due to its higher energy efficiency.

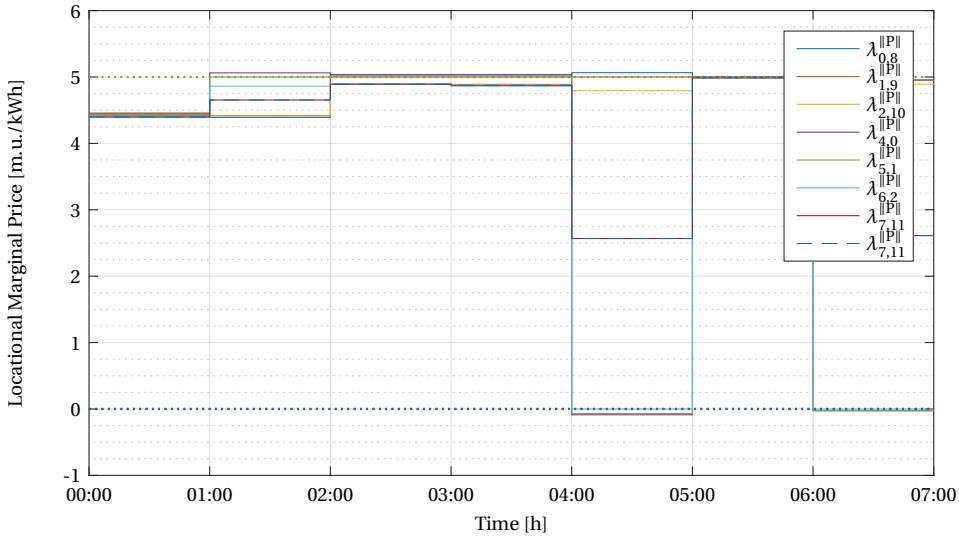

Figure 4.14: The LMP in the grid change over time. The dotted lines show the marginal cost of the sources. The price in the beginning is driven high by the storage it stays at 90 %of the price between 03:00 and 04:00 due to the efficiency of the ESS. Between 04:00 and 05:00 it can be seen how the pole-to-pole connection LMP is the average of the pole-to-neutral ones.

4.4.3. CASE 3: DC DISTRIBUTION GRID WITH TWO LV/MV CONVERTERS

For the third case study a bigger grid is assumed. The schematic is shown in Fig. 4.15. The dc grid is connected at two points to a higher level grid with identical time dependent prices. It is assumed that the higher level grid a so large that its prices are not affected by the dc grid. The converters are connected pole-to-pole, so only balanced power can be taken out of the grid. Their power limit is 100 kW in each direction.

On the left 4 electric vehicles are connected. Two of them can only charge while the other two can also discharge back into the grid. In the middle two time dependent loads exist. Further two small stationary energy storage systems are installed. A combined heat and power plant is assumed to be available at demand for at a high marginal cost. Two PV systems are available. The system is intentionally put in unbalance giving a smaller size to the negative pole PV pannel.

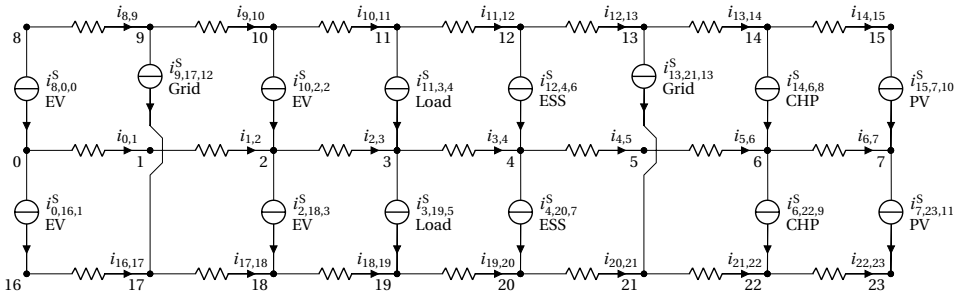

Figure 4.15: Circuit diagram of Case 3. A ±350 V network with positiv pole on top and negative pole on the bottom. Two LV/MV converters with a 700 V pole-to-pole connection connect to the higher level grid. All other sources are pole-to-neutral. The left side has loads, while the right side consists of generators. Two energy storage systems are in the middle.

A optimization for two days is made. The effects are shown in the following figures and are explained in the respective captions.

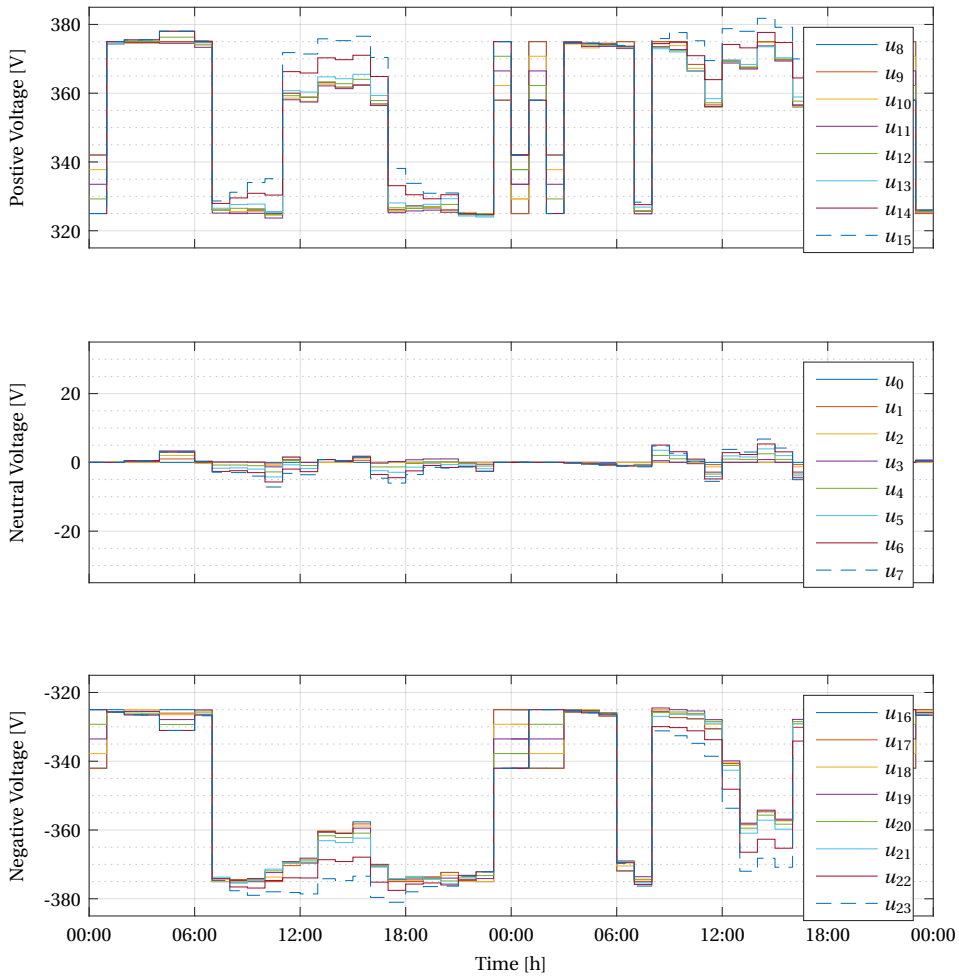

Figure 4.16: The node voltages over time. It can be seen that the voltage is in this case often not at the maximum (minimum) limit. The reason for this is on one hand the unbalance of over 50 % which results in less losses if the current of the neutral conductor is decreased, which is the result of reducing the voltage of the less loaded conductor and increasing its current. On the other hand, the voltage is also reduced if the marginal prices are negative. This is the case from 01:00 until 06:00 on the negative conductor. Further the voltage spread can be seen as a result of high current flow. This is the case in the middle of the day, when the photo voltaic systems feed power into the grids.

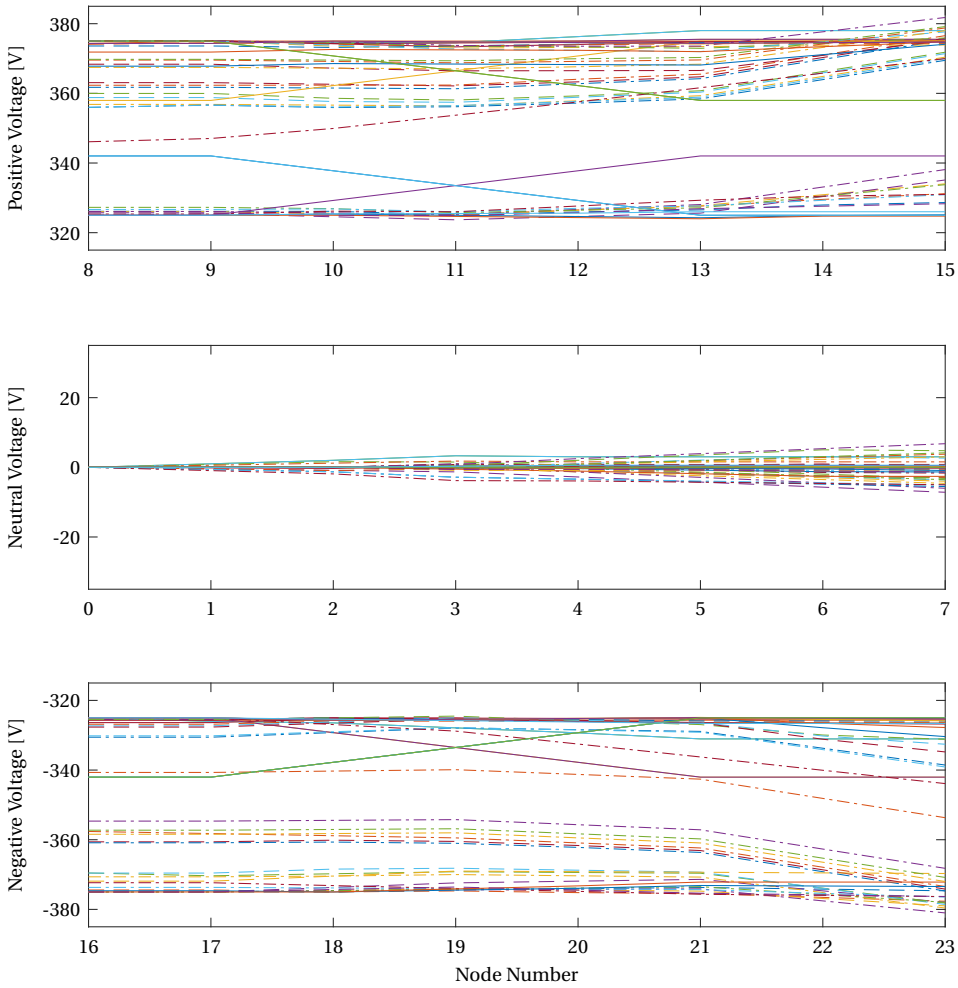

Figure 4.17: In this figure an overview of the voltage profiles along the line is shown. It can be seen that the profile is quite flat some times but in other times there is significant voltage drop. In no case the full voltage range was used, so there did not occur curtailment because of voltage drop constraints. The voltage constraints are applied between the positive and negative pole at connections. Therefore the absolute value with respect to ground (Node 0) can be higher than the applied limit of 375 V as can be seen at Node 15.

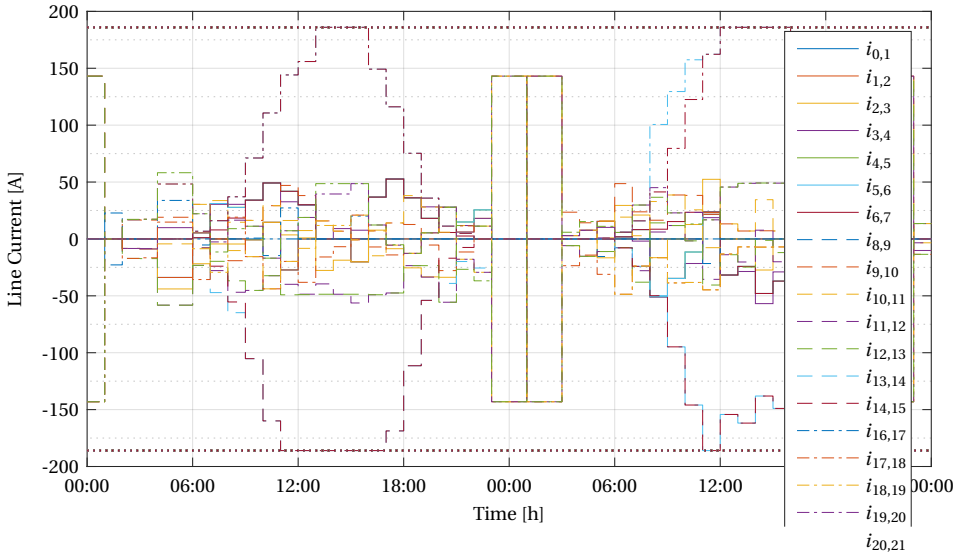

Figure 4.18: The line currents in each individual conductor are shown. The dotted lines are the current limit. It is identical for all lines. It is reached for the lines connecting the photo voltaic systems around noon. This congestion leads to nodal prices of zero as will be shown in a later figure.

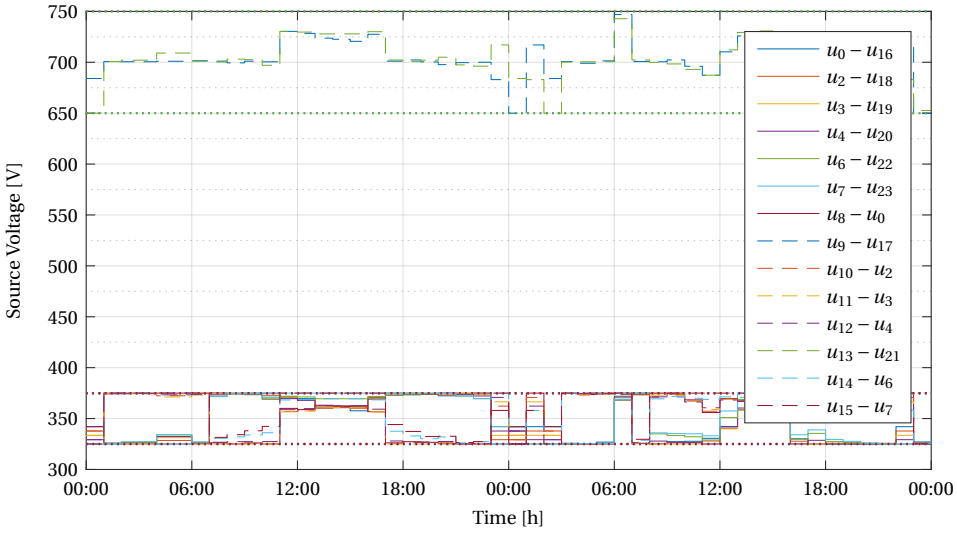

Figure 4.19: Voltages across the source terminals. This voltages are subject to the voltage constraints shown as dotted lines. The pole-to-pole connected converters have a limit of 650 V to 750 V while the pole-to-neutral connected converters should operate between 325 V and 375 V.

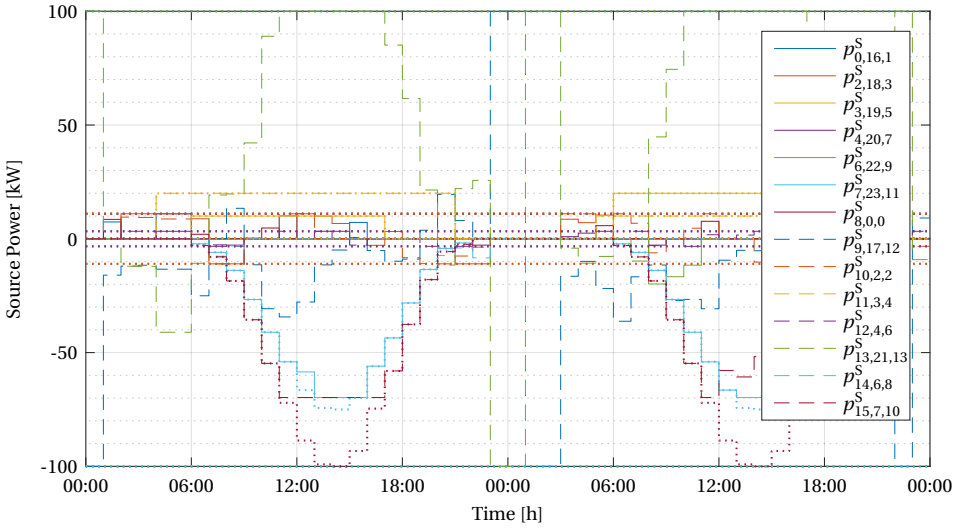

Figure 4.20: Power of generators (negative) and loads (positive). The dotted lines show the limits. It can be seen that the photo voltaic systems are curtailed and don't use their full power around noon.

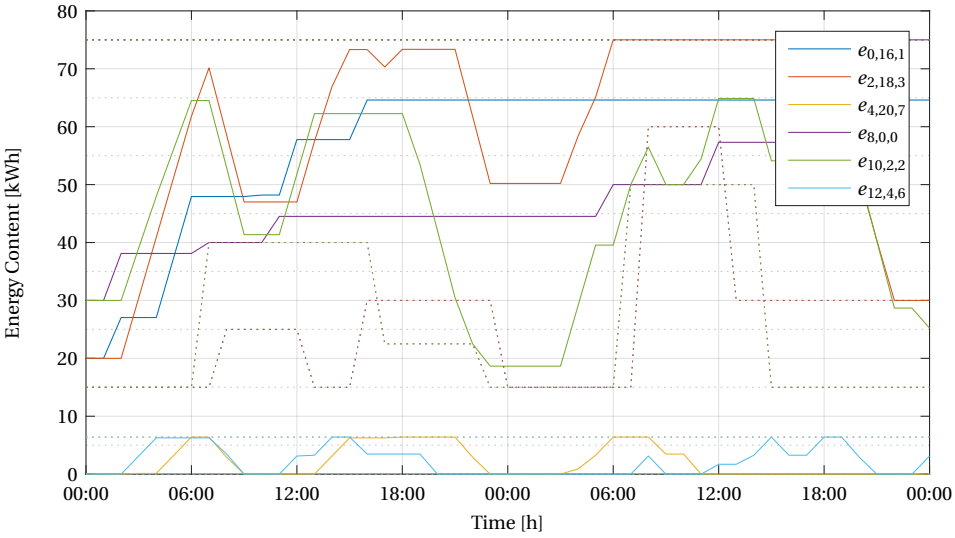

Figure 4.21: The stored energy in the storage systems and electric vehicles. The upper and lower energy limits are shown it dotted lines. These limits change over time for the electric vehicles. This is due to the energy needed to drive to the destination at a scheduled time. In this example the electric vehicle do not perform that travel but instead stay connected. Two electric vehicles can only charge while the others can also discharge. The two stationary energy storage systems are very small compared to the electric vehicles and have fixed limits.

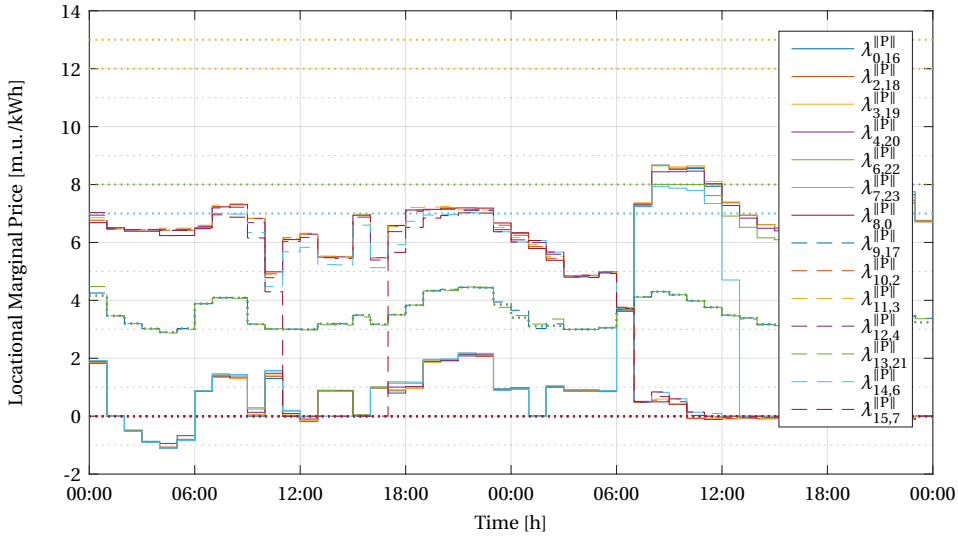

Figure 4.22: The LMP in the grid changes over time. It can be seen that the pole to pole connected grid converters that connect to a higher level grid link the prices on the two poles. The are the average of the two individual prices. As their price is determined by the higher level grid as long as they are active they can drive one of the pole prices negative as can be seen from 02:00 until 06:00. It can be seen how the prices at the pv system drop to zero where the line congestion occurs at 11:00 till 17:00.

4.4.4. CASE 4: VARIABLE TIME PERIOD

Case 4 is identical with case 3 except that now variable time steps are used. Variable time steps can be used to reduce the computation time used for events further in the future where generally also the uncertainty is bigger. The data of several hours is averaged for the further away time periods. The time steps are given inputs. This approach would favorably be used with a moving horizon. The result can be seen in the following figures.

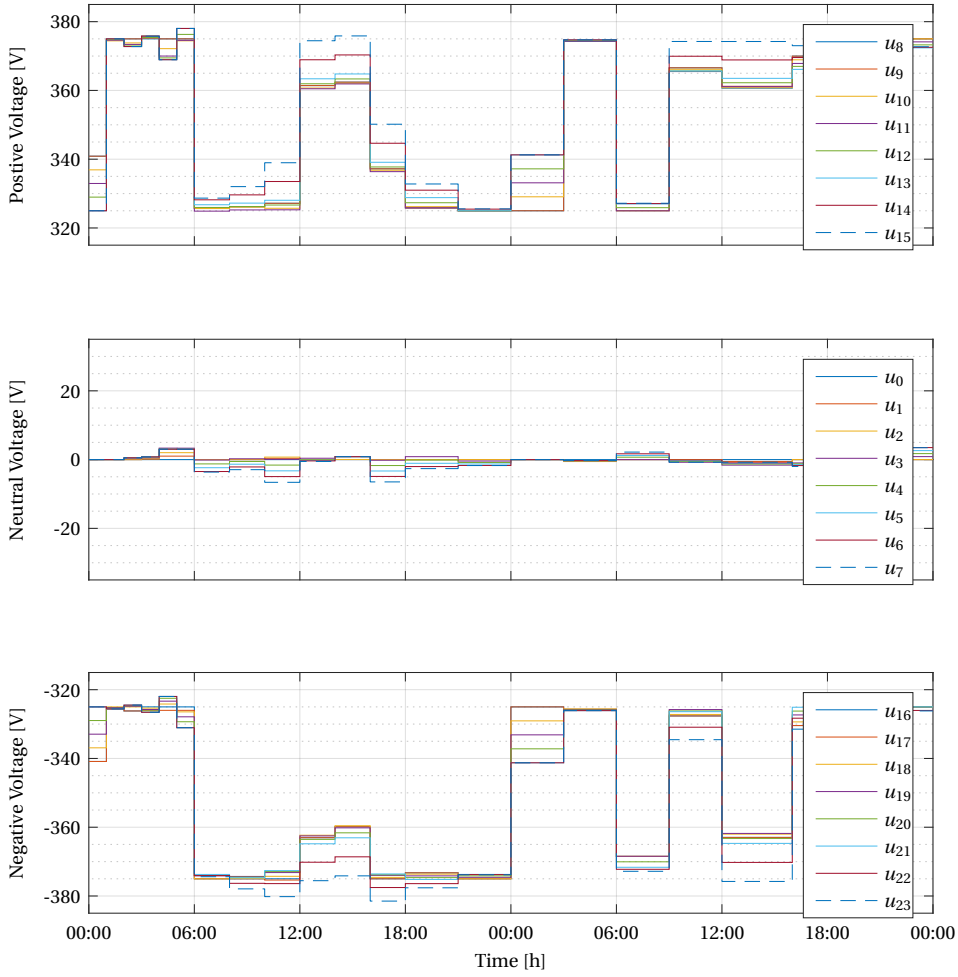

Figure 4.23: The voltages over time.

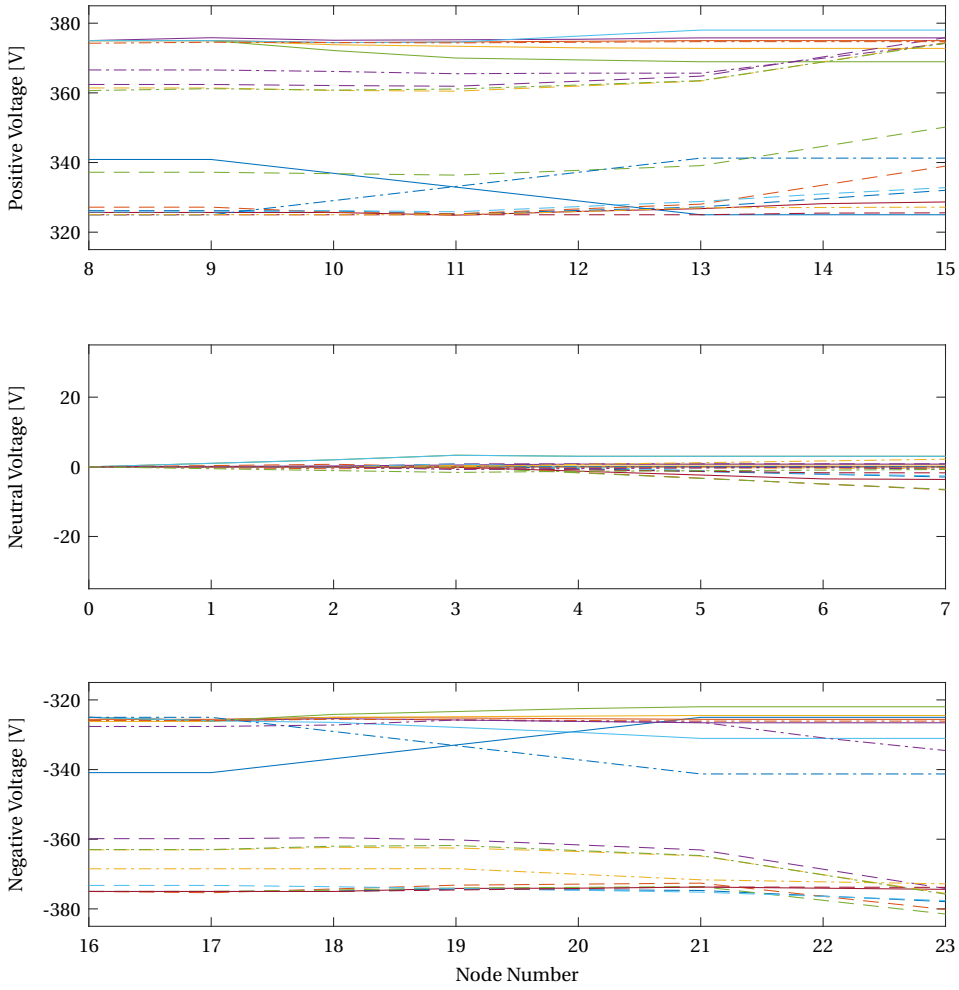

Figure 4.24: Voltage drop along the line.

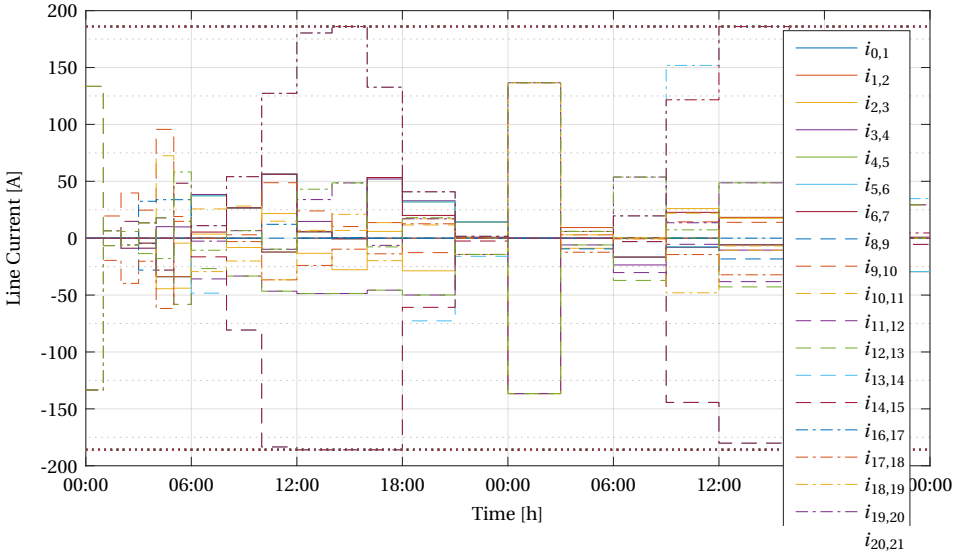

Figure 4.25: Line Currents.

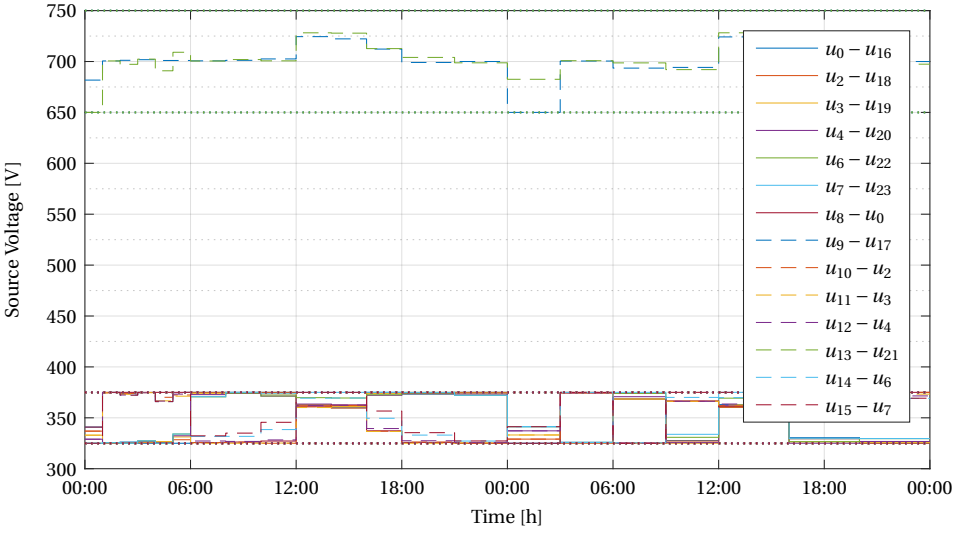

Figure 4.26: Voltages across the source terminals.

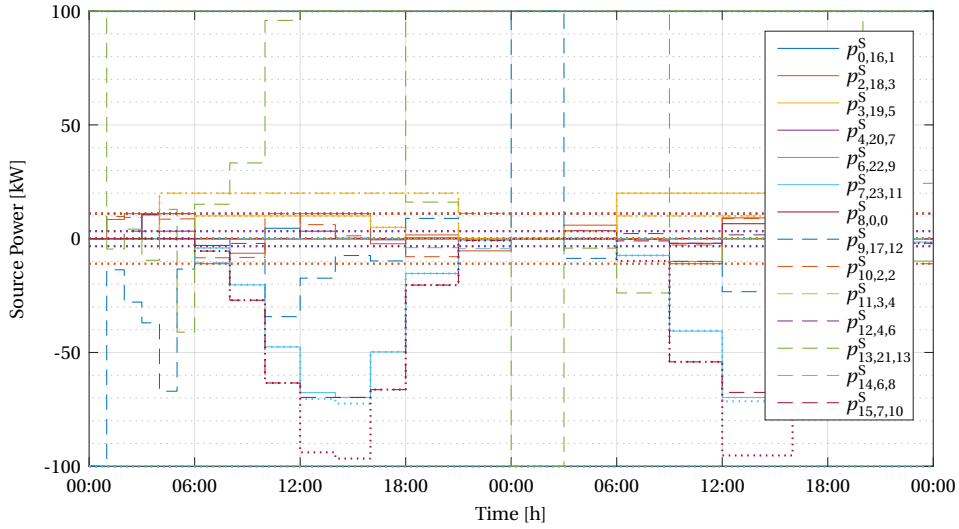

Figure 4.27: Power of the sources.

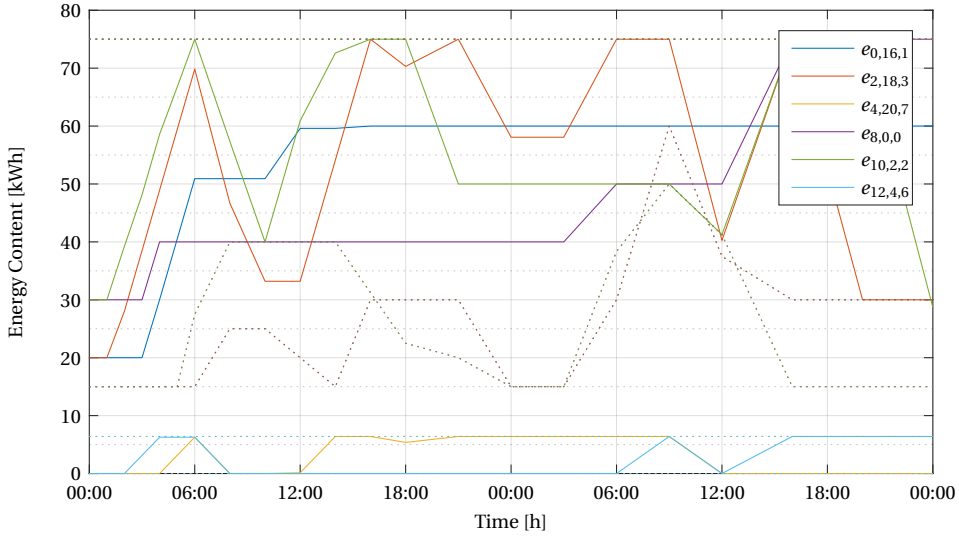

Figure 4.28: The stored energy.

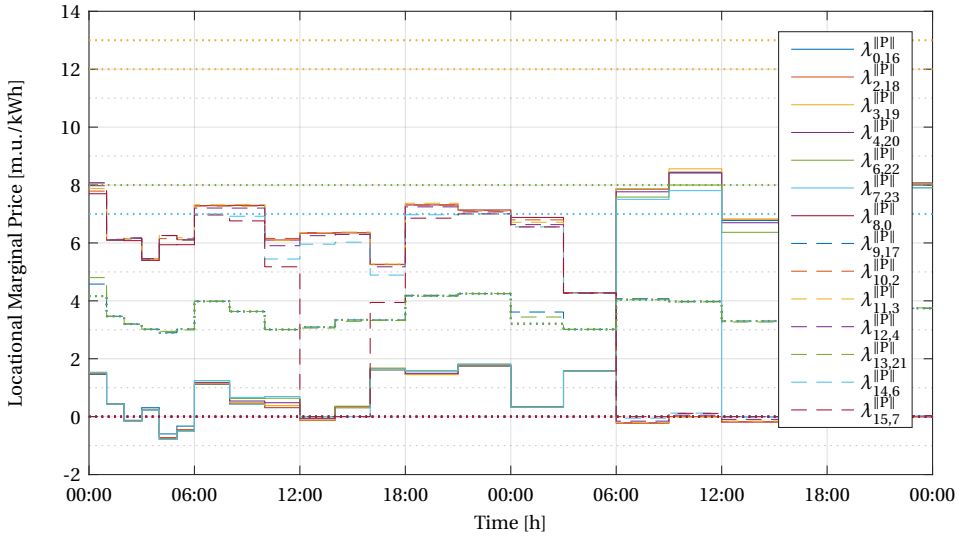

Figure 4.29: The LMP in the grid change over time.

4.5. CONCLUSION

In this chapter a general method for the optimal operation of bipolar dc distribution grids with asymmetric loading over a time horizon has been presented. It can be used in general optimal power flow application in bipolar dc grids. Storage operation as the fundamental element that needs a time horizon for optimization, has been modeled. The impact of storage operation and congestion on the LMP was shown. Examples illustrate the effects that storage operation has in bipolar dc distribution grids. Especially the difference between unipolar and bipolar connection of storage units was shown.

This model sets a foundation for optimal power flow in bipolar dc distribution grids. It can be used to implement model predictive control using a receding horizon with variable time step size. In this way short therm future can be modeled with high precision while reducing computation time for the long term future where details are anyway subject to uncertainty.

Further elements can be added to this model such as converters linking multiple voltage levels or power flow control converters. The storage model used is simple and effective for fast optimization. It could be enhanced with load dependent efficiency, battery chemistry and lifetime degradation effects. However, this would increase complexity and computation times and a trade-off has to be made. Load shifting and charging of plug-able appliances, such as electric vehicles, could further be added.

REFERENCES

[1] L. Mackay, T. G. Hailu, G. R. Chandra Mouli, L. Ramirez-Elizondo, J. A. Ferreira, and P. Bauer, "From DC Nano- and Microgrids Towards the Universal DC Distribution System – A Plea to Think Further Into the Future," in *PES General Meeting*. IEEE, 2015.

[2] L. Mackay, T. Hailu, L. Ramirez-Elizondo, and P. Bauer, "Towards a DC Distribution System – Opportunities and Challenges," in *DC Microgrids, IEEE First International Conference on*, 2015.

[3] L. Mackay, R. Guarnotta, A. Dimou, G. Morales-Espana, L. Ramirez-Elizondo, and P. Bauer, "Exact Optimal Power Flow in Bipolar DC Distribution Grids with Asymmetric Loading," *Smart Grid, IEEE Transactions on*, 2017.

[4] A. Castillo, X. Jiang, and D. F. Gayme, "Lossy DCOPF for optimizing congested grids with renewable energy and storage," in *2014 American Control Conference*. IEEE, jun 2014, pp. 4342–4347. [Online]. Available: http://ieeexplore.ieee.org/document/6859489/

[5] G. Rajasekhar, K. R. Vadivelu, and G. V. Marutheswar, "Study of optimal placement of energy storage units within a deregulated power system," in *2015 International Conference on Advanced Computing and Communication Systems*. IEEE, jan 2015, pp. 1–6. [Online]. Available: http://ieeexplore.ieee.org/document/7324123/

[6] J. C. Beardsall, C. A. Gould, and M. Al-Tai, "Energy storage systems: A review of the technology and its application in power systems," in *2015 50th International*

Universities Power Engineering Conference (UPEC). IEEE, sep 2015, pp. 1–6. [Online]. Available: http://ieeexplore.ieee.org/document/7339794/

[7] L. Gan and S. H. Low, "Optimal Power Flow in Direct Current Networks," *IEEE Transactions on Power Systems*, vol. 29, no. 6, pp. 1–13, 2014.

[8] J. Beerten, S. Cole, and R. Belmans, "A sequential ac/dc power flow algorithm for networks containing multi-terminal vsc hvdc systems," in *Power and Energy Society General Meeting, 2010 IEEE*, July 2010.

[9] R. P. O'Neill, P. M. Sotkiewicz, B. F. Hobbs, M. H. Rothkopf, and W. R. S. Jr., "Efficient market-clearing prices in markets with nonconvexities," *European Journal of Operational Research*, vol. 164, no. 1, pp. 269 – 285, 2005.

[10] T. Wu, M. Rothleder, Z. Alaywan, and A. D. Papalexopoulos, "Pricing Energy and Ancillary Services in Integrated Market Systems by an Optimal Power Flow," *IEEE Transactions on Power Systems*, vol. 19, no. 1, pp. 339–347, 2004.

[11] D. P. Chassin and S. E. Widergren, *Market Operations*, 2009.

[12] Y. F. Y. Fu and Z. L. Z. Li, "Different models and properties on LMP calculations," *2006 IEEE Power Engineering Society General Meeting*, 2006.

[13] D. Gautam and M. Nadarajah, "Influence of distributed generation on congestion and LMP in competitive electricity market," *World Academy of Science, Engineering and Technology*, vol. 39, no. 3, pp. 822–829, 2009.

[14] N. Kaur and K. Singh, "Optimal Placement of Distributed Generator in Transmission System Using an Algorithmic Approach," 2014.

[15] M. S. H. Nabavi, S. Hajforoosh, and M. A. Masoum, "Placement and Sizing of Distributed Generation Units for Congestion Management and Improvement of Voltage Profile using Particle Swarm Optimization," *IEEE PES Innovative Smart Grid Technologies, ISGT Asia 2011 Conference: Smarter Grid for Sustainable and Affordable Energy Future*, 2011.

[16] E. Litvinov, "Design and operation of the locational marginal prices-based electricity markets," *IET Generation, Transmission & Distribution*, vol. 4, no. 2, p. 315, 2010. [Online]. Available: http://digital-library.theiet.org/content/journals/10.1049/iet-gtd.2009.0046

5

Low Short-Circuit Current Protection Philosophy for DC Distribution Grids

Protection of low voltage dc grids with traditional protection methods is challenging. Both large short-circuit currents and missing natural current zero-crossing make the use of mechanical protection devices difficult for high power applications. On the other hand, the trend in power electronics to reduce the size of passive components (i.e., capacitors) by using higher switching frequencies, can lead to difficulties in supplying high enough short-circuit currents for a long enough time period to allow selective fault detection in small dc nano- and microgrids, e.g., with only small PV sources. DC distribution grids, made out of connected dc microgrids, can experience both high and low short-circuit currents. In this chapter, the low short-circuit current protection philosophy is presented as a way to tackle these challenges. It comprises the removal of need for high short-circuit currents, the prevention of high short-circuit currents where available and the adaption of other system components to allow the previous. The adaptations to the system are required in order to allow fast fault detection, discrimination and clearance by solid-state breakers. These adaptations, upcoming challenges and future research in this direction are introduced. Further, a classification of protection zones for dc systems is proposed. Finally, field measurements from an operational dc street lighting system, using over-current tripping, and experimental laboratory results of a more advanced di/dt-based solid-state circuit breaker prototype are shown as examples of the introduced protection philosophy.

This chapter is based on L. Mackay, N. Gouvalas, T. Hailu, H. Stokman, L. Ramirez-Elizondo, and P. Bauer, "Low Short-Circuit Current Protection Philosophy for DC Distribution Grids," in Energies, *under review.*

5.1. INTRODUCTION

Protection is the main challenge to be solved for dc grids to emerge from small dc nano- and microgrids to a full scale dc distribution grid [1]. Opening circuits is not as easy as in ac systems due to the missing current zero-crossing that supports eliminating switching arcs [2]. Therefore, more effort has to be put into the development of dc protection devices and strategies.

In literature, the protection aspect of dc microgrids has often been neglected and left for future work. However many interdependencies, e.g., with control design, can exist. One important aspect to consider is that dc nano- and microgrids are often assumed to be connected to each other by means of a converter that would separate control and protection aspects to a certain level. In general, however, this is not an optimal solution. Moreover, it is not appropriate to assume that converters will be placed at every house entrance (possible boundary of a dc nanogrid, see Figure 5.1) or meter box, especially when thinking of larger dc distribution grids [1]. The example can be taken from the ac power systems where – at least in densely populated areas – there are no individual transformers installed for every house. Not having individual converters for each household implies that they will all be connected on the same voltage level and that the protection system should be able to selectively protect parts of the system.

The contribution of this chapter is to propose a low short-circuit protection philosophy as a fundamental design criterion for the standardization of dc distribution grids. This philosophy is derived through the analysis of the future use cases that can result in very large and/or very small systems [1] and the properties of distributed sources and power electronic converters compared with traditional protection devices and philosophies. Further, the general options for the needed fast fault detection are shown and challenges for future research are identified. The classification of protection zones based on the associated danger is introduced, which has been brought forward into the ongoing standardization process. The feasibility of the proposed philosophy is underlined by measurements from an operational, commercially available, dc street lighting system, as well as experimental results obtained from, specifically built, more advanced solid-state breakers using $\frac{di}{dt}$ tripping. The focus of this chapter is protection of dc distribution grids. Possible connection to ac grids and effects thereof on the dc grid are not described.

The remainder of this chapter is organized as follows. In Section 5.2, short-circuit behavior in dc distribution grids is looked at and in Section 5.3, traditional protection strategies are discussed. Section 5.4 describes the properties of solid-state circuit breakers. In Section 5.5, the low short-circuit current protection philosophy is presented. The requirements for fault detection, device behavior and selectivity are discussed in Section 5.6. Section 5.7 describes the classification of different protection zones that can appear in dc distribution grids. In Section 5.8, measurements of an operational dc street lighting system and an experimental lab setup are shown. Finally, conclusions are drawn in Section 5.9.

5.2. SHORT-CIRCUIT BEHAVIOR IN DC DISTRIBUTION GRIDS

DC distribution grids can consist of interconnected microgrids and nanogrids as shown in Figure 5.1 [1]. These subgrids should be able to continue operation in case of faults

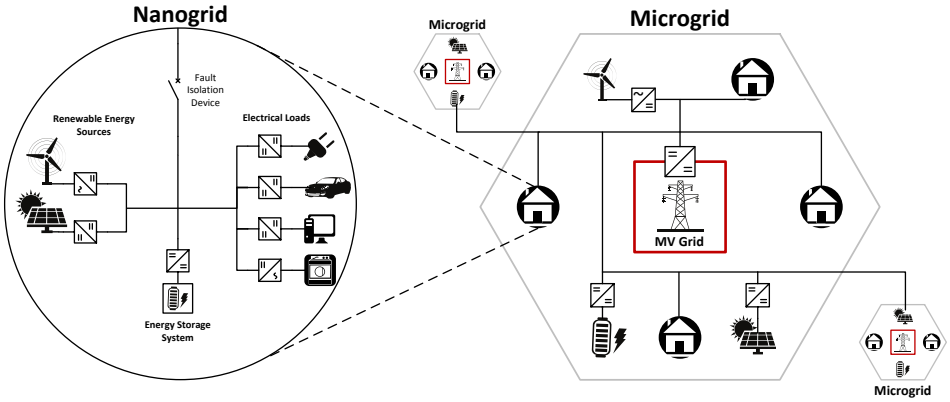

Figure 5.1: On the right: a dc microgrid connecting a neighborhood with multiple dc nanogrid inside buildings and some larger distributed energy resources. It can be connected to other dc microgrids on the same voltage levels (including meshed connections) and to a medium voltage grid at the substation (center). On the left: a dc nanogrid inside a building is shown in detail with various energy resources. It can be separated from the microgrid that connects the neighborhood by a fault isolation device. [1]

in other parts of the grid. As they are interconnected by fault isolation devices, the same fault can produce very different results depending on the connection state of these devices. While a large connected grid could provide large short-circuit currents, an islanded nanogrid with a small PV panel might only have a very low capacitance and therefore, can only provide low short-circuit current.

An important aspect to consider is the use of power electronic converters in dc distribution grids. In general, power electronic converters can only provide short-circuit currents higher than their nominal current for very limited time. This can also be a problem in ac systems where, in regions with high PV penetration, short-circuit current is low in sunny days due to the large distances and therefore large impedance to rotating masses. This can prevent tripping of circuit breakers in case of faults. A possible but expensive measure is to oversize the power electronic converters.

Additionally, the emergence of distributed energy resources leads to power flows, not only top down, but also bottom up. Furthermore, meshed dc distribution grids, that can enable more direct power flow between distributed resources [3], add further complexities to the protection requirements, particularly as large galvanically connected systems emerge.

Large grids with many connections and components have complex short-circuit behavior with fast transients that are affected heavily by frequency dependent cable parameters. Therefore, there is a need for research on fast transient models for low voltage dc distribution grids. For illustration purposes, in this chapter, only the ideal discharge of one capacitor will be shown. The under-damped short-circuit current response of a capacitor discharging in an RL circuit, with the initial conditions $v_C(0) = V_0$ and $i_L(0) = I_0$, is

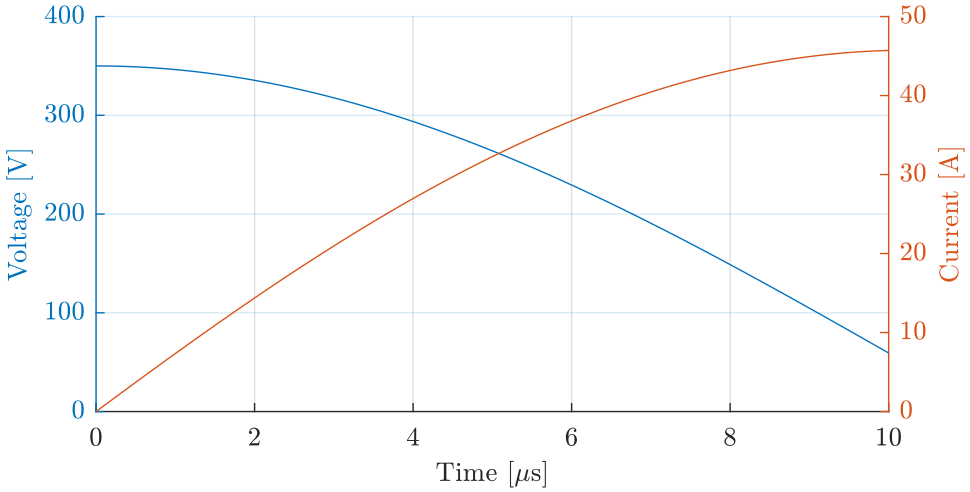

Figure 5.2: Initial discharge of a capacitor $C = 1\,\mu$F trough and limiting inductor $L = 47\,\mu$H with fault resistance $R = 1\,\Omega$. It can be seen how the voltage collapses withing micro seconds. This would mean the loss of selectivity if a fault is not cleared fast enough.

$$i_{SC}(t) = -\frac{I_0\omega_0}{\omega}e^{-\delta t}\sin(\omega t - \beta) + \frac{V_0\omega L}{\omega}e^{-\delta t}\sin(\omega t) \tag{5.1}$$

where $\delta = R/2L$, $\omega^2 = 1/LC - (R/2L)^2$, $\omega_0 = \sqrt{\delta^2 + \omega^2}$, $\beta = \arctan(\omega/\delta)$ with R the combined resistance of cable and fault, L the total cable inductance and C the output capacitance of the converter [4].

For high frequency converters, the output capacitance can be very small. For example, there is a 1.7 kW converter on the market with 1 MHz switching frequency and only $C = 1\,\mu$F output capacitance. In this case, when assuming $L = 47\,\mu$H, $R = 1\,\Omega$, according to the integral of (5.1), the capacitor could be discharged in less than 4 μs from 350 V to 300 V. This discharge is illustrated in Figure 5.2. This poses a challenge if selective protection should be provided such that only faulty parts of the grid are disconnected while the non-affected parts of the grid continue operation.

Therefore, regarding protection of dc distribution grids, new strategies, that avoid oversizing of converters, connectors and protection devices, should be investigated. This, however, is heavily inter-dependent with all other design considerations of dc grids.

5.3. Traditional DC Protection

Until now, traditional ac protection strategies are often adapted for dc systems [5]. A high short-circuit current is guaranteed by big capacitors or directly connected battery banks. This provides the energy necessary to detect fault currents and trip circuit breakers (CBs) or fuses. In the following subsections, the properties of different protection devices are briefly reviewed.

5.3.1. FUSES

The voltage and current ratings of fuses are given in rms values, which is thermally equivalent to dc ratings, and thus should be applicable for both ac and dc systems [6]. The use of fuses in dc system applications covers a wide range of applications including dc traction, mining, battery (storage) protection and low voltage power supplies protection circuitry [7, 8].

The application of fuses in dc systems is not only affected by the current and voltage ratings but also by the system L/R time constant [9]. Thus, the use of fuses is more adequate in low-impedance systems with higher rate of current rise ($\frac{di}{dt}$), which can ensure that the required time for the fuse melting point is kept at a minimum, leading to a fast acting protection [6, 8]. However, the application of fuses in dc systems is limited not only due to the high time constants and slow breaking operation [6], but also due to the difficulty in discriminating between faults [10]. That means that fuses are not capable to distinguish a temporary fault condition from a permanent, with the risk of nuisance tripping and isolation of an important part of the network. On top of that, fuses employed in dc systems should also have the ability to withstand low overcurrents and/or overloads as well as fault transient effects, preventing in this way undesirable malfunction operation.

In view of the above mentioned requirements and restrictions, the use of fuses in dc systems is limited as it lacks in reliability, performance and coordination with other protective devices in the system and when applicable should be used as secondary (back up) protection [8, 10, 11].

5.3.2. ELECTRO-MECHANICAL CIRCUIT BREAKERS

The application of electro-mechanical CBs has been used extensively in ac power networks over the past decades. The experience gained so far in designing CB protection equipment is actually based upon the natural current zero-crossing that holds only in ac. However, mechanical CBs, used in dc systems, require special design and proper de-rating of the breaker tripping levels in order to be optimally applicable [12]. In most cases, this adjustment takes the form of suitable multiplying factors, in the range of 1.1-1.4 times the ac magnetic-tripping current level [13]. The CB protection equipment, more adequate for application in LVdc systems and also commercially available, comprises molded-case circuit breakers (MCCB), LV power circuit breakers (LVPCB) and isolated-case circuit breakers (ICCB) [12, 14, 15]. These types of CBs are widely used in low voltage, high power traction and marine applications as well as in residential premises and commercial centres [16].

The mechanical CB switch-off operation due to the inherent arc-related extinction process, results in typical opening times, without considering detection and tripping time delays, in the range of tens to hundreds of ms [14, 17, 18]. However, one of the superior advantages that CBs have to show compared to alternative protection technologies (i.e. hybrid circuit breakers, solid-state circuit breakers) is the lower contact (on-state) resistance, which lies in the range of few to tens of $\mu\Omega$ [19–21]. Nevertheless, the slow interrupting response (tens of ms) of electro-mechanical CBs makes the later inadequate for converter-fed LVdc systems comprising sensitive power electronic devices of limited fault current withstand capability (2-3 times nominal current for tens of μs) [22] and high

values of prospective short-circuit currents (up to 10 kA or more), caused by converters output filter capacitors rapid discharge [7, 23].

5.3.3. HYBRID CIRCUIT BREAKERS

The slow opening time of the mechanical breaker operation has led to the development of hybrid breakers, which is a combination of a mechanical breaker and a solid-state path [24–26]. The basic operation of a hybrid CB is based on an arc-less opening of the mechanical switch when the fault occurs. This is achieved by allowing the solid-state switches to commutate at the instant that the breaker contacts start to separate quenching the arc. The different stages at which the fault current is interrupted as well as a more detailed description of multiple ways for dissipating the stored fault energy through combination of hybrid CBs, snubbers and resonant circuits can be found in [24]. The hybrid CB has low conduction losses since a mechanical breaker with a low contact resistance is normally-on supplying the nominal load current. However, despite the low on-state losses, the total interruption time is of the order of few hundred μs [27, 28]. There are also some problems related to the solid-state part of the hybrid breaker, such as sensitivity to electro-magnetic interference (EMI) and lack of physical/galvanic isolation due to leakage currents during the semiconductors off-state [29]. Nevertheless, hybrid technology has been the focus of extensive research conducted in the past, mainly for high-power dc system applications [24, 26–28, 30].

5.3.4. OVERSIZING

The above discussed protection devices all have, compared to dc system dynamics, a relative long clearance time, in the range of ms to tens of ms. Further, they need a certain amount of short-circuit current. Power electronic converters have a limited over-current withstand capability (around 2-3 times the nominal load current for tens of μs) [22]. Oversizing these converters for higher currents is possible, but expensive. Another option is to oversize only the output capacitors which are the first providers of short-circuit energy. This goes, however, against the general trend in power electronics which is to increase the switching frequency in order to reduce the size of passive components such as capacitors and thus material usage and cost.

Nevertheless, also high short-circuit capacity of large converters can be a challenge if the fault is only cleared after tens of ms as the dc fault current rises very fast. Further, freewheeling diodes (for example in ac/dc converters) could proved large short circuit currents. All components and cables need to be able to withstand the thermal stress and electromagnetic forces that act during a short-circuit. In order to prevent extreme thermal and mechanical stress over the power circuit elements, the use of a fast dc circuit breaker is deemed preferable. Also, a faster short-circuit interruption will enhance power quality by improving the transient response of the network system leading to lower voltage sags during and lower over voltages after the fault clearance [17, 31, 32]. Therefore, in the next section solid-state circuit breakers are looked at.

5.4. SOLID-STATE CIRCUIT BREAKERS

Solid-state circuit breakers utilize power semiconductor devices enabling them to supply nominal load currents but also to interrupt fault currents in the μs range based on lower over-current (compared to traditional circuit breakers or fuses) and/or rate of current rise thresholds [7]. The solid-state protection technology is a promising solution for fast dc protection since it has fast opening response time, in the range of few to tens of μs [33–36], and is also free from arc-related effects caused by contact separation in conventional breakers [37]. However, the higher conduction losses of the later compared to conventional mechanical CBs has prevented its mass production, since it requires an additional heating management system (i.e heat-sinks) for cooling thus increasing both physical size and cost [29]. The rapid advancements in semiconductor industry, however, has led to the development of power semiconductor devices with on-state resistance of few tens of mΩ or less [38] with improved current and voltage ratings.

The most commonly used power semiconductors for solid-state protection include insulated-gate bipolar transistors (IGBTs), gate turn-off thyristors (GTOs) and insulated-gate commutated thyristors (IGCTs) due to their superior switching characteristics, increased controllability performance and on-state losses [17, 39]. The IGCTs and GTOs switches have slower turn-off capability (6 times slower) compared to IGBTs due to the inherent current limiting properties of thyristor types devices [17]. However, the high conduction losses of IGBTs compared to IGCTs make them an unfavorable choice for voltages higher than 2000 V [22, 40]. For voltages lower than 2000 V, IGBTs are still more preferable compared to the faster Si MOSFETs, mainly due to the much higher (x10 at 1200 V) on-resistance of the later. On the other hand, superjunction MOSFET technology has to show much faster turn-off speed along with low on-resistance in the range of few tens of mΩ with blocking voltages up to 800 V at the moment due to fabrication limitations [22, 38]. However, the use of ultralow on-resistance normally-on WBG devices can also serve as ideal candidates to meet the strict protection requirements of SSCB applications in future LVdc distribution systems. Promising low voltage (<1500 V) experimental prototype paradigms are already found in literature (SiC JFET [41], SiC VJFET [42], SiC - SIT [43], GaN HEMT [22]).

5.5. LOW SHORT-CIRCUIT CURRENT PROTECTION PHILOSOPHY

In Section 5.2, the different sizes and connection states of dc distribution grid that need to be considered have been discussed. The trend in power electronics is to go to higher switching frequencies that need only very small capacitors and thus limit even the initial short-circuit current capability of converters. This poses challenges for traditional dc protection methods and devices. While solid state-breakers can act fast, one of their properties is that they cannot withstand high currents. This results in a chicken-egg problem as it is very expensive to size them for traditional high short-circuit currents.

The core idea of the low short-circuit current protection philosophy is therefore proposed as follows:

1. Avoid oversizing of converters and capacitors by not requiring high short-circuit

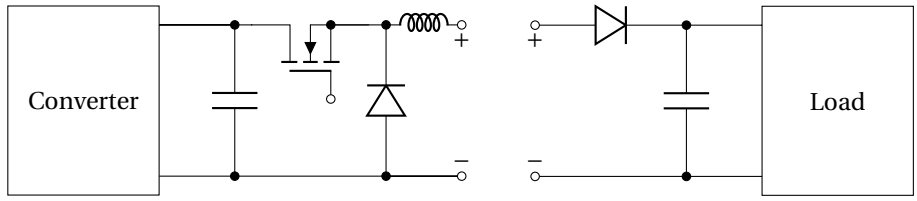

Figure 5.3: (a) Source or bi-directional converter with its internal low short-circuit current protection solid-state circuit breaker including limiting inductor after the output capacitor and freewheeling diode. (b) Load with blocking diode to prevent fault current contribution from the input capacitor.

current capability for fault detection.

2. Prevent high short-circuit currents if capability is available, e.g., fast fault clearance.

3. Adapt system and component design to allow the realization of the previous.

This philosophy has effect on large parts of the system and includes several problems that can only be solved together.

In this section, the adaptations to the converters and loads in order to prevent high short-circuit currents are discussed. The next section discusses fast fault detection and its requirements.

5.5.1. SOURCES AND BI-DIRECTIONAL CONVERTERS

Converters should have the capability to protect themselves during a fault and, at the same time, protect the connected grid. Mainly, semiconductors of the converters and terminal capacitors are prone to high fault current. For the protection of semiconductors, a fast pulse width modulation (PWM) based method is normally implemented. However, this approach does not prevent terminal capacitors from discharging the complete stored energy which contributes large fault currents to the system, especially during bolted fault. Figure 5.3a shows a converter with a possible solid-state circuit breaker to protect terminal capacitors. This breaker uses an inductor to limit the rate of change of current and therefore, the peak breaking current. The free-wheeling diode prevents voltage spikes during fault isolation.

5.5.2. LOADS

Figure 5.3b shows a typical load with power electronics interface and its terminal capacitor. The value of input capacitors depends on the size of individual loads and their switching frequency. Small devices could have negligible filter capacitors.

Input capacitors of loads can introduce high inertia which is particularly advantageous for stability. However, the input capacitors also contribute high fault current during a short-circuit event. To avoid such high short-circuit currents, diodes are used as shown in Figure 5.3b. These diodes make the input capacitors' stored energy not us-

able by the system during disturbance. Therefore, only energy stored in sources' output capacitors can be used for stability. This has to be considered in control design.

5.5.3. SOLID-STATE CIRCUIT BREAKERS

When the converters and loads have their respective measures taken still significant amount of short-circuit current could occur if many of them are connected closely together. Solid-state circuit breakers can segment areas and in that way limit the short-circuit current. This is additional to providing selective protection, i.e., only a small area containing the fault is switched off while the rest of the system can continue normal operation.

5.6. FAST FAULT DETECTION

Fast fault detection is mandatory to allow fault clearance before the short-circuit current goes too high as described in the previous section. This could be in the range of μs instead of tens of ms as in traditional protection strategies, which is 4 to 5 orders of magnitude faster. While fast fault detection is a challenge, fast selectivity is even more challenging. In this section, the main approaches and research directions for fault detection, discrimination and selectivity are discussed, as well as their system level and component level implications.

5.6.1. DETECTION METHODS

OVER CURRENT

Traditionally, faults are detected by using current measurements and over current limits with time grading [11, 44]. In systems where the short-circuit current can be guaranteed to reach the over current limits, this may be feasible. However, this may not be the case for dc nanogrids. DC nanogrids could normally be connected to a large grid and thus have high nominal currents (e.g. 32 A) and over current limits. When the nanogrid is operated in islanded mode only partial supply may be possible and a small distributed source converter may not be able to provide this current. Thus, the over current protection would not trip and selectivity may be lost as the converter protection is activated due to overload.

FAULT TRANSIENTS

New detection methods based on the characteristics of the fault transients are therefore an interesting alternative. The current rate of change ($\frac{di}{dt}$) is the most prominent indicator, however also voltage and its derivative and a combination of all measurements are discussed in literature [45–47]. Based on the fault transients, the fault detection can be very fast (in the range of hundreds of ns), however, false positives need to be prevented. Filtering noise and adding certain time delays is crucial and can improve reliability of these measurements, however, further measures have to be taken as will be discussed in the following subsections.

5.6.2. Fast Fault Discrimination

Differentiation between fault and normal operation very early in the transient is mandatory for fast fault detection. In order to achieve this, the characteristics of faults and normal operation need to be sufficiently different in the multidimensional space of measurements. While traditional protection allows for a longer detection time and thus more time for false positives to be filtered out, for fast protection this has to happen already in the beginning of the transient. Specific measures have to be taken on system and component level to allow this discrimination. The challenge is that it has implication on other parts of the system, which are traditionally not looked at together.

Inrush Currents

Inrush currents are mainly caused by the charging of load input capacitors during grid connection. They can easily reach 100 times the nominal current and also pose problem in traditional ac protection, e.g., multiple LED drivers on one circuit breaker. These inrush currents would trip any fast fault detection device, but they also reduce the lifetime of components and cause significant stress on the system such that it needs to be overrated (e.g. bigger CB rating). Therefore, industry is starting to take measures in order to reduce inrush currents of appliances.

In order to allow fast fault detection without false positives, the inrush currents need to be limited and standardized. Different inrush current limiting possibilities exist for implementation in devices.

In addition, for fixed installations, low inrush currents can be assured by slowly energizing the grid when re-closing circuit breakers. This is mandatory anyway in order to prevent transients on the grid upstream side of the circuit breaker. It could be implemented using a linear current source or closing the solid-state breaker slowly in linear mode. It has to be ensured that loads do not start up before the grid is fully energized. This could be achieved by introducing some start-up delay, counting from the time the steady-state voltage is reached.

Soft Start / Load Changes

Also during operation, it has to be ensured that no transients will trigger fault detection. Loads should not start or change their power too fast. Exact guidelines have yet to be developed. A challenge is that many loads can be connected in parallel. Therefore, simple limits might not be sufficient. Monitoring input voltage could be a possibility as it reflects the state of the grid. This voltage can be strongly influenced by $\frac{di}{dt}$ through line inductance. Also random start-up delays could be considered. Limiting the rate of change of loads would also have a positive impact on the system stability. For fast peak power requirements, local energy buffers would need to be implemented.

5.6.3. Selectivity

Selectivity is a very important topic in dc distribution grids. It is essential that healthy parts of the grid continue operation and only the minimal faulted part is disconnected. Additional challenges are that the power flow can be bi-directional and that the distribution grid topology could be meshed. Many open research questions and opportunities exist in order to achieve fast selectivity in meshed dc distribution grids with bi-directional power flow in order to have resilient connected dc microgrids. In literature,

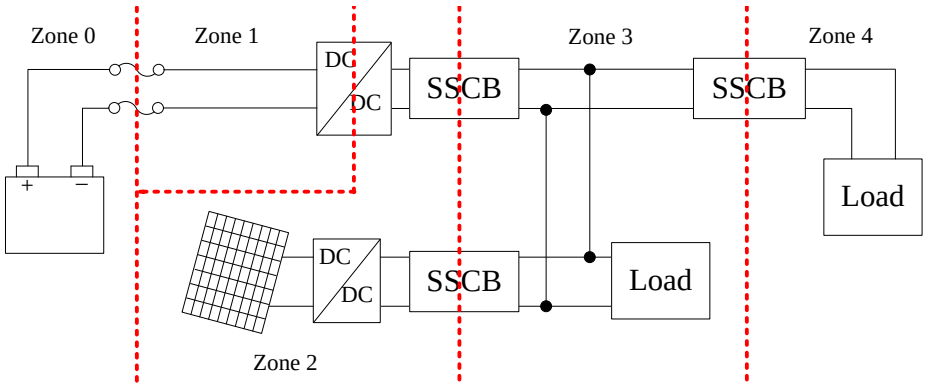

Figure 5.4: An example dc application to demonstrate all different protection classification zones. From the left: at the battery very high short-circuit can occur in Zone 0. Fuses or circuit breakers separate Zone 1, while Zone 2 can only be fed by converters with current limiting capability. It can not guarantee circuit breaker tripping. Zone 3 has low short-circuit protection philosophy applied with multiple sources. Zone 4 is similar, but has only one source of power and is therefore safe if disconnected.

fast communication links have been used for protection coordination [48]. Communication links limit the speed of fault detection to the range of ms and are expensive additional infrastructure. For a general dc distribution grid it would be preferable to not have mandatory high speed communication for protection purposes. By considering the design and behavior of the complete system, an elegant protection solution may be possible.

5.7. CLASSIFICATION OF DC PROTECTION ZONES

The discussed low short-circuit protection philosophy can be applied to large parts of a dc distribution grid. Nevertheless, some parts of the system will have different protection properties with varying danger levels. Therefore, a classification of these levels and clear designation in the field are proposed. This has been put forward into the national standardization process at NEN in the Netherlands and into the IEC LVdc working group by Direct Current B.V. [49]. In this chapter, only very brief descriptions are presented while more detailed specifications, such as current thresholds, are currently discussed for standardization. These zones could be used for the qualification level of installation and maintenance staff and for risk assessment. Figure 5.4 shows an overview of the zones in an example application for illustration. While the example shows a radial grid, the principle is equally applicable to meshed grids. The different zones are proposed as follows:

DC ZONE 0

Very high short-circuit currents occur in this zone. It is not protected by fuses or circuit breakers. This is the most dangerous zone. This could be, e.g., directly at the contacts of batteries before any protection device.

DC ZONE 1
High short-circuit currents occur. Therefore, fuses or mechanical circuit breakers can be used. The risk level is high. This zone could be situated after the protection device of a battery.

DC ZONE 2
High short-circuit currents are not guaranteed in this zone. They may not sufficient to trip fuses or circuit breakers with certainty, thus making application of traditional fault selectivity methods challenging. However, the current is limited and converters go into a current limiting mode. There is a normal risk level.

DC ZONE 3
The short-circuit current in this zone is low. It is protected by solid state breakers that isolate faults fast. Residual ground fault detection is mandatory. There is a normal risk level. This zone corresponds to the low short-circuit current protection philosophy proposed in this chapter.

DC ZONE 4
Same as Zone 3 but power is uni-directional and only comes from one source. This ensures that once a circuit breaker is opened, no other sources can power the grid. The risk is moderate due to the single disconnector.

5.8. IMPLEMENTATION EXAMPLES
In this section, two examples implementing the proposed low short-circuit current protection philosophy are provided in order to indicate its feasibility. Firstly, an operational dc street-lighting system with over current detection is shown. Secondly, an experimental solid state breaker prototype has been built that features current derivative based fault detection.

5.8.1. DC STREET LIGHTING SYSTEM WITH OVERCURRENT DETECTION
Direct Current B.V. has developed and implemented a street lighting system featuring low short-circuit currents. It has been implemented in several locations in the Netherlands with over 1000 light poles in total. DC has several advantages over ac in this application. This includes the removal of the power factor correction stage and the associated electrolytic capacitor from the LED drivers with increases the lifetime and therefore reduces the maintenance with is very expensive on streetlights. Further the strings can be much longer because they are not limited by the necessary steady state short-circuit current for ac circuit breakers. Also the system can be protected for residual ground faults to increase human safety. This is not feasible in ac grids because of the leakage currents trough the parasitic cable capacitance. Also the losses in the cable are reduced due to the higher average voltage or alternatively the cable diameter can be reduced.

Figure 5.5 shows the location and schematic of the field test location. The system is operated by CityTec B.V.. The string length is around 1.6 km. The system is a bipolar dc grid with ±350 V and 22 LED drivers with a maximum power rating of 60 W each are connected alternatively between the two poles and the neutral conductor. This reduces the

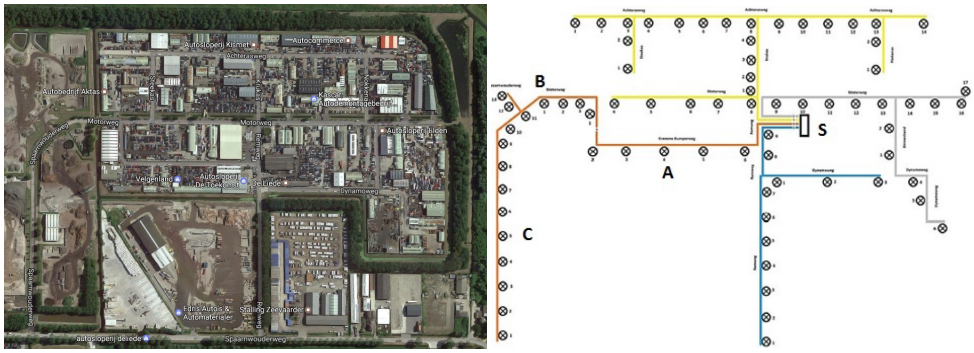

(a) (b)

Figure 5.5: Location of the dc street lighting system at the industrial area "De Liede" close to the airport of Amsterdam, the Netherlands. (a) Satellite image of the area [50] and (b) schematic of the dc feeders starting at substation (S) in the center. The measurements were taken on the left feeder at the locations marked A, B and C.

losses by half compared to unipolar configuration without increasing the cost of the LED drivers. Further reasoning on the voltage level selection can be found in [1]. Over current protection limit is implemented with a MOSFET, limiting inductor and freewheeling diode (as illustrated in Figure 5.3a) after the output capacitors of the sources. Therefore the system falls into protection classification Zone 4 as described in the previous section. The over current limit is set to 3 A at a normal operation current of around 2 A. Inrush current is eliminated as drivers wait for a stable voltage before charging their input capacitor.

In Figure 5.6 measurements of a short-circuit fault between positive and neutral conductor at point A are shown. It can be seen that the short-circuit current only reaches 7 A. After fault clearance, the grid energy mainly stored in the line inductance continues to discharge. Diodes in the LED drivers prevent their input capacitors to discharge and contribute to the fault current.

5.8.2. EXPERIMENTAL PROTOTYPE USING CURRENT DERIVATIVE

In this section a general experimental solid state circuit breaker is described that is not only intended for the specific application of LED lighting as in the previous section. A $\frac{di}{dt}$-based fault detection and protection scheme was tested experimentally by conducting short-circuit tests in a lab environment using a 350 V uni-directional solid-state breaker prototype. The schematic of the experimental uni-directional solid-state breaker setup is shown in Figure 5.7b. This breaker is designed for the negative pole of a possibly bipolar dc grid. Only the negative pole breaker is shown. In practice also the neutral pole should be disconnected depending on the type of fault and the allowable neutral voltage. It could also be an option to let the positive pole continue operation in case of a pole to neutral fault.

The 350 V dc-supply, with a 25 μF capacitor at its output, supplies a pure resistive load of 4.5 kΩ through a series connected 47 μH $\frac{di}{dt}$-limiting inductor in normal opera-

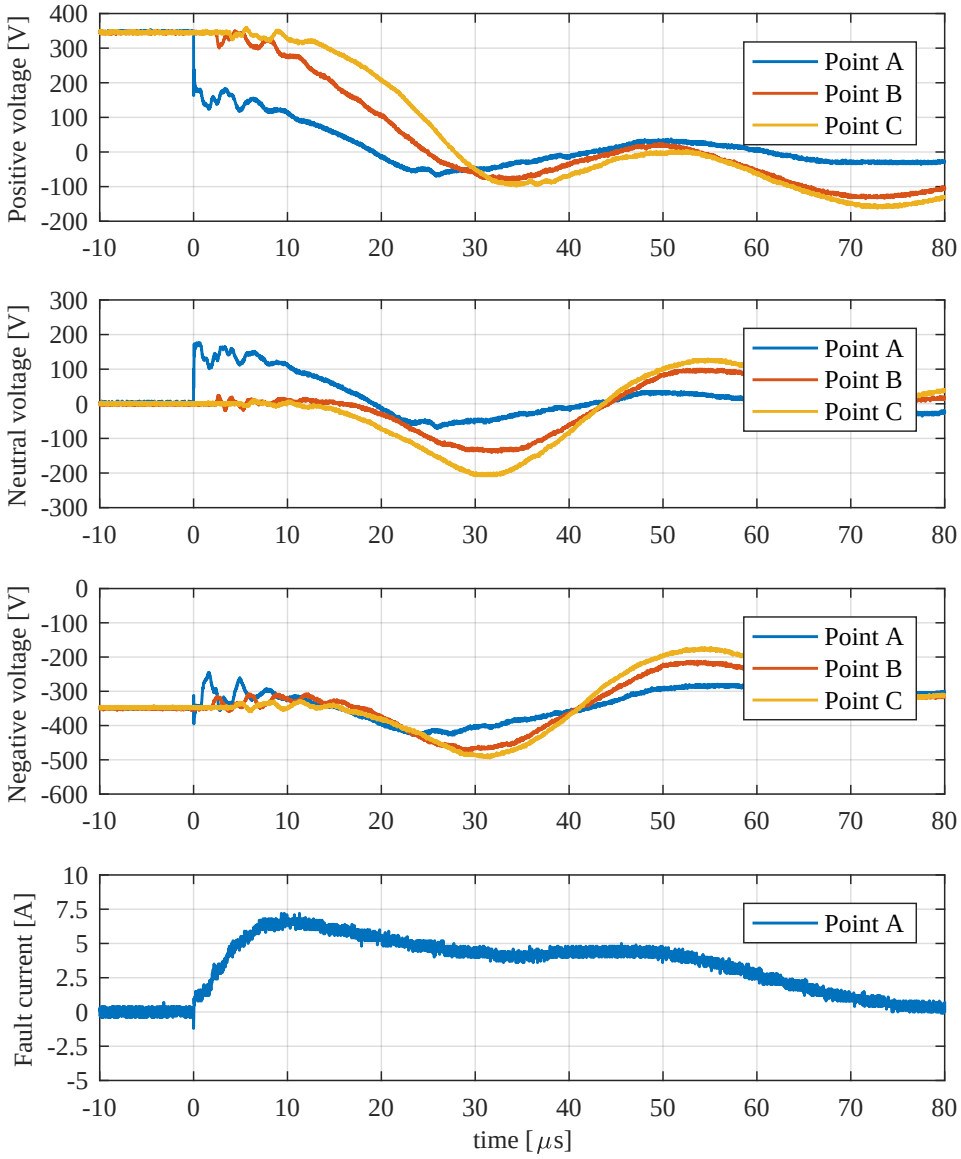

Figure 5.6: Measurements of a short-circuit fault between positive and neutral conductor at point A. The measurements are grouped together for comparison. On top the positive pole voltages followed by the neutral voltages, the negative voltages and the fault current. All voltage measurements are with respect to local PE conductor. It can be seen that the fault current stops rising after 8 μs.

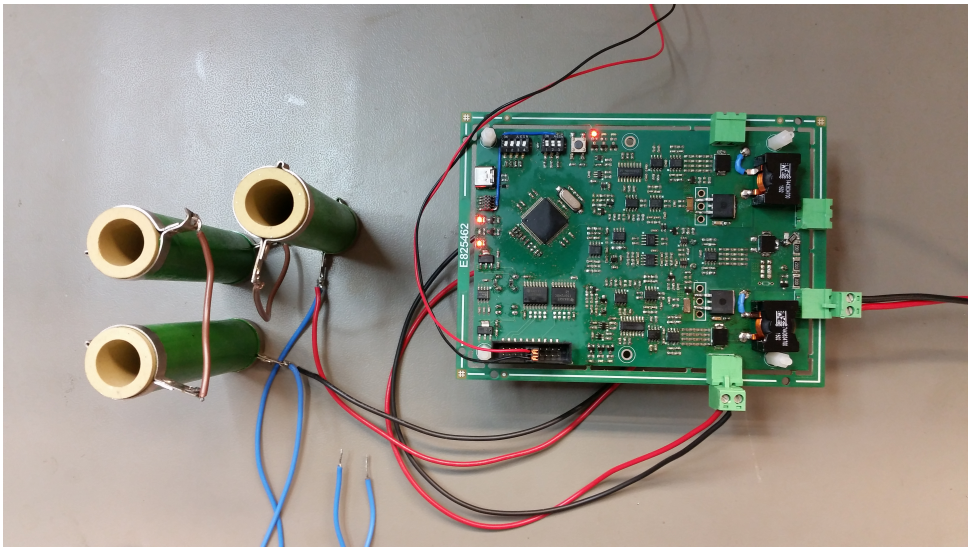

(a)

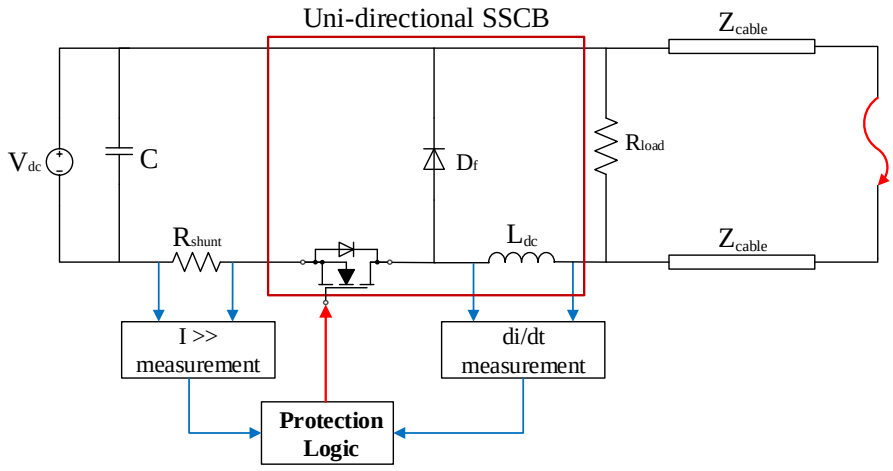

(b)

Figure 5.7: Photograph (a) and schematic representation (b) of the experimental uni-directional solid-state breaker setup. The 350 V dc-supply is connected across a 25 μF capacitor and feeds through a series connected 47 μH fault limiting inductor a pure resistive load of 4.5 kΩ. A short-circuit is made through physical connection at the end of the 2 m conductors.

tion. The top cable conductor represents the 'neutral' while the bottom conductor the 'negative' pole.

A short-circuit is generated at the end of a cable of 2 m length. The solid-state breaker is placed at the bottom side of the power circuit (negative pole) in order to avoid additional high-voltage gate driver circuitry requirements (i.e. use of charge-pump or bootstrap circuit). Thus, the main components of the solid-state breaker include a 650V IPB65R045C7 power MOSFET, a dc inductor of 47 μH and an ultra-fast recovery freewheeling diode. The 25 μF filter capacitor and the shunt resistor in series with the MOSFET are also parts of the hardware included on the PCB which is shown in Figure 5.7a.

The protection circuit is based primarily on $\frac{di}{dt}$ fault detection while overcurrent detection is also employed as back-up fault protection and/or sustained overload detection. The $\frac{di}{dt}$ measurement is extracted from the voltage drop across the limiting inductor (L_{dc}) while an overcurrent condition is being sensed by measuring the voltage across a shunt resistance (R_{shunt}) connected in series with the solid-state switch. The $\frac{di}{dt}$ and overcurrent measurements are sent as inputs to the protection logic circuit which in case of a fault trips and drives the MOSFET off. The analog protection signals measured in [V] for a short-circuit fault between the neutral and negative pole are shown in Figure 5.8 (bottom). The $\frac{di}{dt}$ of the line current through the inductor is being constantly measured and compared with a threshold value of 1.75 V corresponding to 750 kA/s. When the $\frac{di}{dt}$ of the line current exceeds the predetermined threshold, the opamp-based comparator of the protection circuit gives a high output (trip signal) which is then fed into the gate driver that drives the MOSFET off. From Figure 5.8, it can be seen that the $\frac{di}{dt}$ fault detection circuit responds within 400 ns from the fault event (t=0 s) at which point the trip signal goes high (3.3 V). The MOSFET gate is drained to zero in about 100 ns after the generated $\frac{di}{dt}$ trip signal, with the gate-to-source voltage (V_{GS}) dropping from 15 V to 0 V.

In Figure 5.8 (top), the voltage and current measurements of the power circuit during fault interruption are depicted. The fault current is interrupted within 700 ns from the fault event at almost 5 A above the nominal load current. After fault interruption, the diode starts to commutate and the fault current slowly (high $\frac{L}{R}$ time constant) discharges through the free-wheeling path (D_f - Z_{cable} - L_{dc}). The free-wheeling diode included in the solid-state breaker acts also as a snubber preventing excessive overvoltage stress across the solid-state switch during turn-off. Therefore, as shown in Figure 5.8 during MOSFET turn-off, the drain-to-source voltage (V_{DS}) rises up to the 350 V dc-supply (neutral) with a small voltage-spike and then settles to the open-circuit voltage approximately 800 ns from the fault instant.

Finally, from the experimental results, the total opening response time of the unidirectional solid-state circuit breaker prototype is 700 ns after the fault event consisting of 400 ns fault detection time delay ($\frac{di}{dt}$-based), 100 ns gate-driver delay and 200 ns MOSFET turn-off switching delay.

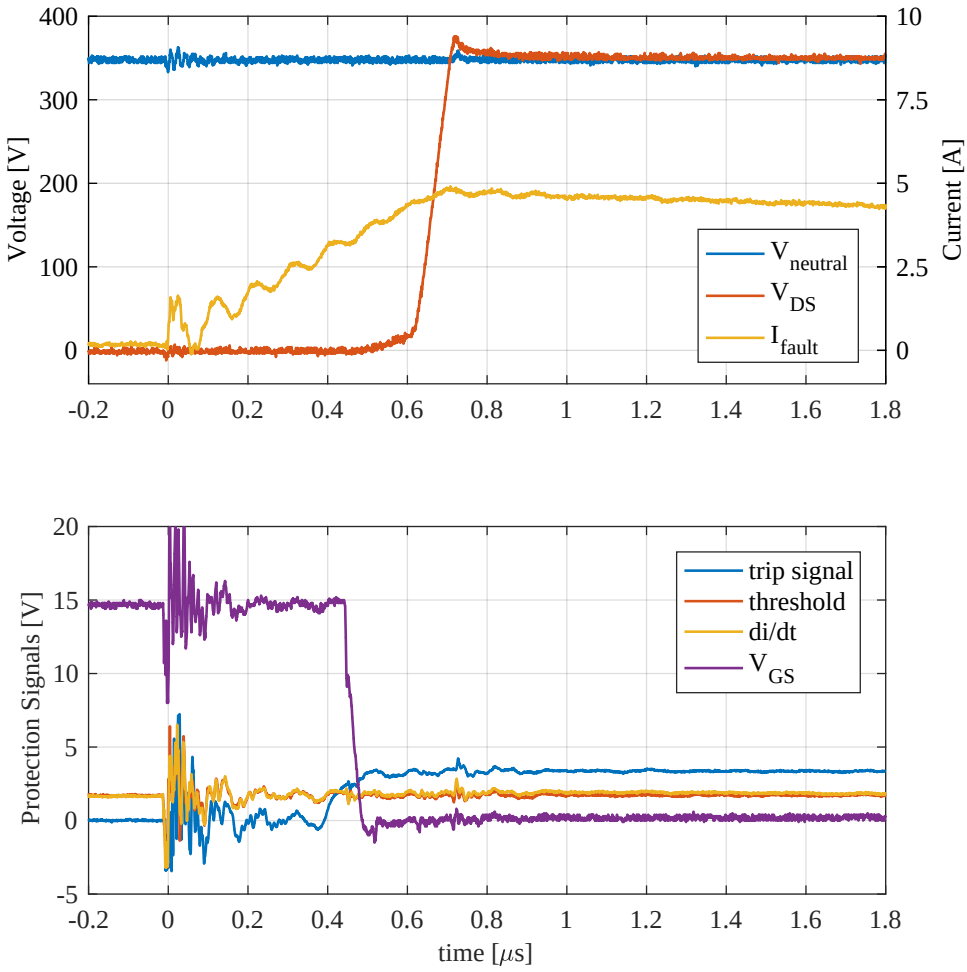

Figure 5.8: Experimental measurements of a short-circuit fault between neutral and negative conductor using the uni-directional solid-state circuit breaker prototype. On the top figure the neutral pole voltage along with the MOSFET drain-to-source voltage and the fault current during the fault interruption. It can be seen that the voltage across the breaker (V_{DS}) rises up to the 350 V dc-supply (neutral) and the fault current is interrupted within 700 ns from the fault event (t=0 s) at almost 5 A. On the bottom figure, the analog protection signals are shown. The $\frac{di}{dt}$ fault detection circuit response is 400 ns and the gate-to-source voltage (V_{GS}) is drained to zero in about 100 ns later.

5.9. CONCLUSION

In this chapter, the low short-circuit protection philosophy for dc distribution grids was proposed, considering the challenges of dc protection, the fault behavior and the development of power electronics. It comprises avoiding oversizing of converters and capacitors for fault current contribution, prevention of high short-circuit currents by fast fault clearing and the adaption of other system components in order to achieve this. Necessary component modifications for sources and loads were discussed. Further, the fast fault detection, discrimination and selectivity were addressed. These pose a vast field of challenges and open research questions that have to be investigated in future work. The introduced philosophy may be applied to large parts of dc distribution grids, however there will be parts that will be protected in other ways. Therefore, a classification of protection zones was proposed, that can be used also for risk assessment and staff qualification. Moreover, measurements of an operational dc street lighting system and the experimental implementation of a $\frac{di}{dt}$-based solid-state circuit breaker were shown as an indication of feasibility of the introduced philosophy. The former still relies on the traditional overcurrent detection and its implementation is limited to radial grids with unidirectional power flow while the latter uses fault transient detection which, after further research, could lead to selective short-circuit protection of meshed dc grids with bidirectional power flow.

While low short-circuit current protection philosophy adds more complexity initially, it may offer significant savings in material and component cost in larger dc distribution grids that may be deployed in future. The challenge is that it has effects on many other aspects of the system that are traditionally looked at independently. Nevertheless, a lot can be gained if these considerations are included in the ongoing low voltage dc standardization process.

ACKNOWLEDGMENT

The author would like to thank Dimitris Petropoulos for his work on the dc street lighting system measurements during his MSc thesis [51]. Appreciation also is due to CityTec B.V. and Direct Current B.V. for allowing and supporting measurements on the operational street lighting system.

REFERENCES

[1] L. Mackay, N. H. van der Blij, L. Ramirez-Elizondo, and P. Bauer, "Toward the Universal DC Distribution System," *Electric Power Components and Systems*, vol. 45, no. 10, pp. 1032–1042, 2017. [Online]. Available: http://www.tandfonline.com/doi/abs/10.1080/15325008.2017.1318977

[2] L. Mackay, A. Shekhar, B. Roodenburg, L. Ramirez-Elizondo, and P. Bauer, "Series Arc Extinction in DC Microgrids using Load Side Voltage Drop Detection," in *DC Microgrids, IEEE First International Conference on*. IEEE, 2015.

[3] L. Mackay, T. Hailu, L. Ramirez-Elizondo, and P. Bauer, "Decentralized Current Limiting in Meshed DC Distribution Grids," in *DC Microgrids, IEEE First International Conference on*, 2015.

[4] J. Yang, J. E. Fletcher, and J. O'Reilly, "Short-circuit and ground fault analyses and location in VSC-based DC network cables," *IEEE Transactions on Industrial Electronics*, vol. 59, no. 10, pp. 3827–3837, 2012.

[5] ABB, "ABB circuit breakers for direct current applications," Tech. Rep., 2010. [Online]. Available: https://library.e.abb.com/public/de4ebee4798b6724852576be007b74d4/1SXU210206G0201.pdf

[6] D. Salomonsson, L. Söder, and A. Sannino, "Protection of low-voltage DC microgrids," *IEEE Transactions on Power Delivery*, vol. 24, pp. 1045–1053, 2009.

[7] R. M. Cuzner and G. Venkataramanan, "The status of DC micro-grid protection," *Conference Record - IAS Annual Meeting (IEEE Industry Applications Society)*, pp. 1–8, 2008.

[8] Y. Xie, J. Ning, Y. Huang, J. Jia, and Z. Jian, "A review of DC micro-grid protection," *Advances in Brain Inspired Cognitive Systems: 6th International Conference, Lecture Notes in Computer Science*, vol. 7888. Springer, Berlin, Heidelberg, pp. 338–347, 2013.

[9] J. P. Brozek, "DC overcurrent protection-where we stand," *IEEE Transactions on Industry Applications*, vol. 29, no. 5, pp. 1029–1032, 1993.

[10] J. Candelaria and J. D. Park, "VSC-HVDC system protection: A review of current methods," *IEEE/PES Power Systems Conference and Exposition, PSCE 2011*, pp. 1–7, 2011.

[11] R. Cuzner, D. MacFarlin, D. Clinger, M. Rumney, and G. Castles, "Circuit breaker protection considerations in power converter-fed dc systems," *IEEE Electric Ship Technologies Symposium (ESTS)*, pp. 360–367, 2009.

[12] G. D. Gregory, "Applying low-voltage circuit breakers in direct current systems," *IEEE Transactions on Industry Applications*, vol. 31, no. 4, pp. 650–657, 1995.

[13] J. S. Morton, "Circuit Breaker and Protection Requirements for DC Switchgear used in Rapid Transit Systems," *IEEE Transactions on Industry Applications*, vol. IA-21, no. 5, 1985.

[14] ABB, "Working with the Trip Characteristic Curves of ABB SACE Low Voltage Circuit-Breakers," *White Paper*, Sept. 2007.

[15] C. Kimblin and R. Long, "Low-voltage power circuit breakers and molded case circuit breakers-a comparison of test requirements," *IEEE Industrial and Commercial Power Systems Technical Conference*, p. 7, 1999.

[16] W. Y. Kong, "Review of dc circuit breakers for submarine applications," *Maritime Platforms Division, Defence Science and Technology Organisation (DSTO)*, March 2012.

[17] C. Meyer, S. Schröder, and R. W. De Doncker, "Solid-state circuit breakers and current limiters for medium-voltage systems having distributed power systems," *IEEE Transactions on Power Electronics*, vol. 19, no. 5, pp. 1333–1340, 2004.

[18] Secheron, "High-speed DC circuit-breakers for Rolling Stock Type UR6,UR10 and UR15," *Technical Brochure*, 2015. [Online]. Available: http://www.secheron.com[Accessed:06.10.15]

[19] M. J. Sprague, "Service-life evaluations of low-voltage power circuit breakers and molded-case circuit breakers," *IEEE Transactions on Industry Applications*, vol. 37, no. 1, pp. 145–152, 2001.

[20] Omicron, "Cibano 500, 3-in-1 test system for medium-and high-voltage circuit breakers," *Technical Guide*, August 2015. [Online]. Available: http://www.omicron.at[Accessed:09.10.15]

[21] Megger, "Circuit breaker testing guide," *Technical Guide*, 2012. [Online]. Available: http://www.megger.com[Accessed:14.10.15]

[22] Z. J. Shen, G. Sabui, Z. Miao, and Z. Shuai, "Wide-bandgap solid-state circuit breakers for DC power systems: Device and circuit considerations," *IEEE Transactions on Electron Devices*, vol. 62, no. 2, pp. 294–300, 2015.

[23] S. Fletcher, P. Norman, S. Galloway, and G. Burt, "Solid state circuit breakers enabling optimised protection of DC aircraft power systems," *Proceedings of the 14th European Conference on Power Electronics and Applications*, pp. 1–10, 2011.

[24] A. Shukla and G. D. Demetriades, "A Survey on Hybrid Circuit-Breaker Topologies," *IEEE Transactions on Power Delivery*, no. 2, pp. 627–641, apr.

[25] C. W. Brice, "Review of technologies for current-limiting low-voltage circuit breakers," *IEEE Transactions on Industry Applications*, vol. 32, no. 5, pp. 1005–1010, 1996.

[26] P. V. Gelder and J. Ferreira, "Zero volt switching hybrid DC circuit breakers," *Conference Record of the 2000 IEEE Industry Applications Conference. Thirty-Fifth IAS Annual Meeting and World Conference on Industrial Applications of Electrical Energy (Cat. No.00CH37129)*, vol. 5, pp. 2923–2927, 2000.

[27] J. M. Meyer and A. Rufer, "A DC hybrid circuit breaker with ultra-fast contact opening and integrated gate-commutated thyristors (IGCTs)," *IEEE Transactions on Power Delivery*, vol. 21, no. 2, pp. 646–651, 2006.

[28] H. Polman, J. a. Ferreira, M. Kaanders, B. H. Evenblij, and P. Van Gelder, "Design of a bi-directional 600V/6kA ZVS hybrid DC switch using IGBTs," *Conference Record - IAS Annual Meeting (IEEE Industry Applications Society)*, vol. 2, no. C, pp. 1052–1059, 2001.

[29] R. Mehl and P. Meckler, "Comparison of advantages and disadvantages of electronic and mechanical Protection systems for higher Voltage DC 400 V," *in Proceedings of the 35th International Telecommunications Energy Conference (INTELEC)*, pp. 236–242, 2013.

[30] M. Callavik, B. A., H. J., and J. B., "The Hybrid HVDC Breaker: An innovation breakthrough enabling reliable HVDC grids," vol. Technical Paper, ABB Grid Systems, Nov. 2012.

[31] A. Emhemed and G. Burt, "Protection analysis for plant rating and power quality issues in LVDC distribution power systems," in *IEEE Power and Energy Society General Meeting*, 2015.

[32] S. D. A. Fletcher, P. J. Norman, S. J. Galloway, and G. M. Burt, "Mitigation against overvoltages on a DC marine electrical system," *IEEE Electric Ship Technologies Symposium, ESTS 2009*, pp. 420–427, 2009.

[33] Z. Miao, G. Sabui, A. Chen, Y. Li, and Z. J. Shen, "A Self-Powered Ultra-Fast DC Solid State Circuit Breaker Using a Normally-on SiC JFET," *IEEE Applied Power Electronics Conference and Exposition (APEC)*, pp. 767–773, 2015.

[34] M. Kempkes, I. Roth, and M. Gaudreau, "Solid-state circuit breakers for Medium Voltage DC power," *2011 IEEE Electric Ship Technologies Symposium*, no. 781, pp. 254–257, 2011.

[35] Z. X. Z. Xu, B. Z. B. Zhang, S. Sirisukprasert, X. Z. X. Zhou, and a.Q. Huang, "The emitter turn-off thyristor-based DC circuit breaker," *2002 IEEE Power Engineering Society Winter Meeting. Conference Proceedings*, vol. 1, pp. 288–293, 2002.

[36] S. Juvekar, B. Compton, and S. Bhattacharya, "A fast acting DC solid state fault isolation device (FID) with Si and SiC devices for MVDC distribution system," *2012 IEEE Energy Conversion Congress and Exposition, ECCE 2012*, pp. 2005–2010, 2012.

[37] S. Krstic, E. Wellner, a. Bendre, and B. Semenov, "Circuit Breaker Technologies for Advanced Ship Power Systems," *Electric Ship Technologies Symposium (ESTS)*, pp. 201–207, 2007.

[38] Infineon Technologies, "CoolMOS™ C7 : Mastering the Art of Quickness," *Technical Datasheet*, pp. 1–30, April 2013.

[39] T. Dragicevic, X. Lu, J. C. Vasquez, and J. M. Guerrero, "DC Microgrids - Part II: A Review of Power Architectures, Applications, and Standardization Issues," *IEEE Transactions on Power Electronics*, vol. 31, no. 5, pp. 3528–3549, may 2016.

[40] R. F. Schmerda, S. Krstic, E. L. Wellner, and a. R. Bendre, "IGCTs vs. IGBTs for circuit breakers in advanced ship electrical systems," *Electric Ship Technologies Symposium, 2009. ESTS 2009. IEEE*, pp. 400–405, 2009.

[41] K. Handt, G. Griepentrog, and R. Maier, "Intelligent, compact and robust semiconductor circuit breaker based on silicon carbide devices," *PESC Record - IEEE Annual Power Electronics Specialists Conference*, pp. 1586–1591, 2008.

[42] V. Veliadis, D. Urciuoli, H. Hearne, H. C. Ha, R. Howell, and C. Scozzie, "600-V / 2-A Symmetrical Bi-Directional Power Flow Using Vertical-Channel JFETs Connected in Common Source Configuration ," *Materials Science Forum*, pp. 1147–1150.

[43] Y. Sato, Y. Tanaka, A. Fukui, M. Yamasaki, and H. Ohashi, "SiC-SIT circuit breakers with controllable interruption voltage for 400-V DC distribution systems," *IEEE Transactions on Power Electronics*, vol. 29, no. 5, pp. 2597–2605, 2014.

[44] ALSTOM, *Network Protection & Automation Guide*, may 2011 ed. ALSTOM Grid.

[45] S. Fletcher, P. Norman, S. Galloway, and G. Burt, "Analysis of the effectiveness of non-unit protection methods within DC microgrids," *IET Conference on Renewable Power Generation (RPG 2011)*, pp. 111–111, 2011.

[46] S. D. a. Fletcher, P. J. Norman, S. J. Galloway, P. Crolla, and G. M. Burt, "Optimizing the roles of unit and non-unit protection methods within DC microgrids," *IEEE Transactions on Smart Grid*, vol. 3, no. 4, pp. 2079–2087, 2012.

[47] A. Meghwani, S. C. Srivastava, and S. Chakrabarti, "A New Protection Scheme for DC Microgrid using Line Current Derivative," pp. 1–5, 2015.

[48] M. Monadi, C. Gavriluta, J. I. Candela, and P. Rodriguez, "A communication-assisted protection for MVDC distribution systems with distributed generation," in *IEEE Power and Energy Society General Meeting*, 2015.

[49] H. Stokman, "Direct Current B.V." [Online]. Available: http://www.directcurrent.eu

[50] Google, "Google Maps." [Online]. Available: https://maps.google.com

[51] D. Petropoulos, "Transient Analysis in DC Distribution Grids," 2016.

6

DC Ready Devices – Is Redimensioning of the Rectification Components Necessary?

DC has several advantages over ac. In relation with the changes needed in todays ac power system to deal with dominating amounts of fluctuating renewable energy, it seems wise to consider dc as an alternative. One of the problems with introducing dc grids is the lack of availability of dc devices. DC ready devices that work on both – ac and dc – would simplify a smooth introduction of dc there, where it has its biggest advantage. This is especially interesting for newly built infrastructure, e.g. in developing countries with bad ac infrastructure, but also for upgrading the power of existing ac cables when needed.

As most ac devices today already have dc/dc converters inside, the changes are not as big as one might assume. In this chapter the rectification stage and power factor correction is looked at in detail and it is shown that in most cases there is no need for re-dimensioning of components to make devices dc ready. Other important points are subject of ongoing research as are dc microgrids in general.

This chapter is based on L. Mackay, L. Ramirez-Elizondo, and P. Bauer, "DC Ready Devices – Is Redimensioning of the Rectification Components Necessary?," in Mechatronika 2014 - 16th International Conference on Mechatronics, 2014.

6.1. INTRODUCTION

The war of currents between Edison with dc vs. Westinghouse and Tesla with ac was won by ac for good reasons a century ago [1]. However as time passed and new developments were made, the foundations of this victory are not as stable as one might have expected. Power electronics enable dc/dc conversion and achieve what hundred years ago only ac transformers could do efficiently: the change of voltage levels. DC is again used for HVdc power transmission today as dc line losses are much smaller than ac ones. Other benefits are the prevention of skin effects and less problems with cable capacitance especially for sea cables.

Also from the low voltage side dc is having a come back. Until now it is mostly inside the devices. First ac transformers were used to bring down the voltage to usual application levels, e.g. 20 V, and rectification was done thereafter. Today ac transformers in devices are more and more replaced by dc/dc converters. Due to their higher switching frequencies, typically 100 kHz instead of 50/60 Hz with ac, much smaller passive components can be used, which reduces size, weight and material costs. The ac from the grid needs therefore to be rectified and – to prevent distortion of the ac grid – artificial sinusoidal currents are drawn using power factor correction (PFC). Today even ac motors are more and more driven by motor controllers using ac/dc followed by dc/ac conversion which allows variable speed control.

Distributed renewable energy sources are either dc inherently, e.g. photovoltaics, or use a dc link to decouple rotations speeds from the ac grid such as wind power. Batteries are dc in general and their application is evolving in electric vehicles and other devices.

Therefore it would be reasonable to consider bringing dc one level higher and change the distribution grid connecting these sources and loads from ac to dc, eliminating dc/ac and ac/dc conversions. DC microgrids [2] can improve reliability even with an outage of the higher level grids using available distributed sources and storage. Balancing local supply and demand and financial compensation for grid losses could be done using the dc voltage [3]. Due to the lack of synchronization need in dc, reconnection to higher level grids is straight forward [4]. Centralized ac/dc conversion from low or medium voltage ac grid is more efficient and can even help stabilizing the ac grid, e.g. by supplying reactive power.

The transition from an ac to a dc distribution grid however is a challenge even though dc outperforms ac in many aspects. The high initial investment cost prevent the replacement of a whole ac grid at one time. This results in a chicken-and-egg problem: lack of available dc devices hinders the implementation of small dc grids while the lack of dc grids prevents manufactures to build dc devices.

DC ready devices that work on both – ac and dc – are a solution to this problem. Large volumes of ac consumers would also let play economics of scale for the early adopting dc consumers if costs are not (significantly) higher than ac only devices. As common ac devices (Fig. 6.1) use a bridge rectifier to get a fixed polarity, also a dc voltage at the input leads to the same polarity. So in fact these devices are already dc ready. However only two diodes are conducting constantly instead of four in the ac case. Therefore it could be argued that they would need to be dimensioned bigger because of higher losses. This does not hold in general as will be shown.

This chapter investigates the losses in the rectification stage when operated on dc

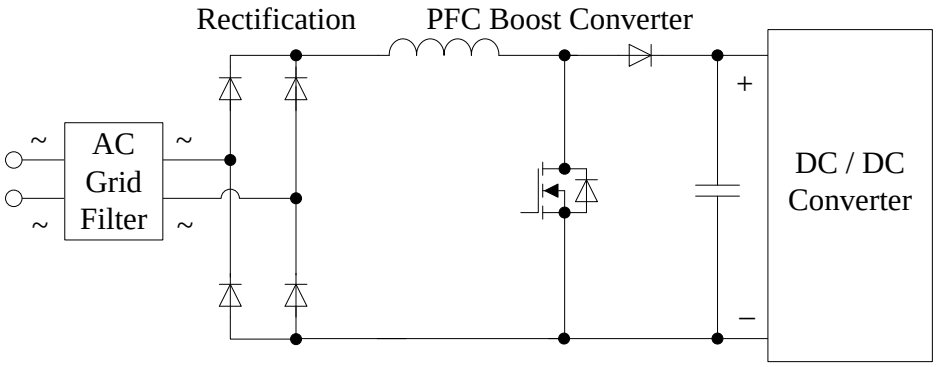

Figure 6.1: A usual power supply consists of a rectification stage, a boost converter for power factor correction and a dc/dc converter.

and determines under which circumstances the losses in an individual component are higher than the ac losses and thus demand for redimensioning. The main contribution is the finding that only diode bridge rectifiers rated for only 230 V ac may have to be redimensioned. For wide input range devices and devices using active rectification the losses in the individual rectification components are found to be smaller for dc voltages above 300 V. The term 'dc ready' instead of 'hybrid ac/dc' [3] is introduced to prevent confusion with hybrid ac/dc distribution systems.

The remainder of this chapter is organized as follows: In Section 6.2 the converter topology, voltage ranges and operation under ac and dc are introduced. In Section 6.3 the rectification losses are derived. These losses are compared in Section 6.4 with the losses when operating on different dc voltages. Further measures to built dc ready devices are discussed in Section 6.5 and conclusions are drawn in Section 6.6.

6.2. POWER SUPPLY WITH POWER FACTOR CORRECTION

In a power supply with power factor correction, as shown in Fig. 6.1, the first step is to rectify the ac input voltage (Fig. 6.2 on top). The resulting voltage is a rectified sine wave as is shown on the bottom of Fig. 6.2. After that rectified sinusoidal currents are drawn by the power factor correction (PFC) boost converter. This will result in sinusoidal ac currents at the input side. The resulting dc link voltage, typically around 380 V, is then converted by a dc/dc converter into the voltage needed by the device.

6.2.1. OPERATION ON DC INSTEAD OF AC

When dc instead of ac is applied, the currents will always flow trough the same two diodes as shown in Fig. 6.3. One could assume that they will produce bigger losses in the individual components that now conduct. This is what will be analyzed in this paper.

An alternative, to supplying ac on the ac input, would be, to add a dc connector to the dc link after the boost converter. In this way the rectification and power factor correction

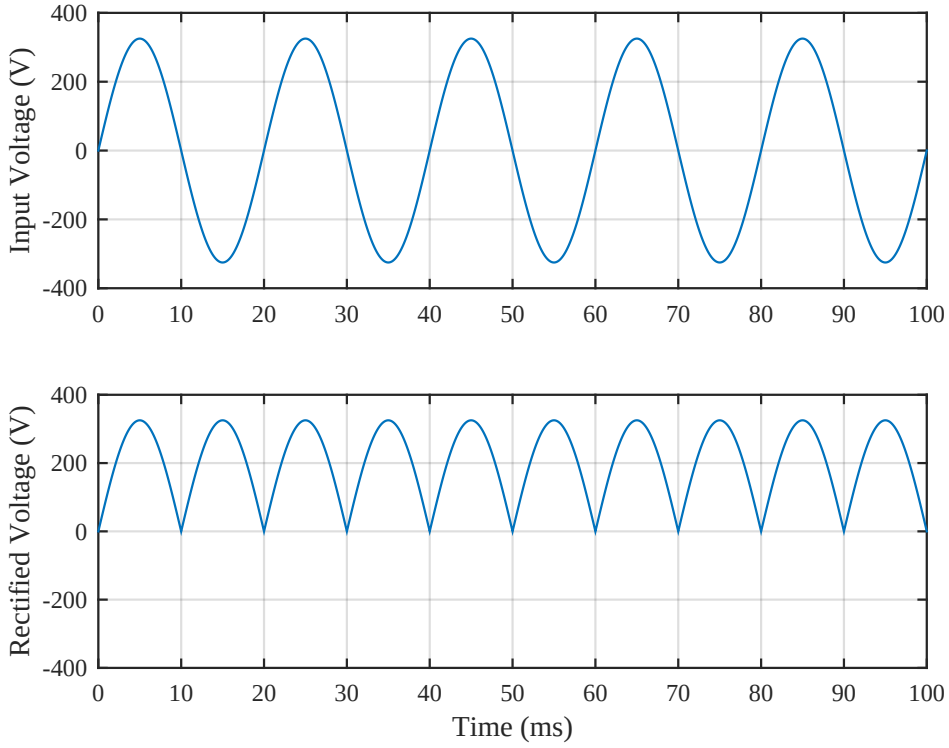

Figure 6.2: An ac voltage of 230 V at 50 Hz on top and the rectified voltage on the bottom.

stage can be bypassed. However this would mean that the device has to be modified and connectors are relatively expensive. If devices are made with replaceable connectors anyway such that they can used with the variety of outlets all over the world, this could however be viable. The rectification and PFC could be placed in the ac plugs, while the rest of the device is native dc. This chapter however focuses on the use of the same input connector for ac and dc.

6.2.2. EVALUATION OF THE COMMON VOLTAGES

For the analysis it has to be taken into account that usual ac voltage levels for devices range from 100 V in Japan to 240 V in the UK. AC devices are often constructed with a wide input voltage and frequency range to simplify mobility and reduce the number of product variants. If a safety margin of ±10 % is included, the lowest rms voltage can be 90 V and the highest 264 V. The latter has a peak voltage of 373 V. All devices have to be able to insulate at least this voltage. Therefore, just from the voltage perspective, these devices can be operated at least until this voltage if used with dc.

Devices only made for 230 V, as used in Europe, have – with a safety margin of ±10 % – a lower bound for the rms voltage of 207 V. This is the voltage at which the current is the highest and component loss dimensioning has therefore to be done.

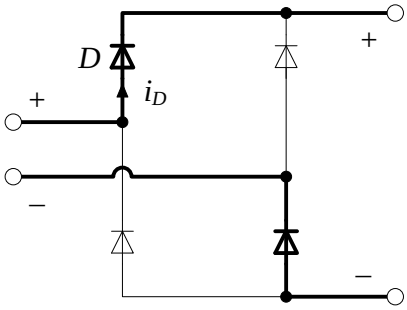

Figure 6.3: The current path true a diode bridge with dc input. Two elements conduct the whole time, while the others are never used.

6.2.3. CURRENTS AND VOLTAGES IN AC AND DC

The currents I in ac as in dc depend on the voltage U of the grid and the power P which is consumed by the device. It is assumed that the PFC stage is ideal so that the ac current is sinusoidal with power factor $\cos\varphi = 1$ meaning that voltage and current are in phase. They relate according to

$$P = U_{AC} \cdot I_{AC} = U_{DC} \cdot I_{DC} \tag{6.1}$$

$$I_{DC} = \frac{P}{U_{DC}} = \frac{U_{AC}}{U_{DC}} \cdot I_{AC}. \tag{6.2}$$

Equation (6.2) shows how I_{DC} can be influenced by choosing U_{DC}. Without needing any additional insulation in rectifying devices, U_{DC} can be as high as the peak voltage $\hat{U}_{AC}$ which is about the 1.4 fold as highest considered ac rms voltage U_{AC}:

$$U_{DC} := \hat{U}_{AC} = \sqrt{2} \cdot U_{AC} \tag{6.3}$$

with corresponding reduction of current

$$I_{DC} = \frac{P}{U_{DC}} = \frac{I_{AC}}{\sqrt{2}}. \tag{6.4}$$

6.3. DERIVATION OF RECTIFICATION LOSSES

The losses of the common rectifiers – diode bridge and active rectification – are derived in the following. The component models are simplified and switching losses are neglected as they only occur when the ac polarity changes twice every cycle. These switching losses that occur only in ac operation would extend the dc operating range. However, their magnitude depends on the specific components and high quality components, that are otherwise used at frequencies hundreds of kHz, have extremely low switching losses at 50 or 60 Hz. Therefore, this theoretical advantage can not be relied on in general terms and is therefore neglected. It is assumed that the thermal time constant is significantly larger than the ac period and thus is not used in the dimensioning of the original ac components. These effects are generally not taken into account when sizing rectifieres [5]. It

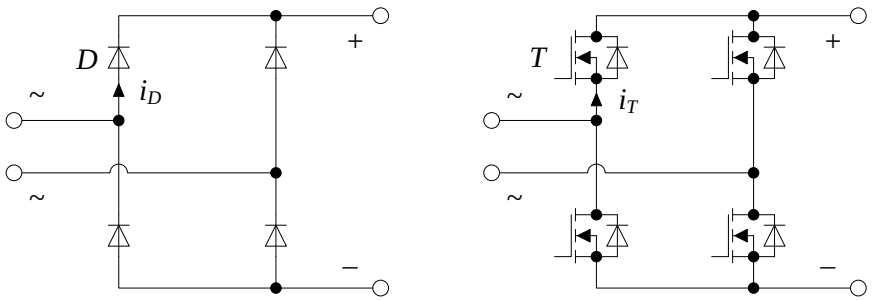

(a) (b)

Figure 6.4: The power electronics involved in rectification. On the left the diode bridge rectifier; on the right the four transistors for active rectification with their parasitic diodes in parallel.

is assumed that the PFC stage is ideal so that the ac current is sinusoidal with power factor $\cos\varphi = 1$ meaning that voltage and current are in phase. Ripples in dc and harmonic distortion are neglected for the loss calculations.

6

6.3.1. DIODE BRIDGE RECTIFICATION – LOSSES LINEAR TO CURRENT

In a full bridge diode rectifier as in Fig. 6.4a, current is flowing through each single diode D only half of the time. The loss of the diode p_D at time t is proportional to the current flowing through it:

$$p_D(t) = U_D \cdot i_D(t) \tag{6.5}$$

where U_D is the forward diode drop voltage – typically 0.7 V for Si-diodes – and i_D the current flowing through the diode.

With ac at frequency f the current of a single diode in the brigde rectifier over time is

$$i_{D,AC}(t) = \begin{cases} \hat{I}_{AC} \sin(\omega t) & \text{if } 0 < \omega t < \pi \\ 0 & \text{if } \pi < \omega t < 2\pi \end{cases} \tag{6.6}$$

with $\omega = 2\pi f$ and $\hat{I}_{AC}$ the peak value of the ac current I_{AC}. The average ac diode loss of each single diode is the integral of the instantaneous losses $p_D(t)$ divided by the time period:

$$\begin{aligned} P_{D,AC} &= \frac{\int_0^{\frac{2\pi}{\omega}} U_D \cdot i_{D,AC}(t)\,\mathrm{d}t}{\frac{2\pi}{\omega}} \\ &= \frac{\frac{1}{\omega} 2 U_D \hat{I}_{AC}}{\frac{2\pi}{\omega}} = \frac{\sqrt{2} U_D I_{AC}}{\pi} = \frac{\sqrt{2} \cdot U_D P}{\pi \cdot U_{AC}}. \end{aligned} \tag{6.7}$$

If the device is operated with dc, only two of the four diodes are used. The (average) dc diode loss in each of the two of them is

$$P_{D,DC} = U_D \cdot I_{DC} = \frac{U_D \cdot P}{U_{DC}}. \tag{6.8}$$

6.3.2. ACTIVE RECTIFICATION – LOSSES QUADRATIC TO CURRENT

Active rectification, also referred to as synchronous rectification, can be used to reduce the loss caused by the forward diode drop voltage U_D. In principle four transistors T are connected in parallel to the diodes (Fig. 6.4b) and conduct if the associated diodes would do. It is worth mentioning that this solution with MOSFETs is not commonly used because of over-voltage vulnerability, also of the drivers. However with new technologies like SiC this might get a more practical option. Bridge-less PFC is an alternative way of doing active rectification. The active low-side transistors are there used to do PFC. This is however not in the scope of this analysis.

The loss in common MOSFETs is quadratic to the current i_T flowing trough it:

$$p_T(t) = u_T(t) \cdot i_T(t) = R_T \cdot i_T^2(t) \tag{6.9}$$

where u_T is the voltage over the transistor and R_T the resistance of it when switched on.

The ac current $i_{T,AC}(t)$ is the same as $i_{D,AC}(t)$ in (6.6) and the average ac single transistor loss $P_{T,AC}$ can be derived from the instantaneous power $p_{T,AC}(t)$ as

$$p_{T,AC}(t) = \begin{cases} R_T \cdot (\hat{I}_{AC} \sin(\omega t))^2 & \text{if } 0 < \omega t < \pi \\ 0 & \text{if } \pi < \omega t < 2\pi \end{cases} \tag{6.10}$$

$$P_{T,AC,rms} = \begin{cases} R_T \cdot I_{AC}^2 & \text{if } 0 < \omega t < \pi \\ 0 & \text{if } \pi < \omega t < 2\pi \end{cases} \tag{6.11}$$

$$P_{T,AC} = \frac{R_T \cdot I_{AC}^2}{2} = \frac{R_T}{2} \left(\frac{P}{U_{AC}} \right)^2 \tag{6.12}$$

where I_{AC} is the rms value of $\hat{I}_{AC}$.

If the device is operated with dc, the current is flowing only in two of the four transistors. The (average) dc transistor loss in each of the two of them is

$$P_{T,DC} = R_T \cdot I_{DC}^2 = R_T \left(\frac{P}{U_{DC}} \right)^2 . \tag{6.13}$$

6.4. COMPARISON OF RECTIFICATION LOSSES

Regarding the losses of the rectification components, the worst-case rms voltages U_{AC} for the two ac voltage range cases are 90 V and 207 V respectively. At these voltages the ac current and thus the losses are the highest. The dc voltage above which losses in the

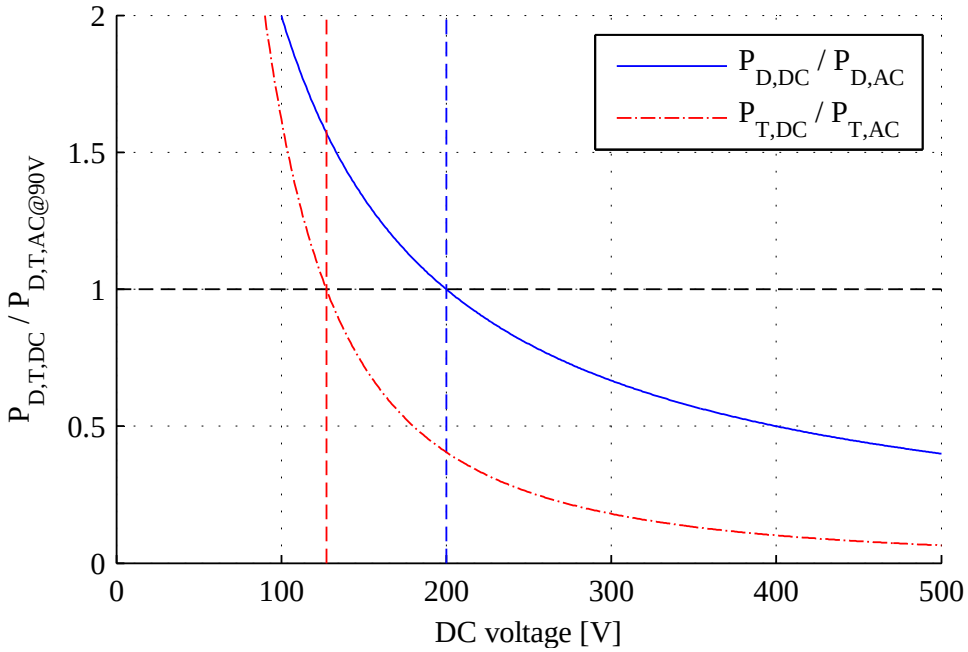

(a)

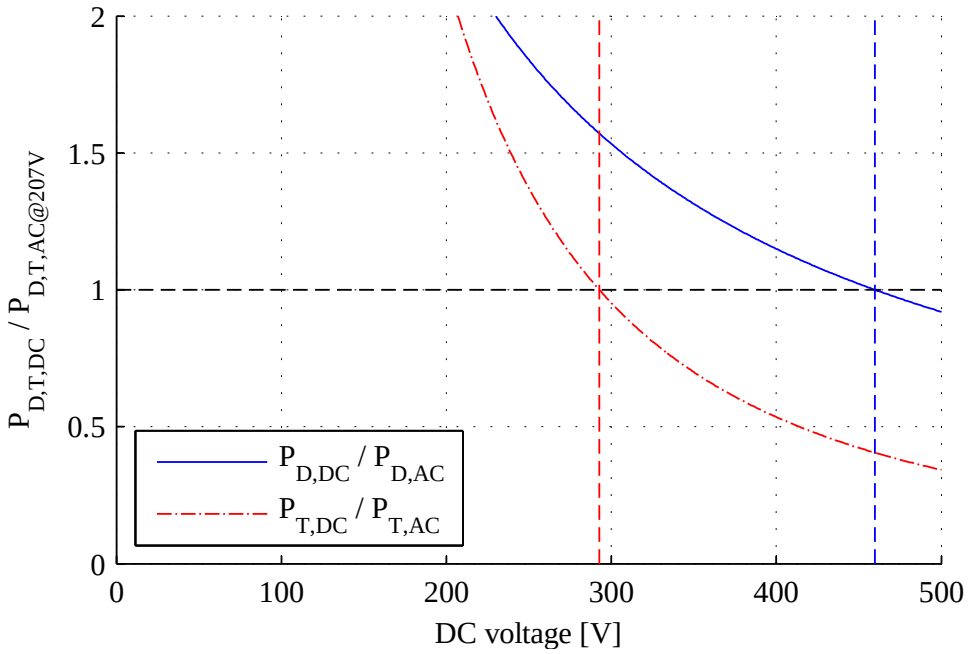

(b)

Figure 6.5: The losses of diode (solid blue) and transistor (dashed red) over the dc voltage spectrum in relation to the worst case losses at 90 V ac (a) and 207 V ac (b). The horizontal line indicates the equilibrium of dc and ac losses. All dc voltages higher than the vertical blue respectively red lines result in lower losses in the operational semiconductors compared to the ac case.

active diodes are lower are derived as follows:

$$P_{D,DC} \overset{!}{\leq} P_{D,AC} \tag{6.14}$$

$$P_{D,DC} = U_D \cdot I_{DC} \overset{!}{\leq} \frac{U_D \cdot \hat{I}_{AC}}{\pi} = P_{D,AC} \tag{6.15}$$

$$U_D \cdot \frac{P}{U_{DC}} \leq \frac{U_D \cdot \sqrt{2}\frac{P}{U_{AC}}}{\pi} \tag{6.16}$$

$$\frac{U_D}{U_{DC}} \leq \frac{\sqrt{2} \cdot U_D}{\pi \cdot U_{AC}} \tag{6.17}$$

$$U_{DC} \geq \frac{\pi}{\sqrt{2}} \cdot U_{AC} \approx 2.22 \cdot U_{AC} \tag{6.18}$$

This yields in a dc voltage U_{DC} of 200 V above which losses in diode bridge rectifier devices are lower than with 90 V ac. Fig. 6.5a shows the diode loss comparison over the dc voltage range (solid blue).

For active rectification, the needed dc voltage is:

$$P_{T,DC} \overset{!}{\leq} P_{T,AC} \tag{6.19}$$

$$P_{T,DC} = R_T \cdot I_{DC}^2 \overset{!}{\leq} \frac{R_T \cdot I_{AC}^2}{2} = P_{T,AC} \tag{6.20}$$

$$R_T \cdot \frac{P^2}{U_{DC}^2} \leq \frac{R_T \cdot P^2}{2 \cdot U_{AC}^2} \tag{6.21}$$

$$U_{DC}^2 \geq 2 \cdot U_{AC}^2 \tag{6.22}$$

$$U_{DC} \geq \sqrt{2} \cdot U_{AC} \approx 1.41 \cdot U_{AC} \tag{6.23}$$

For devices capable of 90 V ac this yields in a dc voltage U_{DC} as low as 127 V as shown in Fig. 6.5a (dashed red). This yields in a dc voltage U_{DC} of 293 V above which losses in active rectification devices are lower than with 207 V ac (Fig. 6.5b, dashed red).

In Fig. 6.5a the losses in diodes and transistors with dc are compared to the losses with the lowest ac voltage of 90 V. One can see that for devices capable of as low as 90 V ac, all dc voltages above 200 V are suitable both for the diode and especially for the transistor case.

For the transistor case a dc voltage above 293 V produces less losses even for devices that are designed only for a minimum ac voltage of 207 V (Fig. 6.5b). If a dc voltage U_{DC} lower than the equilibrium voltage calculated in (6.18) and (6.23) would be used, the graphs in Fig. 6.5a and 6.5b show for which additional losses the components would have to be dimensioned. The relation of losses for the diode bridge can be calculated as

$$\frac{P_{D,DC}}{P_{D,AC}}(U_{DC}) = \frac{\frac{U_D \cdot P}{U_{DC}}}{\frac{\sqrt{2} \cdot U_D P}{\pi \cdot U_{AC}}} = \frac{\pi U_{AC}}{\sqrt{2} U_{DC}} \tag{6.24}$$

and the one for active rectification as

$$\frac{P_{T,DC}}{P_{T,AC}}(U_{DC}) = \frac{R_T(\frac{P}{U_{DC}})^2}{\frac{R_T}{2}(\frac{P}{U_{AC}})^2} = 2\frac{U_{AC}^2}{U_{DC}^2}. \tag{6.25}$$

Decreasing Power at Low DC Voltages

Instead of increasing the size of rectification components, devices could reduce power if the dc voltage is low. This applies in general to any kind of storage devices, e.g. battery charging, where the effect of increased charging time is not too relevant. The amount of power reduction needed can be calculated for the diode bridge as

$$P_{D,DC} = U_D \cdot \frac{P_{DC}}{U_{DC}} \stackrel{!}{=} \frac{U_D \cdot \sqrt{2}\frac{P_{AC}}{U_{AC}}}{\pi} = P_{D,AC} \tag{6.26}$$

$$\left(\frac{P_{DC}}{P_{AC}}\right)_D = \frac{\sqrt{2} \cdot U_{DC}}{\pi \cdot U_{AC}} \tag{6.27}$$

and is shown in solid blue in Fig. 6.6. For active rectification it is calculated as

$$P_{T,DC} = R_T \cdot \frac{P_{DC}^2}{U_{DC}^2} \stackrel{!}{=} \frac{R_T \cdot P_{AC}^2}{2 \cdot U_{AC}^2} = P_{T,AC} \tag{6.28}$$

$$\left(\frac{P_{DC}}{P_{AC}}\right)_T = \frac{U_{DC}}{\sqrt{2} \cdot U_{AC}} \tag{6.29}$$

and is shown in dashed red in Fig. 6.6. For these graphs it is assumed that the components are dimensioned exactly for ac voltages of 90 V respectively 207 V and the maximum power. In practice components are mostly oversized due to quantization. This decreases the amount of needed power reduction. Not considered effects – like switching losses and non-sinusoidal ac currents – further contribute in advantage of dc. They depend strongly on the implementation of the power factor correction.

It should be noted all the presented calculations evaluate the losses in single semiconductors. The overall rectification stage losses when operating devices on dc are generally lower than the relative comparison of ac and dc shown as only two of the four semiconductors are used.

6.5. Further Measures to Design DC Ready Devices

Besides rectification there are other topics that should be considered when building dc ready devices. The PFC stage needs to be able to detect dc and switch of the transistor of the boost converter. This is a control issue and doesn't affect power electronics. Trying to detect an ac sine-wave in dc input could lead to unfavorable results. Losses in this stage are significantly reduced.

The dc/dc converter needs to be designed for the – to be standardized – dc operating voltage range. Another less efficient option would be to use the PFC stage to boost a too low dc input voltage.

Implementing demand response in case of under voltage would be necessary to continue operation of high priority loads in case of insufficient supply [6]. All loads would need to implement this. Inrush currents and load change characteristics are further topics that will probably be covered in future standards and should be complied with. The behavior of the ac grid filter when operated in dc also has to be considered.

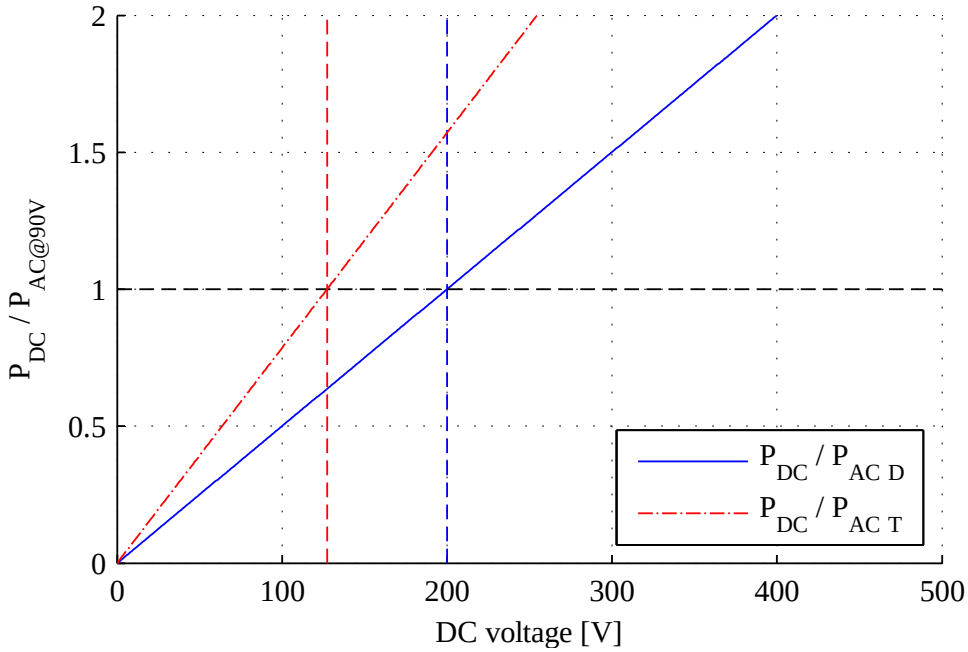

(a)

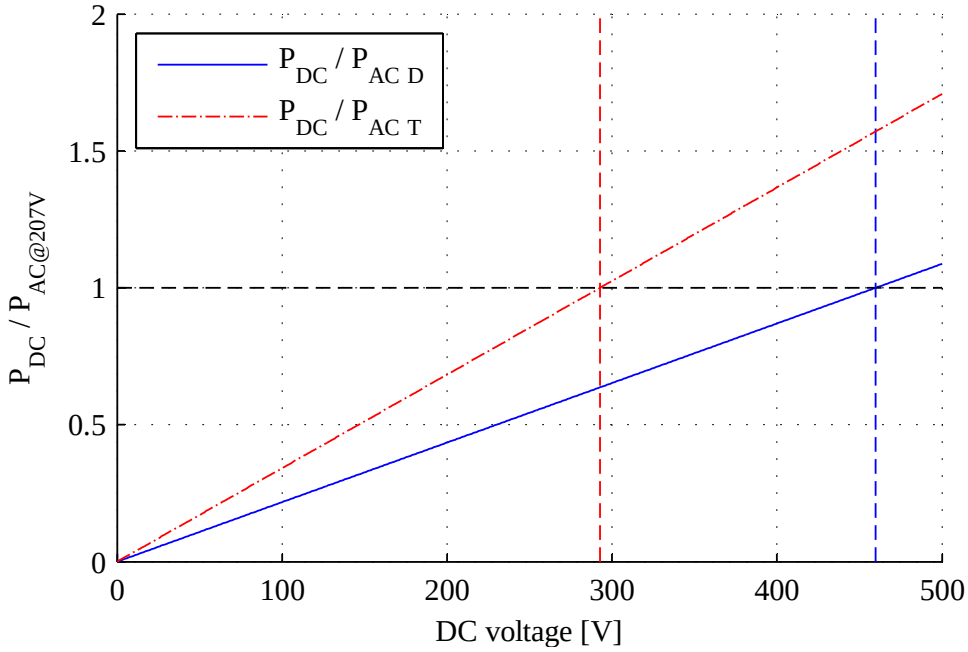

(b)

Figure 6.6: The dc power, in relation to the ac power at 90 V ac (a) and 207 V ac (b), that is allowed to not exceed the ac component losses of diode (solid blue) and transistor (dashed red). The horizontal line indicates the equilibrium of dc and ac power. For dc voltages lower than the vertical blue respectively red lines the dc power could be reduced to match precisely dimensioned components.

6.6. CONCLUSION

It can be concluded that it is easier to make devices dc ready than one might assume. For the discussed dc voltages between 350 V and 400 V nominal, it is shown that no re-dimensioning is necessary for wide input range ac devices. For 230 V only devices it has to be verified that the diodes are correctly dimensioned.

A 'dc ready' label should be introduced to make it recognizable. An adoption of this practice – even by just several suppliers – would decrease initial costs for early dc adopters significantly. It could also be considered to make this change mandatory for new devices. Other measures concerning inrush currents, protection and demand response could be added once a dc standard is established – but could also be connected in front externally later.

REFERENCES

[1] T. McNichol, *AC/DC: The Savage Tale of the First Standards War*. Wiley, 2006.

[2] T. Dragicevic, J. C. Vasquez, J. M. Guerrero, and D. Skrlec, "Advanced LVDC Electrical Power Architectures and Microgrids: A step toward a new generation of power distribution networks." *IEEE Electrification Magazine*, vol. 2, no. 1, pp. 54–65, Mar. 2014. [Online]. Available: http://ieeexplore.ieee.org/lpdocs/epic03/wrapper.htm?arnumber=6774539

[3] L. Mackay, M. Imhof, R. Wiget, and G. Andersson, "Voltage dependent pricing in DC distribution grids," in *PowerTech (POWERTECH), 2013 IEEE Grenoble*. IEEE, 2013, pp. 1–6. [Online]. Available: http://ieeexplore.ieee.org/lpdocs/epic03/wrapper.htm?arnumber=6652227

[4] J. J. Justo, F. Mwasilu, J. Lee, and J.-W. Jung, "AC-microgrids versus DC-microgrids with distributed energy resources: A review," *Renewable and Sustainable Energy Reviews*, vol. 24, pp. 387–405, Aug. 2013. [Online]. Available: http://linkinghub.elsevier.com/retrieve/pii/S1364032113002268

[5] S. Abdel-Rahman, F. Sückler, and K. Siu, "PFC boost converter design guide," 2016.

[6] J. Schonberger, S. Round, and R. Duke, "Autonomous Load Shedding in a Nanogrid using DC Bus Signalling," in *IECON 2006 - 32nd Annual Conference on IEEE Industrial Electronics*. IEEE, Nov. 2006, pp. 5155–5160. [Online]. Available: http://ieeexplore.ieee.org/lpdocs/epic03/wrapper.htm?arnumber=4153721

7

CONCLUSION

In summary, this dissertation covered the general requirements and design considerations for the future universal dc distribution system. The system could feature modular bipolar voltage levels of ±350 V and unbalanced connection of sources and loads. The optimal power flow model for unbalanced bipolar dc distribution grids can handle partial congestion and enable demand response if necessary. In this way operation cost could be minimized and social welfare maximized. Nodal prices can be used to put in place incentives for optimal behavior. This however, needs to be implemented in an automated way due to the low total electricity cost of the individual appliances. Storage operation in these systems could be optimized using multi period optimal power flow. The low short-circuit current protection philosophy can form a fundamental principle for the protection of large dc distribution grids that could also be islanded into multiple small nano- or microgrids in case of faults. DC ready devices could simplify the transition towards dc distribution grids.

In this chapter the research questions that were stated in Chapter 1, are re-addressed and the corresponding conclusions are drawn. This is followed by an overview of the main contributions. In the end, overall conclusions are drawn.

RE-ADDRESSING THE RESEARCH QUESTIONS

How can the dc distribution system be designed to allow for resilience with significant share of distributed renewable energy sources?

In Chapter 2 the general considerations for a universal dc distribution system were elaborated. The universal dc distribution system should be built out of connected dc nano- and microgrids. This enables the continuation of operation of parts of the grid even if they become disconnected, e.g., due to faults, and thereby increases the resilience of the system. There are various possibilities to choose location of separation of nanogrids. However, it was elaborated that in general this does not need to be at a location where a fully rated converter provides isolation. That means that different dc nano- and microgrids can be connected at the same voltage level.

In order to deal with a high share of distributed renewable energy sources, the operational aspects of future dc distribution systems were discussed. Enabling flexibility was described, which can be seen as the main paradigm. It was discussed that load shedding based on the local voltage should be used as a measure of last resort. This would need to be included into mandatory standards. On top of that, active demand response should be enabled for larger appliances. It was discussed that all of this should be enabled without user interaction. The electricity market design was described as an important aspect in enabling flexibility of prosumers. Dynamic prices were discussed to be essential for this and the faster they are updated, the less reserve power would be needed.

How should optimal power flow be implemented in meshed bipolar dc distribution grids in order to achieve minimum operation cost respectively maximization of social welfare, while respecting operation limits of lines and converters?

In Chapter 3 the exact optimal power flow for bipolar dc distribution grids was derived. It is formulated in terms of current and voltage. In this way the exact current limits of lines can be expressed. Likewise, in addition to conventional power limits, the current rating of converters can be considered as well, which is useful for wide voltage operating ranges where the maximum power at low voltages is less, e.g., due to demand response. Further, it was shown how the formulation allows parallel connection of converters and converters connected pole-to-pole as well as pole-to-neutral. The social welfare was maximized by minimizing the cost function such that all constraints were satisfied. Only local optimality is guaranteed due to the possible non-convexity of the bilinear problem formulation.

How can nodal prices for prosumers be derived in dc distribution grids such that they allow for independent economics agents to optimize for their own profit and encourage congestion management?

Also, in Chapter 3, the derivation of the locational marginal prices was presented. These nodal prices were calculated by linearizing the problem at the optimal solution. By using the dual variables of nodal currents, it was shown how general nodal prices for power injection between any two nodes can be calculated. These nodal prices are location dependent and can differ per pole due to asymmetric loading and congestion. Due to unbalance between the poles, prices were shown to be negative in some cases.

How is storage operated optimally in bipolar dc distribution grids and what effect does the operation of storage have on the nodal prices.

It was shown in Chapter 4 how the optimal power flow algorithm is extended for multiple periods. This was necessary for the inclusion of storage operation. The charging and discharging of energy storage systems were modeled by using binary variables due to the possibility that the electricity price could be zero or negative.

Further, it was shown how, in general, storage leads to more equalized prices over time. In unbalanced cases storage was shown to counter-act system unbalance in the case where this could reduce the total losses respectively cost. It was seen that sometimes it is more optimal to reduce the operation voltage of the less used pole in case of excessive unbalance.

What protection philosophy should be applied to large dc distribution grids such that both connected and islanded operation of individual dc microgrids is possible?

In Chapter 5, it was elaborated that dc distribution grids could have both very high and very low short-circuit current capability. On one hand, large capacitors of high power converters can lead to very high currents which are challenging to clear with traditional protection devices due to the missing current zero-crossings. On the other hand, dc nanogrids operated in islanding mode may only have a very small source that would not be able to sustain the fault current long enough in order to keep the systems selective. It was discussed how solid state breakers could clear faults very fast, but cannot sustain large fault currents. Therefore, a low short-circuit current protection philosophy was proposed, comprised of avoiding oversizing of converters and capacitors for fault current contribution, prevention of high short-circuit currents by fast fault clearing and the adaption of the other system components to achieve this.

Do the rectification components of ac devices need to be enhanced if they are operated on dc instead of ac?

It was derived in Chapter 6 that for dc grids with an operating voltage over 300 V, diode bridge rectifiers do not need to be enhanced if they are rated for a wide input voltage range. However, diode rectifiers in devices rated for only 230 V ac need to be looked at in detail in order to be sure that the losses do not exceed the device limits. The power loss of the individual diodes that conduct is 50 % larger if operated at 300 V dc. If active rectification was used, the losses in dc were shown to be smaller above 300 V as a result of the quadratic relation of the losses in MOSFETs.

Main Contributions

This dissertation contributes to the discussion towards a universal dc distribution systems that could be generally applied in various use cases. The main contributions can be seen as follows:

- Vision on the universal dc distribution system with its challenges and opportunities.
- Modeling of unbalanced bipolar dc distribution grids in terms of voltage and current for the purpose of power flow optimization.
- Derivation of locational marginal prices for unbalanced bipolar dc distribution grids.
- Formulation of the low short-circuit protection philosophy as a general direction for protecting larger dc distribution grids.
- Demonstrating ultra fast solid state protection with fault detection based on current derivative.
- Determination of the voltage above which rectification components in common ac devices do not need to be resized in order to be used on dc.

In conclusion, the intention of this dissertation was to set first steps in the direction of the universal dc distribution system. Fundamental considerations have been elaborated that can serve as a basis for future research. As we have seen, many opportunities in dc systems can only be realized if the inter-dependencies are considered and the different parts of the system are designed together, while making the necessary trade-offs. This will be done best in a team covering the different inter-related fields.

ACKNOWLEDGEMENTS

First of all I'd like to thank my promotor Pavol Bauer for allowing me to come to Delft and continue my research on dc distribution grids here. I'm very grateful for the support and guidance from my daily supervisor and copromotor Laura Ramirez Elizondo. Without you, I would not have completed this PhD. Jelena Popovic, thank you for the short time that we could work together here in Delft. I'd like to thank my initial intended promotor Miro Zeman for supporting me during the first two years. Also I'd like to thank my mentor Koen Hindriks for his support during these years.

I would like to thank Harry Stokman for connecting me to the university in the first place and also for the unfortunately limited – but very fruitful – discussions.

The most important part of a research group is to work together in order to achieve things that would not be possible alone. That was the reason why we tried to form a team on dc microgrids. I'd like to take opportunity to thank the master students that I was allowed to work with during this time. I thank all of you for choosing to do your projects with me on these topics. I really enjoyed to be able to work with all of you.

In my first year, we started to form the team and building our dc microgrid research and demonstration framework. Vinay Srisanka did an extra project and did the initial design for a dual active bridge converter. In his master's thesis Panos Kolios built a first prototype for the dual active bridge converter and worked on storage operation in dc distribution grids with only unidirectional communication and voltage dependent demand response. Nil Chaudhuri worked on the control of dc microgrids and we designed the first converter prototype with integrated solid state protection and inrush current limiting. Emanuele Marafante worked on the blackstart of dc microgrids from photovoltaics with micro converters and we implemented and tested an inrush current control circuit. Anastasios Dimou started to work on optimal power flow for bipolar dc distribution grids. Aditya Shekhar investigated series arc detection from load side.

In my second year Robin Guarnotta worked the optimal power flow with storage operation in dc distribution grids. Nikos Gouvalas worked mainly on solid state protection but we also debugged the first converter prototype. Dimitris Petropoulos focused on the transients in dc distribution grids and developed EMTP models as well as a measurement set up for a field study. Elisabeth Vandeventer worked on grounding and ground fault protection in meshed dc distribution grids with multiple grounding points. Ivan Ramirez first developed a microgrid communication framework as an extra project and then focused in his master's thesis on control and voltage dependent demand response in dc microgrids. Nikitas Karatzaferis built a converter for USB-C with Power Delivery that could also be used to research advanced demand response. Sotiris Sakkas focused on zero voltage switching in non-inverting buck-boost converters and power balance control in dc microgrids. Giannis Tsopelopoulos built a non-inverting buck boost converter in an extra project. Suzanne Janssen, Koen Emmer, Ludo van den Buijs, Bart

Kölling, Ron Bentvelsen, Menno Gravemaker worked on the Tesla Powerwall and its control in their bachelor's project.

In my third year, I worked with Kenji Yañez Martinez who focused on capacitive grounding in his master's thesis. Sahil Karambelkar worked on distributed optimal power flow for dc distribution grids. Bryan Oscareino worked on storage balancing without communication in interconnected solar home systems. Ryan Prakoso built a partially rated power flow control converter for meshed dc distribution grids. Shruthi Kashyap worked on the software implementation of USB Power Delivery in an extra project.

Of course I'd like to thank also my fellow PhD students. Rodrigo Teixeira Pinto, I really appreciated your support and the discussions with you during my first weeks in Delft. Todor Todorcevic, thank you for reviewing my first paper and introducing me into the world of power electronics. Minos Kontos, I enjoyed to have you as a colleague and I also appreciate our collaboration on the Multi-Line HVDC Breaker. Tsegay Hailu, I would really like to thank you for all the interesting discussions especially the first two years and also for being a good friend. Nishant Narayan, I'm glad that our paths have crossed and enjoyed that collaboration we could have. Udai Shipurkar, I enjoyed the time with you and our discussions on dc wireless power transfer. Nils van der Blij and Pavel Purgat thank you for being my office mates for the last years and helping me through this time. Longjian Piao, I wish you all the best in the dc markets. Soumya Bandyopadhyay, maybe do some things on dc and what about USB Power Delivery? Gautham Ram Chandra Mouli, I guess, that I chose a printer anyway in the end. Venogupal Prasanth, thank you for your calm advice. Aditya Shekhar, thank you for initiating and sustaining all the controversial discussions. Victor Vega, thanks for letting me improve my Spanish skills at the end of your progress meetings. Shantanu Chakraborty thank you for your collaboration and discussions.

I'd like to also thank our lab technicians Bart Roodenburg and Joris Koeners for your support and our discussions and our secretary Sharmila Rattansingh for organizing everything and spreading some good mood every day.

I'd like to thank Caroline Bruens for supporting me during the last two years (and for making the cover). Last but not least, many thanks to my family and friends for all your support until this day.

List of Publications

Conference Papers

1. L. Mackay, M. Imhof, R. Wiget, and G. Andersson, "Voltage Dependent Pricing in DC Distribution Grids," in IEEE PowerTech 2013 Conference Grenoble, 2013. Published.

2. L. Mackay, L. Ramirez-Elizondo, and P. Bauer, "DC Ready Devices – Is Redimensioning of the Rectification Components Necessary?," in Mechatronika 2014 - 16th International Conference on Mechatronics, 2014. Published.

3. L. Mackay, T. G. Hailu, G. R. Chandra Mouli, L. Ramirez-Elizondo, J. A. Ferreira, and P. Bauer, "From DC Nano- and Microgrids Towards the Universal DC Distribution System – A Plea to Think Further Into the Future," in PES General Meeting, 2015. Published.

4. L. Mackay, P. Kolios, L. Ramirez-Elizondo, and P. Bauer, "Voltage Dependent Demand Response with Dynamic Hysteresis Thresholds in DC Microgrids," in IEEE PowerTech 2015 Conference Eindhoven, 2015. Published.

5. L. Mackay, A. Shekhar, B. Roodenburg, L. Ramirez-Elizondo, and P. Bauer, "Series Arc Extinction in DC Microgrids using Load Side Voltage Drop Detection," in DC Microgrids, IEEE First International Conference on, 2015. Published.

6. L. Mackay, T. Hailu, L. Ramirez-Elizondo, and P. Bauer, "Towards a DC Distribution System – Opportunities and Challenges," in DC Microgrids, IEEE First International Conference on, 2015. Published.

7. L. Mackay, T. Hailu, L. Ramirez-Elizondo, and P. Bauer, "Decentralized Current Limiting in Meshed DC Distribution Grids," in DC Microgrids, IEEE First International Conference on, 2015. Published.

8. L. Mackay, A. Dimou, R. Guarnotta, G. Morales-Espania, L. Ramirez-Elizondo, and P. Bauer, "Optimal Power Flow in Bipolar DC Distribution Grids with Asymmetric Loading," in IEEE Energycon Leuven, 2016. Published.

9. L. Mackay, L. Ramirez-Elizondo, and P. Bauer, "Current Pricing: Avoiding Marginal Losses in Locational Marginal Prices for DC Grids," in IEEE PowerTech Manchester, 2017. Published.

10. L. Mackay, K.F. Yanez Martinez, E. Vandeventer, L. Ramirez Elizondo, and P. Bauer, "Capacitive Grounding for DC Distribution Grids with Two Grounding Points," in DC Microgrids, IEEE Second International Conference on, 2017. Published.

11. L. Mackay, P. Kolios, L. Ramirez-Elizondo, and P. Bauer, “Physical Market Clearing for Dynamic Pricing in DC Distribution Grids with Storage,” in DC Microgrids, IEEE Second International Conference on, 2017. Accepted.

12. E. Marafante, L. Mackay, T. Hailu, G. R. Chandra Mouli, L. Ramirez-Elizondo, and P. Bauer, “PV Architectures for DC Microgrids using Buck or Boost Exclusive Microconverters,” in IEEE PowerTech 2015 Conference Eindhoven, 2015. Published.

13. T. Hailu, L. Mackay, L. Ramirez-Elizondo, J. Gu, and J. A. Ferreira, “Voltage Weak DC Microgrids,” in DC Microgrids, IEEE First International Conference on, 2015. Published.

14. T. Hailu, L. Mackay, L. Ramirez-Elizondo, J. Gu, and J. A. Ferreira, “Weakly Coupled DC Grid for Developing Countries : ‘ Less is More ,’” in Africon, 2015. Published.

15. A. Shekhar, L. Mackay, L. Ramirez-Elizondo, and P. Bauer, “State Space Model for n-Parallel Connected DC-DC Converters with Predictive Current Control Strategy,” in International Exhibition and Conference for Power Electronics, Intelligent Motion, Renewable Energy and Energy Management, PCIM, 2016. Published.

16. A. Shekhar, L. Mackay, L. Ramirez-Elizondo, and P. Bauer, “Experimental design of a series arc load side detection algorithm for DC microgrid protection,” in 2016 International Symposium on Power Electronics, Electrical Drives, Automation and Motion (SPEEDAM), 2016, pp. 343–347. Published.

17. A. Shekhar, L. Mackay, L. Ramirez-Elizondo, and P. Bauer, “DC microgrid protection by selective detection of series arcing using load side power electronic devices,” in 2016 18th European Conference on Power Electronics and Applications (EPE’16 ECCE Europe), 2016. Published.

18. I. Ramirez-Fonseca, L. Mackay, N. H. Van Der Blij, T. G. Hailu, L. Ramirez-Elizondo, and P. Bauer, “Impact of Voltage Dependent Demand Response on the Dynamics of DC Microgrids,” in Sustainable Green Buildings and Communities, IEEE First International Conference on, 2016. Published.

19. E. Vandeventer, L. Mackay, L. Ramirez Elizondo, and P. Bauer, “Circulating Net Currents in Meshed Bipolar DC Distribution Grids due to Asymmetrical Line Resistance,” in Sustainable Green Buildings and Communities, IEEE First International Conference on, 2016. Published.

20. T. Hailu, L. Mackay, M. Gagic, and J. A. Ferreira, “Protection Coordination of Voltage Weak DC Distribution Grid: Concepts,” IEEE Southern Power Electronics Conference, 2016. Published.

21. T. Hailu, M. Gagic, L. Mackay, and J. A. Ferreira, “From Voltage Stiff to Voltage Weak: Opportunities and Challenges,” IEEE Southern Power Electronics Conference, 2016. Published.

22. P. Purgat, L. Mackay, R. A. Prakoso, L. Ramirez-Elizondo and P. Bauer, "Power Flow Control Converter for Meshed LVDC Distribution Grids," 2017 IEEE Second International Conference on DC Microgrids (ICDCM), Nuremburg, 2017, pp. 476-483. Published.

23. D. Petropoulos, L. Mackay, L. Ramirez-Elizondo, M. Popov, and P. Bauer, "Transient Analysis of DC Distribution Grids," in DC Microgrids, IEEE Second International Conference on, 2017. Published.

24. P. Purgat, R. A. Prakoso, L. Mackay, Z. Qin, and P. Bauer, "A Partially Rated DC-DC Converter for Power Flow Control in Meshed LVDC Distribution Grids," in IEEE APEC Conference, 2018. Accepted.

25. S. Karambelkar, L. Mackay, S. Chakraborty, L. Ramirez-Elizondo, and P. Bauer, "Distributed Optimal Power Flow for DC Distribution Grids," in IEEE PES General Meeting, 2018. Under Review.

26. P. Purgat, L. Mackay, Z. Qin and P. Bauer, "On the Protection of the Power Flow Control Converter in Meshed Low Voltage DC Networks," ECCE, 2018. Under Review.

JOURNAL PAPERS

1. L. Mackay, N. H. van der Blij, L. Ramirez-Elizondo, and P. Bauer, "Toward the Universal DC Distribution System," Electric Power Components and Systems, 2017, no. 10, pp. 1032–1042. Published.

2. L. Mackay, R. Guarnotta, A. Dimou, G. Morales-Espania, L. Ramirez-Elizondo, and P. Bauer, "Optimal Power Flow for Unbalanced Bipolar DC Distribution Grids," in IEEE Access, 2018. Published.

3. L. Mackay, N. Gouvalas, T. Hailu, H. Stokman, L. Ramirez-Elizondo, and P. Bauer, "Low Short Circuit Current Protection Philosophy for DC Distribution Grids," in Energies, 2018. Under Review.

4. E. Kontos, T. Schultz, L. Mackay, L. Ramirez-Elizondo, C. Franck, and P. Bauer, "Multi-Line Breaker for HVDC Applications," in IEEE Transactions on Power Delivery, 2017. Published.

5. A. Shekhar, L. Ramirez-Elizondo, S. Bandyopadhyay, L. Mackay, and P. Bauer, "Detection of Series Arcs using Load Side Voltage Drop for Protection of Low Voltage DC Systems," in Smart Grid, IEEE Transactions on, 2017. Published.

6. T. Hailu, L. Mackay, M. Gagic, L. Ramirez-Elizondo, and J. A. Ferreira, "Voltage Weak DC Distribution Grids," in Taylor and Francis Electric Power Components and Systems, 2017. Published.

7. T. Hailu, M. Gagic, L. Mackay, and J. A. Ferreira, "Piece-wise linear droop control for Load Sharing in Low Voltage DC Distribution Grid ," in Power Delivery, IEEE Transactions on. Under Review.

LETTERS

1. L. Mackay, E. Vandeventer, and L. Ramirez Elizondo, “Circulating Net Currents in Meshed DC Distribution Grids: A Challenge for Residual Ground Fault Protection,” in IEEE Transactions on Power Delivery, 2018. Published.

PATENTS

1. L. Mackay and E. Kontos, “DC switch yard and method to operate such a DC switch yard,” WO 2017/034408, 2015.

CURRICULUM VITÆ

Laurens MACKAY

19-09-1985	Born in Zeist, the Netherlands.

EDUCATION

2005	Matura Gymnasium Kirschgarten, Basel, Switzerland
2011	Bachelor of Science in Electrical Engineering and Information Technology Swiss Federal Institute of Technology (ETH), Zürich, Switzerland
2012	Master of Science in Electrical Engineering and Information Technology Swiss Federal Institute of Technology (ETH), Zürich, Switzerland *Master's Thesis:* DC Distribution Grid with Voltage Dependent Pricing and Distributed Renewable Generation *Examiner:* Prof. G. Andersson